The Susceptibility of an Urban Ash Canopy to the Emerald Ash Borer – A Temporal and Spatial Analysis from Winnipeg, Manitoba, Canada

by

Brett MacDonald

A Thesis submitted to the Faculty of Graduate Studies of The University of Manitoba

in partial fulfilment of the requirements of the degree of

MASTER OF ENVIRONMENT

Department of Environment and Geography

University of Manitoba

Winnipeg

Abstract

The invasive emerald ash borer (*Agrilus planipennis* Fairmaire; Coleoptera: Buprestidae) was first detected in Winnipeg, Manitoba in 2017 and has the potential to become a serious threat to the city's extensive ash (*Fraxinus* spp.) canopy. The objectives of this thesis were to predict *A. planipennis* emergence and peak activity patterns in Winnipeg; and to determine the potential susceptibility of neighbourhoods to infestation. To predict adult emergence and peak activity of *A. planipennis*, we used local weather station data to calculate the number of degree-days accumulated in each year for the 1970–2019 period using three different degree-day accumulation models. The estimated mean emergence dates for the 50-year period were June 14 ± 8.5 days (double sine model), June 14 ± 8.5 days (single sine model), and June 19 ± 9.1 days (standard model). The peak activity dates were July 16 ± 8.8 days (double sine model), July 17 ± 8.7 days (single sine model), and July 21 ± 9.4 days (standard model). To determine the potential susceptibility of neighbourhoods, ash density (trees/ha) maps, Moran plots, and correlograms were developed to model how *A. planipennis* might spread throughout Winnipeg and the potential corridors that may facilitate beetle movement. This study found that private green ash trees along riverbanks may be of most concern to city managers as these trees have significant potential to influence how EAB disperses throughout Winnipeg. The management of private green ash (*Fraxinus pensylvanica* Marsh.) trees along riverbanks will be a major variable in how successful *A. planipennis* dispersal is throughout the city. The results from this study will provide managers with information regarding the predicted temporal and spatial behavior of *A. planipennis* in Winnipeg allowing for improved timing of control measures and monitoring.

Acknowledgements

The completion of this thesis would not have been possible without the support of my advisor Rick Baydack, and my advisory committee David Walker, Richard Westwood, and Kerienne La France. Rick: thank you for your support, encouragement, and advice throughout the duration of my degree. Your student-orientated approach always steered me in the right direction, and I greatly appreciate everything you did for me. Enjoy your retirement! Dave: thank you for sticking with me through long meetings and helping me, especially with the spatial modelling. Your guidance and assistance are much appreciated! Richard: thank you for your assistance and advice throughout this project, especially with the degree-day component. I greatly appreciate the expertise that you provided to my project! Keri: I am grateful for your genuine interest and support of this project! Your comments and forestry experience contributed significantly in shaping this project to be of great use to the City of Winnipeg.

I would like to thank the City of Winnipeg's Urban Forestry Department for providing me with datasets and information that allowed me to complete several of the analyses and models.

Lastly, I would like to thank my friends and family for their support and encouragement through the years.

Table of Contents

List of Tables

List of Figures

Chapter 1: Emerald Ash Borer in North America

1.1 Introduction

The emerald ash borer (EAB; *Agrilus planipennis* Fairmaire; Coleoptera: Buprestidae) is an invasive wood boring beetle that was first detected in North America near Detroit, Michigan and Windsor, Ontario in 2002 (Haack et al., 2002; Poland & McCullough, 2006). Dendrochronological evidence suggests that EAB likely became established in North America in the early 1990s (Siegert et al., 2014) and has since killed tens of millions of ash (*Fraxinus spp.*) trees (Herms & McCullough, 2014; McCullough et al., 2009a). Within the current North American distribution of EAB, forested sites have experienced as much as 100% mortality of ash trees with significant economic and ecological cost (Flower et al., 2013; Herms & McCullough, 2014; Klooster et al., 2014, 2018). Complete mortality of affected urban ash stands is usually observed within 6-10 years after EAB is first detected in the area (Knight et al., 2013; Morin et al., 2017; Government of Canada, 2021). This delay in EAB detection and ash mortality is due to a lag effect whereby local beetle populations take time to grow large enough to kill trees rapidly (Haavik, 2016). Infested individual mature ash trees usually die in 2–5 years; however, trees with high larval densities can die in under two years (Wang et al., 2010; Knight et al., 2013; Herms & McCullough, 2014). Ash of all sizes ranging from saplings to mature trees are susceptible to EAB (McCullough, 2020; Knight et al., 2013). EAB is difficult to detect at low densities at the beginning of an infestation because infestations generally begin in the upper tree canopy and few visible symptoms are present (Cappaert et al., 2005). Locating newly infested trees and trees with low densities of EAB is difficult because these trees do not exhibit the external symptoms that characterize heavily infested trees (McCullough et al., 2009b). Since its detection in 2002, EAB has killed ash trees in forest, riparian, and urban areas becoming one of the most destructive and costly forest insects to ever invade North America (Aukema et al., 2011).

EAB is native to northeastern China, the Korean peninsula, Japan, Mongolia, and eastern Russia (Baranchikov et al., 2008; Valenta et al., 2017). In its native range, EAB functions as a secondary pest colonizing and killing unhealthy ash trees (Liu et al., 2003). However, North American ash species have no evolutionary history with EAB and thus they are very susceptible to the insect (Valenta et al., 2017; Villari et al., 2016). It is suspected that different phloem chemistry and defensive proteins between Asian and North American ash species result in the

varying EAB susceptibility (Whitehill et al., 2011; Whitehill et al., 2012). While trees under stress are preferred, EAB also attacks and kills healthy trees in North America which could result in the extirpation of native ash species from North American forest systems (Herms & McCullough, 2014; Klooster et al., 2014). Six native ash species endemic to North America are threatened by EAB. These include white ash (*Fraxinus americana* L.), green ash (*Fraxinus pensylvanica* Marsh.), black ash (*Fraxinus nigra* Marsh.), blue ash (*Fraxinus quadrangulata* Michx.), Carolina ash (*Fraxinus caroliniana* Mill.), and pumpkin ash (*Fraxinus profunda* (Bush) Bush). All native North American ash species within the EAB's current invasive range are known to be susceptible to EAB attack (Poland & McCullough, 2006) and the continued loss of mature ash trees from forest communities will present challenges for conserving genetic diversity in ash (Granger et al., 2020). The most abundant ash species in North America are white, green, and black ash (Herms & McCullough, 2014). These three species especially serve as potential hosts for EAB and face extirpation from forest communities (Villari et al., 2016). All three of these species are highly susceptible and are critically endangered because of the threat posed by EAB (IUCN, 2021; Steiner et al., 2019). Green, white, and black ash may experience functional extirpation to the point that they no longer provide significant ecosystem functions and services as EAB continues to spread (Flower et al., 2013). Since its introduction, EAB has expanded its range significantly and now threatens ash trees in 35 US states (USDA, 2021) and five Canadian provinces (Canadian Food Inspection Agency, 2021).

1.2 Biology

EAB has a one-year or two-year life cycle depending on geographical location and infestation stage (Liu, 2018). In unhealthy trees, nearly all EAB develop within one-year with larvae feeding from mid-summer into autumn during which time they complete four instars before they overwinter as prepupae (J-stage) in the bark (Herms & McCullough, 2014; Wang et al., 2010). EAB adults emerge from the pupal stage during mid-spring through mid-summer depending on location where they complete 1-2 weeks of maturation feeding on ash leaves (Poland & McCullough, 2006; Villari et al., 2016; Wang et al., 2010). After this 1-2 week period, they are reproductively mature and they begin to disperse via flight (Cappaert et al., 2005). Upon mating, females oviposit (lay eggs) on bark surfaces or in crevices and eggs hatch within 10–14 days (Herms & McCullough, 2014). Larvae then bore through the outer bark and begin feeding in

galleries in the phloem and cambium during the summer, after which they create a pupal chamber in the sapwood in which to overwinter and pupate (Crook & Mastro, 2010). Tree mortality occurs after extensive damage from the larval galleries and feeding which disrupts water and nutrient transport leading to canopy dieback and tree mortality (Cappaert et al., 2005; Cipollini & Peterson, 2018).

1.3 Impacts

EAB is the most economically destructive non-native forest pest to ever invade the United States due to widespread tree mortality (Aukema et al., 2011). In Canada, EAB has already caused tens of millions of dollars in damage to governmental bodies (municipal, provincial, and federal) and has the potential to inflict millions more (Hope et al., 2020; McKenny et al., 2012). Economic costs associated with EAB largely reflect the abundance of ash trees in landscapes, parks, and along roads in urban areas (McCullough, 2020). This is because cultivars of green ash, white ash, and black ash are common landscape and roadside trees in many US and Canadian municipalities, often comprising more than 25% of the public urban forest canopy (City of Ottawa, 2017; City of Winnipeg, 2020; McCullough & Mercader, 2012; Poland & McCullough, 2006; Sadof et al., 2017). Forest inventories report almost eight billion ash trees in US forests and woodlands valued at $282.25 billion USD (Poland et al., 2015). Detailed spatial data on ash volumes are not available for much of Canada; therefore, the true extent of the Canadian ash population is not completely understood (Government of Canada, 2018; McKenny et al., 2012). Estimates based on forestry data suggest that the population of black ash in Canada is in the range of 162 million mature trees (Government of Canada, 2018) while other ash species, most notably green ash, do not have approximated national populations. Although the national projection may be lacking, many Canadian cities have urban tree inventories where green ash is reported to be among the most common planted species. Green ash represented 26% of the city-managed tree population in Thunder Bay, Ontario (Davey Resource Group, 2011); 30% in Winnipeg, Manitoba (City of Winnipeg, 2020); 20-25% in Ottawa, Ontario (City of Ottawa, 2017); 35% in Regina, Saskatchewan (City of Regina, 2022); and 25% in Edmonton, Alberta (City of Edmonton, 2012). In Canada, there are approximately four million ash street trees in urban areas; however, this estimate is likely conservative as it excludes backyard, park, and greenspace trees (Hope et al., 2020).

A study of invasive forest insects in the US projected that by 2019, economic costs of EAB would exceed $1 billion USD annually, most of which will be borne by municipalities and private property owners (Aukema et al., 2011). Kovacs et al. (2010) modeled the spread and economic impact of EAB from 2009 to 2019 and estimated the costs of treating or removing 37.9 million urban ash trees across 25 American states. They found that the estimated cost of treatment, removal, and replacement would be $10.7 billion USD, and twice that if ash in adjacent suburban communities were included (Kovacs et al., 2010). A subsequent projection of EAB expansion through 2020 showed costs associated with landscape ash removal, replacement, and treatment would likely exceed $12.5 billion USD (Kovacs et al., 2011). Projected costs for removal and replacement of ash trees growing in parks, private land, and along streets in communities in four Midwestern states were estimated at $26 billion USD (Sydnor et al., 2011). There have been no updates on the findings of these studies at the time of writing this thesis. In Canada, Hope et al. (2020) found that under a simulation with no EAB regulation (of long-distance dispersal events), the predicted costs of EAB damage were approximately $1.422 billion (CAD). They also found that the cost of removing and replacing urban street trees at risk in Canada was estimated to be around $1.384 billion to the year 2035 should no regulation occur (Hope et al., 2020). It should be noted that these estimates in Hope et al. (2020) did not include backyard (private) trees, ash trees in parks and recreational areas, or the social values associated with loss of ash. The economic cost projections in (Kovacs et al., 2010, 2011; Syndor et al., 2011; Hope et al., 2020) do not consider lost ecological services such as urban stormwater capture, CO_2 capture, effects on nutrient cycling, biodiversity loss, forest productivity, and other social losses.

Ecologically, EAB is very destructive to the North American landscape threatening multiple native ash species with functional extirpation, and significantly impacting the species that depend on them. Ash species provide cover and food for several small animal species (Brakie, 2013), many bird species use ash for habitat, food, nesting sites, and roosts (Twedt & Best, 2004), and ash trees provide browse, thermal cover, and protection for a variety of wildlife species (Liu, 2018). Wagner & Todd (2016) reported 21 species of ash-feeding moths which depend on the survival of ash trees. In addition, 43 native arthropod species exclusively use ash for feeding or breeding purposes (Gandhi & Herms, 2010). Ash also plays an important ecological role in many southern Canadian ecosystems as ash is a common riparian species and

its loss will likely impact water quality for both wildlife and humans (Kreutzweiser, 2010). Canopy space opened by the death of ash trees may be occupied over time by invasive plants which will lead to further habitat alteration, species displacement, and the loss of species diversity (Liu, 2018). European buckthorn (*Rhamnus Cathartica*) is an invasive plant species in Winnipeg that may occupy such canopy space, especially in natural areas and riverbanks. The loss of ash due to EAB will likely result in native species diversity that is dependent on ash being reduced or lost (Schrader et al., 2021).

1.4 EAB in Winnipeg

EAB was first detected in Winnipeg in December 2017 (Government of Canada, 2017) and threatens Winnipeg's extensive ash inventory. Based on the City of Winnipeg Public Tree Inventory, there were 85,004 public green ash trees and 8,671 public black ash trees at the time this research was initiated in May 2020 (City of Winnipeg, 2020). Pre-emptive removals of public ash done by the City of Winnipeg as of May 2020 were accounted for in the ash datasets for this study. The combination of green and black ash comprises approximately 30% of all public trees in Winnipeg (K. La France, Pers. Comm., City of Winnipeg Urban Forestry Branch, August 5, 2020). Public trees in these studies refer to those that are located on boulevards and city parks. A private ash inventory was completed by the Urban Forestry Branch in 2017 and at that time, included 240,851 green ash trees and 6,533 black ash trees. It is noted that subsequent plantings and removals of private ash are not captured beyond 2017. Therefore, for the purpose of this project, the total number of green and black ash trees in Winnipeg was estimated to be 341,059 at the time of writing this thesis. There are other ash cultivars in Winnipeg that are known to have various levels of susceptibility to EAB. These species include white ash, Northern treasure ash (*Fraxinus x* 'Northern Treasure'), and Mancana Manchurian ash (*Fraxinus mandshurica* 'Mancana'); however, given that these species account for 1.5% of Winnipeg's public tree inventory and 2.8% of Winnipeg's private ash inventory, the threat that EAB poses to Winnipeg's green and black ash canopy is of more serious concern. The city began planting ash after Dutch elm disease was introduced into Winnipeg's monoculture of American elms in 1975 (K. La France, Pers. Comm., City of Winnipeg Urban Forestry Branch, August 5, 2020). City blocks with older tree plantings tend to be dominated by elm, but areas that were developed post-1975 are dominated by ash (Needoba et al., 2021). Winnipeg's extensive ash inventory combined

with the recent appearance of EAB creates the potential for significant economic and ecological losses.

1.5 Study Objectives

The objectives of this study were to better understand EAB's life cycle in Winnipeg by predicting adult EAB emergence and peak flight activity periods; and to determine ash counts (number of trees), ash densities (trees/ha), and ash hotspots across Winnipeg's neighbourhoods for several ash inventories.

The first objective of better understanding EAB's life cycle is addressed in Chapter 2 by determining when adult EAB emergence and peak flight activity thresholds would have been reached in Winnipeg using weather station data from the past 50 years. We also wanted to determine if climate warming would have a significant impact on the emergence and peak activity periods in Winnipeg and if continued climate warming would make it necessary to update prediction estimates on a regular basis. Prediction of first adult emergence and peak adult activity will allow pest control managers to better plan and execute EAB control initiatives and develop long-term management strategies.

The second objective of determining the potential susceptibility of neighbourhoods to EAB infestation is addressed in Chapter 3, where the effects of ash density (trees/ha), total ash count, and the influence of riverbank corridors in Winnipeg are explored. Currently it is unknown how EAB might spread throughout Winnipeg and the potential corridors that might facilitate beetle movement. It is also relatively unknown how the ash inventory in Winnipeg is dispersed and the differences that tree ownership (public or private) and tree species (green or black) may have on management. Modelling these parameters individually and better understanding potential hotspots and corridors would significantly assist city managers in preparing for EAB infestations.

In Chapter 4, the main points from Chapters 2 and 3 are summarized, and recommendations are made for how management methods can be improved as well as areas for future research.

1.6 Organization

This thesis is organized in four chapters, with the two data chapters (2 and 3) formatted as journal article submissions to enhance the opportunity for graduate student publication upon

completion. Chapter 1 provides background and a general introduction, in Chapter 2 we examine EAB emergence and peak activity patterns based on accumulated growing degree-days, in Chapter 3 we explore potential EAB movement patterns and levels of neighbourhood susceptibility, and Chapter 4 provides an overall interpretation of all the results from the full study concluding in further recommendations for EAB management in Winnipeg. Chapter 2 was published as a journal article prior to the completion of this thesis paper (MacDonald et al., 2022).

1.7 References

Aukema, J. E., Leung, B., Kovacs, K., Chivers, C., Britton, K. O., Englin, J., Frankel, S. J., Haight, R. G., Holmes, T. P., Liebhold, A. M., McCullough, D. G., & von Holle, B. (2011). Economic impacts of Non-Native forest insects in the continental United States. *PLoS ONE*, *6*(9). https://doi.org/10.1371/journal.pone.0024587

Baranchikov, Y., Mozolevskaya, E., Yurchenko, G., & Kenis, M. (2008). Occurrence of the emerald ash borer, Agrilus planipennis in Russia and its potential impact on European forestry. *EPPO Bulletin*, *38*(2), 233–238. https://doi.org/10.1111/j.1365-2338.2008.01210.x

Brakie, M. (2013). *Plant Guide—Green Ash (Fraxinus Pennslyvanica Marsh). USDA – Natural Resources Conservation Service.* https://www.nrcs.usda.gov/Internet/FSE_PLANTMATERIALS/publications/etpmcpg11869.pdf

Canadian Food Inspection Agency. (2021). *Areas regulated for the emerald ash borer*. https://inspection.canada.ca/plant-health/invasive-species/insects/emerald-ash-borer/areas-regulated/eng/1347625322705/1367860339942

Cappaert, D., Mccullough, D. G., Poland, T. M., and Siegert, N. W. (2005). Emerald ash borer in North America: a research and regulatory challenge. *American Entomologist, 51*, 152–165. https://doi.org/10.1093/ae/51.3.152

Cipollini, D., & Peterson, D. L. (2018). The potential for host switching via ecological fitting in the emerald ash borer - host plant system. *Oecologia*, *187*, 507–519. https://doi.org/10.1007/s00442-018-4089-3

City of Edmonton. (2012). *Urban Forest Management Plan*. https://www.edmonton.ca/public-files/assets/document?path=PDF/Urban_Forest_Management_Plan.pdf

City of Ottawa. (2017). *Putting Down Roots for the Future—Urban Forest Management Plan: 2018-2037*. Urban Forest Innovations, INC, Beacon Environmental LTD, Kenney, W.A. https://documents.ottawa.ca/sites/documents/files/final_ufmp_en.pdf

City of Regina. (2022). *Emerald Ash Borer*. https://www.regina.ca/home-property/tree-yard/pests-wildlife/emerald-ash-borer/

City of Winnipeg. (2020). *City of Winnipeg Open Data Services*. https://data.winnipeg.ca/Parks/Tree-Inventory/hfwk-jp4h

Crook, D. J., & Mastro, V. C. (2010). Chemical ecology of the emerald ash borer agrilus planipennis. *Journal of Chemical Ecology*, *36*(1), 101–112. https://doi.org/10.1007/s10886-009-9738-x

Davey Resource Group. (2011). *Urban Forest Management Plan—City of Thunder Bay, Ontario*. https://www.thunderbay.ca/en/city-hall/resources/Documents/Urban-Forest-Management-Plan.pdf

Flower, C. E., Knight, K. S., & Gonzalez-Meler, M. A. (2013). Impacts of the emerald ash borer (Agrilus planipennis Fairmaire) induced ash (Fraxinus spp.) mortality on forest carbon cycling and successional dynamics in the eastern United States. *Biological Invasions*, *15*, 931–944. https://doi.org/10.1007/s10530-012-0341-7

Gandhi, K. J. K., & Herms, D. A. (2010). North American arthropods at risk due to widespread Fraxinus mortality caused by the alien Emerald ash borer. *Biological Invasions*, *12*(6), 1839–1846. https://doi.org/10.1007/s10530-009-9594-1

Government of Canada. (2017). *Emerald ash borer confirmed in Winnipeg*. https://www.canada.ca/en/food-inspection-agency/news/2017/12/emerald_ash_borerconfirmedinwinnipeg.html

Government of Canada. (2018). *Black Ash (Fraxinus nigra): COSEWIC assessment and status report 2018*. https://www.canada.ca/en/environment-climate-change/services/species-risk-public-registry/cosewic-assessments-status-reports/black-ash-2018.html

Government of Canada. (2021). *Emerald ash borer*. https://www.nrcan.gc.ca/our-natural-resources/forests/wildland-fires-insects-disturbances/top-forest-insects-and-diseases-canada/emerald-ash-borer/13377

Granger, J. J., Zobel, J. M., & Buckley, D. S. (2020). *Differential Impacts of Emerald Ash Borer (Agrilus planipennis Fairmare) on Forest Communities Containing Native Ash (Fraxinus spp.) Species in Eastern North America*, *66*(1), 38–48. https://doi.org/10.1093/forsci/fxz063

Haack, R., Jendek, E., Liu, H., Marchant, K., Petrice, T. R., Poland, T. M., et al. (2002). The emerald ash borer: a new exotic pest in North America. *Journal of Chemical Information and Modelling,* 47, 1–5. https://www.fs.usda.gov/treesearch/pubs/11858

Haavik, L. (2016). *How Fast Does Emerald Ash Borer Kill Trees in Our Forests?* https://entomologytoday.org/2016/12/09/how-fast-does-emerald-ash-borer-kill-trees-in-our-forests/

Herms, D., & McCullough, D. (2014). Emerald Ash Borer Invasion of North America: History, Biology, Ecology, Impacts, and Management. *Annual Review of Entomology*, *59*, 13–30. https://doi.org/10.1146/annurev-ento-011613-162051

Hope, E., Sun, L., McKenny, D., Bogdanski, B., Pedlar, J., Macaulay, L., MacDonald, H., & Lawrence, K. (2020). Emerald Ash Borer, Agrilus planipennis: An Economic Analysis of Regulations in Canada. *Natural Resources Canada - Canadian Forest Service*. https://publications.gc.ca/collections/collection_2020/rncan-nrcan/Fo143-2-454-eng.pdf

IUCN. (2021). *The IUCN Red List of Threatened Species*. IUCN Red List of Threatened Species. https://www.iucnredlist.org/en

Klooster, W. S., Gandhi, K. J. K., Long, L. C., Perry, K. I., Rice, K. B., & Herms, D. A. (2018). Ecological impacts of emerald ash borer in forests at the epicenter of the invasion in North America. *Forests*, *9*(5). https://doi.org/10.3390/f9050250

Klooster, W. S., Herms, D. A., Knight, K. S., Herms, C. P., McCullough, D. G., Smith, A., Gandhi, K. J. K., & Cardina, J. (2014). Ash (Fraxinus spp.) mortality, regeneration, and seed bank dynamics in mixed hardwood forests following invasion by emerald ash borer (Agrilus planipennis). *Biological Invasions*, *16*, 859–873. https://doi.org/10.1007/s10530-013-0543-7

Knight, K. S., Brown, J. P., & Long, R. P. (2013). Factors affecting the survival of ash (Fraxinus spp.) trees infested by emerald ash borer (Agrilus planipennis). *Biological Invasions*, *15*(2), 371–383. https://doi.org/10.1007/s10530-012-0292-z

Kovacs, K. F., Haight, R. G., McCullough, D. G., Mercader, R. J., Siegert, N. W., & Liebhold, A. M. (2010). Cost of potential emerald ash borer damage in U.S. communities, 2009-2019. *Ecological Economics*, *69*(3), 569–578. https://doi.org/10.1016/j.ecolecon.2009.09.004

Kovacs, K. F., Mercader, R. J., Haight, R. G., Siegert, N. W., McCullough, D. G., & Liebhold, A. M. (2011). The influence of satellite populations of emerald ash borer on projected economic costs in U.S. communities, 2010–2020. *Journal of Environmental Management*, *92*(9), 2170–2181. https://doi.org/10.1016/j.jenvman.2011.03.043

Kreutzweiser, D. (2010). “Ecological implications of emerald ash borer infestations and management”, in *Workshop Proceedings: Guiding Principles for Managing the Emerald Ash Borer in Urban Environments,* eds D.B. Lyons and T.A. Scarr (Natural Resources Canada and Ontario Ministry of Natural Resources), 18-21. https://d1ied5g1xfgpx8.cloudfront.net/pdfs/32017.pdf

Liu, H. (2018). Under Siege: Ash management in the wake of the emerald ash borer. *Journal of Integrated Pest Management*, *9*(1). https://doi.org/10.1093/jipm/pmx029

Liu, H., Bauer, L. S., Gao, R., Zhao, T., Petrice, T. R., & Haack, R. A. (2003). Exploratory survey for the emerald ash borer, Agrilus planipennis (Coleoptera: Buprestidae), and its natural enemies in China. *Great Lakes Entomologist*, *36*(2). https://scholar.valpo.edu/tgle/vol36/iss2/11/

MacDonald, B., Baydack, R., Westwood, A.R., & Walker, D. (2022). Predicting Emerald Ash Borer Adult Emergence and Peak Flight Activity in Winnipeg, Manitoba, Canada. *Frontiers in Ecology and Evolution, 10:846144*. https://doi.org/10.3389/fevo.2022.846144

McCullough, D. G. (2020). Challenges, tactics and integrated management of emerald ash borer in North America. *Forestry*, *93*(2), 197–211. https://doi.org/10.1093/forestry/cpz049

McCullough, D. G., & Mercader, R. J. (2012). Evaluation of potential strategies to SLow Ash Mortality (SLAM) caused by emerald ash borer (Agrilus planipennis): SLAM in an urban forest. *International Journal of Pest Management*, *58*(1), 9–23. https://doi.org/10.1080/09670874.2011.637138

McCullough, D. G., Poland, T., & Cappaert, D. (2009b). Attraction of the emerald ash borer to ash trees stressed by girdling, herbicide treatment, or wounding. *Canadian Journal of Forest Research*, *39*(7), 1331–1345. https://doi.org/10.1139/X09-057

McCullough, D. G., Poland, T. M., Anulewicz, A. C., & Cappaert, D. (2009a). Emerald Ash Borer (Coleoptera: Buprestidae) Attraction to Stressed or Baited Ash Trees. *Environmental Entomology*, *38*(6), 1668–1679. https://doi.org/10.1603/022.038.0620

McKenny, D., Pedlar, J., Yemshanov, D., Lyons, D. B., Campbell, K., & Lawrence, K. (2012). Estimates of the Potential Cost of Emerald Ash Borer (Agrilus planipennis Fairmaire) in

Canadian Municipalities. *Arboriculture & Urban Forestry*, *38*(3), 81–91. https://cfs.nrcan.gc.ca/publications?id=33763

Morin, R.S., Liebhold, A.M., Pugh, S.A., & Crocker, S.J. (2017). Regional assessment of emerald ash borer, *Agrilus planipennis*, impacts in forests of the Eastern United States. *Biological Invasions, 19,* 703-711. http://doi.org/10.1007/s10530-016-1296-x

Needoba, A., Lefrancois, C., Shields, M., Bellis, E., MacDonald, M., Shah, T., & Williams, D. (2021). Winnipeg Comprehensive Urban Forest Strategy – State of the Urban Forest. *Diamond Head Consulting Ltd.* https://wfpquantum.s3.amazonaws.com/pdf/2021/63937_State%20of%20the%20Urban%20Forest%20April%202021.pdf

Poland, T. M., Chen, Y., Koch, J., & Pureswaran, D. (2015). Review of the emerald ash borer (Coleoptera: Buprestidae), life history, mating behaviours, host plant selection, and host resistance. *Canadian Entomologist*, *147*(3), 252–262. https://doi.org/10.4039/tce.2015.4

Poland, T. M., & McCullough, D. G. (2006). Emerald ash borer: Invasion of the urban forest and the threat to North America's ash resource. *Journal of Forestry*, *104*(3), 118–124. https://doi.org/10.1093/jof/104.3.118

Sadof, C. S., Hughes, G. P., Witte, A. R., Peterson, D. J., & Ginzel, M. D. (2017). Tools for staging and managing emerald ash borer in the urban forest. *Arboriculture & Urban Forestry*, *43*(1), 15–26. http://www.emeraldashborer.info/pdf/Sadof2017.pdf

Schrader, G., Baker, R., Baranchikov, Y., Dumouchel, L., Knight, K. S., McCullough, D. G., Orlova-Bienkowskaja, M. J., Pasquali, S., & Gilioli, G. (2021). How does the Emerald Ash Borer (Agrilus planipennis) affect ecosystem services and biodiversity components in invaded areas? *EPPO Bulletin*, *51*(1), 216–228. https://doi.org/10.1111/epp.12734

Siegert, N. W., Mccullough, D. G., Liebhold, A. M., & Telewski, F. W. (2014). Dendrochronological reconstruction of the epicentre and early spread of emerald ash borer in North America. *Diversity and Distributions*, *20*(7), 847–858. https://doi.org/10.1111/ddi.12212

Steiner, K. C., Graboski, L. E., Knight, K. S., Koch, J. L., & Mason, M. E. (2019). Genetic, spatial, and temporal aspects of decline and mortality in a Fraxinus provenance test following invasion by the emerald ash borer. *Biological Invasions*, *21*, 3439–3450. https://doi.org/10.1007/s10530-019-02059-w

Sydnor, D., Bumgardner, M., & Subburayalu, S. (2011). Community Ash Densities and Economic Impact Potential of Emerald Ash Borer (Agrilus planipennis) in Four Midwestern States. *Arboriculture & Urban Forestry*, *37*(2), 84–89. https://www.nrs.fs.fed.us/pubs/37642

Twedt, D. J., & Best, C. (2004). Restoration of floodplain forests for the conservation of migratory landbirds. *Ecological Restoration*, *22*(3), 194–203. https://doi.org/10.3368/er.22.3.194

USDA (2021). *Emerald Ash Borer. USDA – Animal and Plant Health Inspection Service.* https://www.aphis.usda.gov/aphis/ourfocus/planthealth/plant-pest-and-disease-programs/pests-and-diseases/emerald-ash-borer

Valenta, V., Moser, D., Kapeller, S., & Essl, F. (2017). A new forest pest in Europe: A review of Emerald ash borer (Agrilus planipennis) invasion. *Journal of Applied Entomology*, *141*(7), 507–526. https://doi.org/10.1111/jen.12369

Villari, C., Herms, D. A., Whitehill, J. G. A., Cipollini, D., & Bonello, P. (2016). Progress and gaps in understanding mechanisms of ash tree resistance to emerald ash borer, a model for wood-boring insects that kill angiosperms. *New Phytologist*, *209*(1), 63–79. https://doi.org/10.1111/nph.13604

Wagner, D., and Todd, K. (2016). New ecological assessment for the emerald ash borer: a cautionary tale about unvetted host-plant literature. *American. Entomologist, 62*, 26–35. https://doi.org/10.1093/ae/tmw005

Wang, X., Yang, Z.-Q., Gould, J. R., Zhang, Y.-N., Liu, G.-J., & Liu, E. (2010). The Biology and Ecology of the Emerald Ash Borer, Agrilus planipennis , in China. *Journal of Insect Science*, *10*(128), 1–23. https://doi.org/10.1673/031.010.12801

Whitehill, J.G., Opiyo, S.O., Koch, J.L., Herms, D.A., Cipollini, D.F., & Bonello, P. (2012). Interspecific comparison of constitutive ash phloem phenolic chemistry reveals compounds unique to manchurian ash, a species resistant to emerald ash borer. *Journal of Chemical Ecology, 38(5),* 499-511. https://doi.org/10.1007/s10886-012-0125-7

Whitehill, J.G., Popova-Butler, A., Green-Church, K., Koch, J.L., Herms, D.A., & Bonello, P. (2011). Interspecific Proteomic Comparisons Reveal Ash Phloem Genes Potentially

Involved in Constitutive Resistance to the Emerald Ash Borer. *PLoS One, 6(9),* e24863. http://doi.org/10.1371/journal.pone.0024863

Chapter 2: Predicting emerald ash borer adult emergence and peak flight activity in Winnipeg, Manitoba, Canada

2.1 Introduction

The calculation of degree-day accumulations is often used to predict the timing of insect development stages and can be used to predict adult emergence dates of insects (Dearborn & Westwood, 2014). Degree-day calculations have been widely used to increase the precision of insecticide applications, and to improve integrated pest management techniques for both invasive and endemic insect pests (Baek et al., 2008; Dearborn & Westwood, 2014; Mironidis et al., 2010; Thöming & Saucke, 2011). The prediction of some or all of an insect's development using a degree-day model requires determination of the lower development threshold temperature for that species (Dearborn & Westwood, 2014). The lower development threshold temperature (LTT) is the temperature point at which an immature insect undergoes development and below which no development occurs. Thus, once the immature insect either begins or resumes development above the LTT, it begins accumulating degree-days. The LTT may vary within an individual species and across various life stages; however, a single threshold temperature has often been used for several larval instars, or several different developmental stages of the same species (O'Neal et al., 2011; Son et al., 2012). On the other hand, upper development threshold temperatures (UTT) are the point at which development slows due to excessive heat (O'Neal et al., 2011; Son et al., 2012).

Once the LTT and UTT have been determined, several methods are available to calculate degree-days. Most methods of calculation are based on the assumption that the relationship between insect development rate and temperature is linear (Johansen, 1997; University of California, 2016). In reality, the relationship between these two variables is usually nonlinear, especially near the upper and lower developmental thresholds (Régnière et al., 2012; Son et al., 2012). Sine models generally better reflect the growth rates for insects as development may be more non-linear close to the upper and lower developmental thresholds (Murray, 2008; Herms, 2004). However, linear degree-day models have been demonstrated to work well enough for practical purposes, such as timing of insect life stages for pest control (Johansen, 1997; O'Neal et al., 2011; University of California, 2016). A simple, but widely used method, involves taking the average daily temperature and subtracting the LTT of the specific development stage(s) of the

species under study [(max daily temp + min daily temp)/2 – LTT]. This is called the standard model (Dearborn & Westwood, 2014). A more complex model fits the daily maximum and minimum temperatures to a sine wave and then calculates the area of the curve above the LTT, represented by a horizontal line, for each day of the insect's development. This can be done using the single sine or double sine method. The single sine method only considers the LTT and does not have a vertical cut-off whereas the double sine method considers both the LTT and a vertical cut-off. The vertical cut-off assumes that no development occurs above the UTT. Other cut-off methods include the horizontal cut-off which assumes development continues at a constant rate at temperatures above the UTT and the intermediate cut-off which assumes development slows, but does not stop, at temperatures above the UTT (University of California, 2016).

Several studies report the threshold temperatures and degree-day requirements for EAB. Adult EAB emergence generally begins in late spring at 230-260 degree-days base=LTT 10°C (DD_{10}) and emergence continues throughout the summer (Cappaert et al., 2005; Gould et al., 2016; Herms et al., 2019; Poland et al., 2011). Herms et al., (2019) used a biofix date (the starting date for degree-day calculations) of January 1 while the other studies did not mention a biofix date. Peak adult flight activity (peak activity) generally occurs in late June or early July at 514–556 degree-days (DD_{10}) and drops off sharply by the end of July at about 833 degree-days (DD_{10}) as the beetles begin to die off and new emergence declines (Brown-Rytlewski & Wilson, 2004; Gould et al., 2016; Herms et al., 2019; McCullough et al., 2009b; Poland et al., 2011). EAB has a one-year or two-year life cycle depending on geographical location and infestation stage (Liu, 2018). In unhealthy trees within the invasive range, nearly all EAB develop within one-year with larvae feeding from mid-summer into autumn during which time they complete four instars before they overwinter as prepupae under the bark (Wang et al., 2010). Although EAB generally has a one-year life cycle, it has been reported that two years may be required to complete development. A longer life cycle may be adaptive in northern locations with cooler climates, when EAB attack densities are low, hosts are vigorous, or when oviposition occurs in late summer (Cappaert et al., 2005; Tluczek et al., 2011; Tussey et al., 2018). In North America, a one-year and two-year larval development cycle can occur in the same location and even on the same trees (McCullough et al., 2009b).

In this study, the objective was to determine when adult EAB emergence and peak activity thresholds would have been reached in Winnipeg using weather station data from the past 50 years. Estimates were developed for a range of days that first adult emergence and peak adult activity would have occurred in Winnipeg based on development data from other jurisdictions. We wanted to determine if climate warming would have a significant impact on the emergence and peak activity periods in Winnipeg and if continued climate warming would make it necessary to update prediction estimates regularly. Prediction of first adult emergence and peak adult activity in Winnipeg will allow pest control managers to better plan and execute EAB control initiatives and develop long-term management strategies. Currently, it is unknown if EAB can complete its life cycle in one year in Winnipeg or if a second year is needed to complete adult development. If EAB requires two years to complete its life cycle, this would have significant implications for management of this species in Winnipeg.

2.2 Methodology

Historic annual temperature records in Winnipeg were analyzed for the previous 50 years (1970-2019) to perform degree-day calculations that predict EAB adult emergence and peak activity using the LTTs and UTTs reported in the literature. This 50-year period was chosen so that potential decadal differences could be examined prior to some of the first reported cases of EAB in Winnipeg, and to determine if there are temperature trends that might influence emergence and peak activity dates predicted by the GDD model outcomes. It is predicted that climate warming will change the emergence and peak activity dates in the future; therefore, determining temperature trends may become increasingly important for effective management. Temperature records from the Environment Canada weather station at the Richardson International Airport on the northwest edge of Winnipeg (49° 54' 21.59" N; -97° 14' 14.40" W) were analyzed for the years 1970-1999 and similar records from the Environment Canada weather station located in central Winnipeg (49° 53' 18" N; 97° 7' 47 W) were analyzed for the years 2000-2019. While the distance between the two weather stations is only 7.1 kilometers; the weather data from the central Winnipeg station was used whenever possible as this location better represents a more developed urban environment and associated temperature conditions in the heart of Winnipeg's urban forest where EAB has been found.

Each temperature dataset consisted of the daily minimum and maximum temperature for every day of the year. There were infrequent gaps in the meteorological record for Winnipeg and in these instances, temperatures from the Steinbach weather station (49.53 °N, 96.69 °W) were used. This station is located 51.5 kilometres from central Winnipeg and 58.5 kilometres from the Richardson International Airport weather stations. For data gaps involving all of the stations in this study, values were interpolated by averaging the temperatures for the days prior and following the missing day. In total over the 50 years used in this study, there were 73 days with missing data (See Supplementary Material). Data for 57 of these days was used from the Steinbach weather station and the remaining 16 days were interpolated using the averaging method described above.

2.2.1 GDD Model Preparation

The double sine, single sine, and standard degree-day models were run for the 50-year study period. The double sine and single sine models were run using the degree-day calculator from the University of California Integrated Pest Management Program http://ipm.ucanr.edu/WEATHER/index.html. This calculator requires that certain parameters be fulfilled to run any model. These parameters include the temperature unit, the LTT, the UTT (optional), the method of calculation (model), and the cutoff method (optional). Degree-days were calculated using the double sine model with a LTT of 10°C (Brown-Rytlewski & Wilson, 2004; Herms et al., 2019; Poland et al., 2011) and a UTT of 37.8°C (Pest Prophet, 2021) with a vertical cut-off. The vertical cut-off assumes that no development occurs above the UTT (37.8°C). Degree-days were calculated using the single sine model with a LTT of 10°C and no UTT. The standard model was also calibrated based on a LTT of 10°C. The Julian date was recorded as well as the calendar date in which the GDD 250 and GDD 550 thresholds occurred in each year and were recorded for each model. The thresholds used in this study were chosen based on results published from jurisdictions closest geographically and climatologically to Winnipeg, including: (Brown-Rytlewski & Wilson, 2004; Cappaert et al., 2005; McCullough et al., 2009a; Poland et al., 2011). For these studies, the observed degree-day range for adult emergence was 230-260 degree-days (DD_{10}) and the range for peak adult activity was 514–556 degree-days (DD_{10}). GDD 250 and GDD 550 were chosen as median threshold values based on mid-range activity ranges provided by these other studies to account for Winnipeg's more northern location. The biofix date selected was January 1.

Six degree-day model combinations were tested (GDD 250 double sine, GDD 550 double sine, GDD 250 single sine, GDD 550 single sine, GDD 250 standard, and GDD 550 standard) with each combination resulting in a degree-day indicator value for either first adult emergence or peak activity. Significance between the decades was tested by expressing adult emergence and peak activity as the number of days from January 1 (Julian date). Years were pooled by decade (1970-1979 – 1970s, 1980-1989 – 1980s, 1990-1999 – 1990s, 2000-2009 – 2000s, and 2010-2019 – 2010s) to determine if the model predictions were significantly different. The decadal breakdown is useful for a general comparison across the study period (50-years) especially for local managers. The blocking of decades also helps reduce the year-to-year variation.

2.2.2 Statistical Analysis

After the creation of the six degree-day model combinations, data for each variable were tested for departure from the normal distribution and Levene's test was used to ensure equality of variances between treatments (Dytham, 2011). An ANOVA test was used to compare degree-day accumulations for first emergence and peak activity between decades and when the ANOVA was significant, a Bonferroni (with correction) post-hoc test was used to test means (Dytham, 2011). Linear regressions were run for each of the six model combinations for the entire 50-year study period for the purpose of determining if there was a difference in threshold dates/trends over time. Prior to all statistical analyses, variables were tested for evidence of non-linearity and equality of variance. All analyses were conducted at the $\alpha < 0.05$ level of significance. All tests were run in SPSS (2017).

2.3 Results

2.3.1 Comparison of differences between degree-day models

Estimated emergence dates for EAB ranged from 23 May to 30 June for the 50-year period across all six model-threshold combinations. For the 1970s, estimated emergence dates ranged from 23 May to 30 June; for the 1980s, estimated emergence dates ranged from 25 May to 30 June; for the 1990s, estimated emergence dates ranged from 31 May to 29 June; for the 2000s, estimated emergence dates ranged from 3 June to 28 June; for the 2010s, estimated emergence dates ranged from 3 June to 22 June.

Mean number of GDD (in Julian date) and standard deviations were calculated for the 50-year period for each of the six model-threshold combinations (Table 2.1) and by decade (Table 2.2). The double sine and single sine models had almost identical results; however, the standard model accrued the most GDD in all combinations tested (Tables 2.1 and 2.2).

Table 2.1. Mean Growing Degree-Days (GDD) using the number of days from January 1 (Julian date) across the three models over the 50-year (1970-2019) period.

Model	First Emergence (GDD 250)		Peak Activity (GDD 550)	
	GDD Mean ± SD	Mean Date	GDD Mean ± SD	Mean Date
Double Sine	164±8.5	June 14	196±8.8	July 16
Single Sine	164±8.5	June 14	197±8.7	July 17
Standard	169±9.1	June 19	201±9.4	July 21

Table 2.2. Mean Growing Degree-Days (GDD) using the number of days from January 1 (Julian date) by decade across the three models. (Bolded data are the lowest values in their respective threshold-model combinations which corresponds to the earliest emergence and peak activity dates).

Model	Decade	First Emergence (GDD 250)		Peak Activity (GDD 550)	
		GDD Mean ± SD	Mean Date	GDD Mean ± SD	Mean Date
Double Sine	1970s	166±11.3	June 16	199±9.1	July 19
Single Sine	1970s	166±11.3	June 16	200±9.0	July 20
Standard	1970s	171±11.7	June 21	205±9.5	July 25
Double Sine	1980s	**161±9.4**	June 11	194±9.9	July 14
Single Sine	1980s	**161±9.5**	June 11	194±9.9	July 14
Standard	1980s	169±11.6	June 19	200±10.7	July 20
Double Sine	1990s	164±6.2	June 14	201±9.4	July 21
Single Sine	1990s	165±6.3	June 15	201±9.4	July 21
Standard	1990s	171±7.4	June 21	206±10.6	July 26
Double Sine	2000s	167±9.4	June 17	197±10.1	July 17
Single Sine	2000s	167±9.4	June 17	197±9.8	July 17
Standard	2000s	170±9.7	June 20	200±10.6	July 20
Double Sine	2010s	**161±6.1**	June 11	**191±5.4**	July 11
Single Sine	2010s	**161±6.0**	June 11	**191±5.6**	July 11
Standard	2010s	**165±5.2**	June 15	**193±5.4**	July 13

2.3.2 Emergence (250 GDD) Results

The ANOVA of emergence degree-days between decades was not significant (GDD 250 double sine $p = 0.479$; GDD 250 single sine $p = 0.488$; GDD 250 standard $p = 0.591$).

The regression analysis of the full study period (50 years) showed for all models that there was no significant increase or decrease in the first emergence dates over the study period (GDD 250 double sine $p = 0.685$; GDD 250 single sine $p = 0.677$; GDD 250 standard $p = 0.282$ (Figure 2.1).

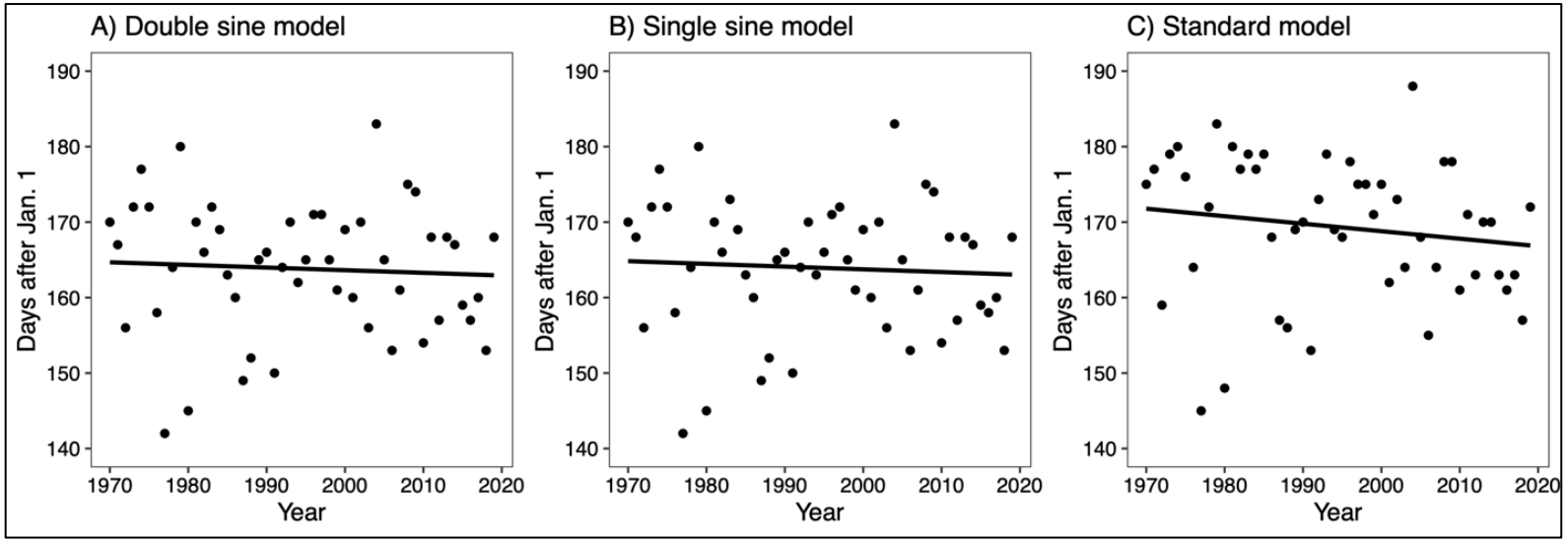

Figure 2.1. Linear regressions for **(A)** the GDD 250 double sine model, **(B)** the GDD 250 single sine model, and **(C)** the GDD 250 standard model. All regressions were not significant (GDD 250 double sine $F = 0.166$, $df = 49$, $p = 0.685$, $R^2 = 0.003$; GDD 250 single sine $F = 0.175$, $df = 49$, $p = 0.677$, $R^2 = 0.004$; GDD 250 standard $F = 1.184$, $df = 49$, $p = 0.282$, $R^2 = 0.024$).

2.3.3 Peak Activity (GDD 550) Results

The ANOVA of peak activity degree-days between decades was significant for the GDD 550 standard model ($p = 0.032$) indicating difference between decades. The other models were not significant (GDD 550 double sine $p = 0.097$; GDD 550 single sine $p = 0.097$). Examination of the peak activity analysis showed that only the GDD 550 standard model accrued significantly more days ($F = 2.90$, $df = 49$, $p = 0.032$, $\eta^2 = 0.205$). Post-hoc tests indicate that these differences are attributable to the 1990-1999 decade in comparison to the 2010-2019 decade (Table 2.3).

Table 2.3. The mean number of days from January 1 (Julian date) and standard deviations for each decade (group) for the GDD 550 standard model predicting adult peak activity. Means with different letters are significantly different $p<0.05$.

Decade	N	Mean Days After Jan 1.	Std. Deviation
1970s	10	205.00[ab]	9.51
1980s	10	200.30[ab]	10.70
1990s	10	206.60[b]	10.56
2000s	10	200.20[ab]	10.59
2010s	10	193.40[a]	5.42
Average	50	201.10	9.36

The regression analysis of the full study period (50 years) showed a significant shift to an earlier date in peak activity for the GDD 550 standard model ($R^2 = 0.114$, $F = 6.16$, $p = 0.017$) (Figure 2.2). The peak activity date for the GDD 550 standard model was July 25 (205±9.5 days after Jan. 1) in 1970-1979, and shifted to July 13 (193±5.4 days after Jan. 1) in 2010-2019. The other models were not significant (GDD 550 double sine $p = 0.09$; GDD 550 single sine $p = 0.095$) (Figure 2.2).

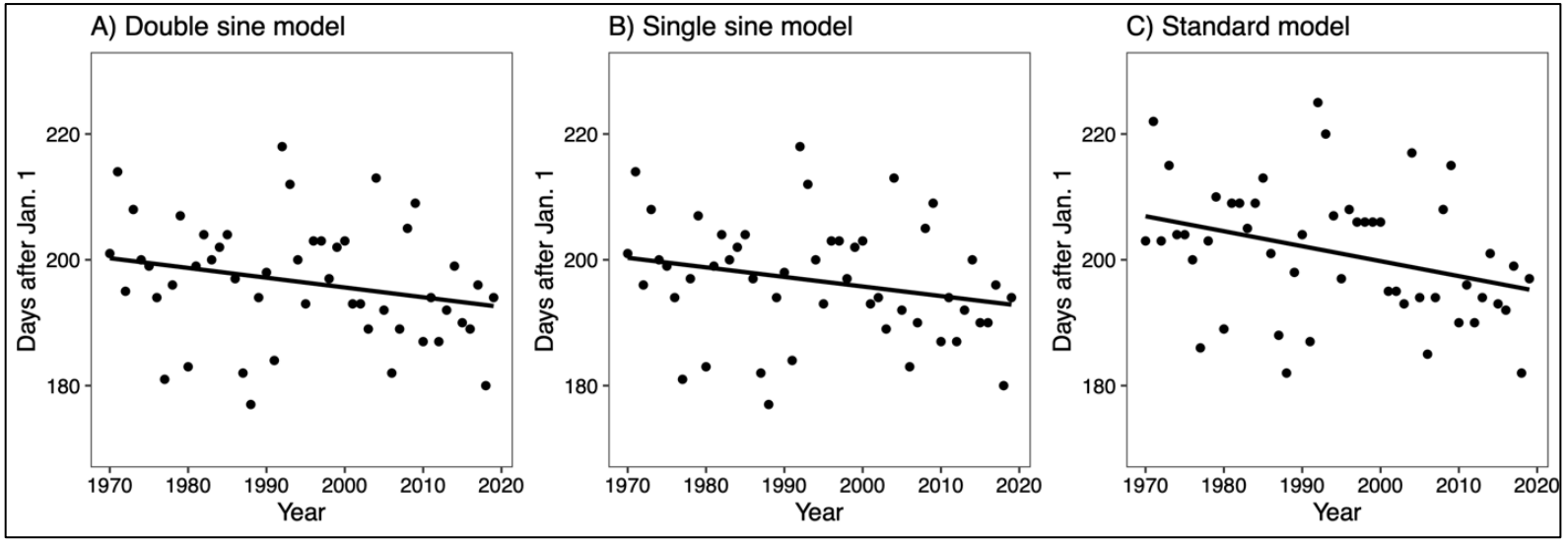

Figure 2.2. Linear regressions for **(A)** the GDD 550 double sine model, **(B)** the GDD 550 single sine model, and **(C)** the GDD 550 standard model. The GDD 550 standard model was significant ($F = 6.158$, $df = 49$, $p = 0.017$, $R^2 = 0.114$), while the other models were not significant (GDD 550 double sine $F = 2.987$, $df = 49$, $p = 0.09$, $R^2 = 0.059$; GDD 550 single sine $F = 2.899$, $df = 49$, $p = 0.095$, $R^2 = 0.057$).

2.4 Discussion

2.4.1 General Discussion

Using degree-day accumulations derived from weather station data to estimate EAB emergence and peak activity will help guide logistical planning for a city wide EAB management program in Winnipeg. It is recommended to use the results from the last decade analyzed (2010-2019) as at least one model showed a significant decline in the date for peak activity by EAB over the 50-year study period. Despite reports of increased temperatures and longer growing seasons in central North America (Cuddington et al., 2018; Liang & Fei, 2014) it appears that climate change that would affect EAB first emergence in the Winnipeg region are not profound enough to produce a significant change in first emergence data in most of the decades in this study. The results from this study did not show any significant changes in emergence dates and did not detect increasing spring temperatures over the 50-year study period. Similarly, a study in eastern Manitoba that examined the effect of climate warming on butterfly phenology using degree-days found that there was no change in spring temperatures, but a significant increase in late summer and fall (Westwood & Blair, 2010). Given this result, first emergence predictions should be based on the most recent decadal data. Management activities that focus on early adult beetle detection (i.e. trap installation) are best initiated prior to the emergence date, which for Winnipeg, is June 11 ± 6.1 days (double sine model), June 11 ± 6.0 days (single sine model), June 15 ±5.2 days (standard model). Management activities that could be implemented prior to the emergence date include setting artificial pheromone traps, branch sampling, and the establishment of trap trees by girdling them. It appears that the effect of climate change on the EAB peak activity range in Winnipeg over the 50-year study period is not consistent as only the GDD 550 standard model showed a significant earlier trend in the peak activity date. Given this result, the peak activity date should be monitored more closely in the future as peak activity dates may continue to trend earlier in the season with warming temperatures depending on the model used. The adult peak activity date could be used to better inform the planning of activities that aim to limit the spread of adult beetles, such as restrictions on ash, wood handling and transport. Management activities that could be implemented with consideration of the peak activity date include conducting visual surveys for the beetles themselves, public outreach, and trap inspections.

Our analysis suggested that climate change in the Winnipeg region would not have significantly impacted the date of first emergence for EAB over the 50 years examined in the study had it been present. When comparing across the five decades, the earliest emergence dates for each model-threshold combination occurred in the 2010 decade. For the GDD 250 double and single sine models, the earliest date of emergence was at 161 Julian days (June 11), which occurred in both the 1980 and 2010 decades. The primary difference in these decades was slightly greater climate variability in the 1980s compared with the 2010s (double sine - std. 9.4 vs 6.1; single sine – std. 9.5 vs 6.0). The GDD 250 standard model's earliest emergence date occurred in the 2010 decade on June 15 (165±5.2).

While there appears to be little change in emergence dates, the analysis suggested that GDD accumulations have been increasing during the summer in the Winnipeg region over time for one of the models. The earliest peak activity dates for each model-threshold combination also occurred in the 2010 decade (GDD 550 double sine model on July 11 191±5.4; GDD 550 single sine model on July 11 191±5.6; GDD 550 standard model on July 13 193±5.4). The GDD 550 standard model was significant showing an earlier peak activity date. Although not significant, the double and single sine models also predict earlier peak activity dates. These findings suggest that summer temperatures have been increasing in the Winnipeg region and peak activity dates are becoming earlier as measured by at least one model. The trends that were observed in Winnipeg over the past 50 years are consistent with climatological data covering summer temperatures in the Winnipeg region (Climate Atlas of Canada, 2019a; Prairie Climate Centre, 2018). Other jurisdictions with confirmed EAB infestations have reported various levels of warming spring and summer temperatures including Detroit Michigan (GLISA, 2017); The Twin Cities, Minnesota (Minnesota Department of Health, 2021; Minnesota Pollution Control Agency, 2021); and London Ontario (Climate Atlas of Canada, 2019b).

The three models allowed us to develop three scenarios for adult emergence and peak activity dates. The models used to predict EAB emergence and peak activity periods in Winnipeg operate with different variables; therefore, comparisons between the models allows for the consideration of different biological factors that would control EAB immature development. However, it is difficult to determine which model is most accurate due to the lack of Winnipeg-specific EAB

data. Further research should determine EAB's GDD thresholds (LTT and UTT) in Winnipeg which would help in resolving which model is more accurate.

Decadal analysis was used to determine if there were differences and trends within a 50-year period that includes the first cases of EAB in Winnipeg. By aggregating over decade periods, interannual variability was reduced. Additionally, given the distinct possibility of a two-year life cycle for EAB in areas with extreme and highly variable climate like Winnipeg, blocking these data over time was appropriate. Evaluation of management prescriptions will similarly need to consider how best to monitor over time considering the potential of a multi-year lag between infection and emergence. While different temporal blocking strategies were not examined in my study, the decadal analysis allowed for comparisons to determine how GDD for those parameters have historically changed in Winnipeg. The GDD 550 standard model showed statistically declining peak emergence dates but not the other models. This decreasing peak activity date is probably indicative of warmer summers. Westwood & Blair (2010) found that for the period 1971-2004, mean monthly temperatures in the autumn and winter increased significantly in southern Manitoba and the butterflies they were studying seemed to be responding to this warming trend over late summer and fall but did not find any changes in spring emergence. In another study, three decades (1982–2008) were analyzed to better understand seasonality shifts in the North American boreal forests (central Manitoba included) and they found that the region has experienced earlier springs especially in the western forests (Buermann et al., 2013). In our study, earlier peak activity date estimates for the GDD 550 standard model was found but emergence date estimates and spring temperatures had no significant change.

Several studies have used GDD and/or air temperatures to predict life cycle timing of other wood-boring insects in North America. Mitton & Ferrenberg (2012) used temperature data from 1970 to 2008 to calculate annual and daily mean air temperatures for each year and degree-days were derived to predict development for the Mountain Pine Beetle (MPB, *Dendroctonus ponderosae*) in Colorado. They found that air temperatures have been increasing in Colorado over the previous two decades, and the flight season for the MPB occurred earlier in the year and was approximately twice as long as the historically reported season (Mitton & Ferrenberg, 2012). This is similar to the results for the GDD 550 standard model in that (peak) flight activity is becoming earlier in the year corresponding with increasing temperatures. Bentz et al. (2013)

tested the influence of air temperature on the timing of adult emergence and flight for MPB in the western United States. They found that MPB life cycle timing is univoltine at warmer sites and a mix of univoltine and semivoltine at cooler sites. Other MPB studies have indicated that MPB populations have evolved local adaptations resulting in genetic differences in development times (Bentz et al., 2011; Bracewell et al., 2013). These studies on MPB suggest that increasing temperatures significantly impact the MPB's life cycle and flight activity, similar to what was found for EAB (GDD 550 standard model).

Kappel et al. (2017) predicted emergence and time to adult maturity for the Asian Longhorned Beetle (ALB; *Anoplophora glabripennis*) by studying the effects of temperature-dependent development and host species abundance throughout the contiguous United States. They found that the southern and eastern US states are at the greatest risk of infestation due to the warmer conditions which promote faster beetle maturation and population growth. Keena & Moore (2010) studied developmental thresholds for ALB by comparing degree-days, larval stages, and constant temperatures in the states of Illinois and New York, USA. The developmental thresholds used in this study were 10°C (LTT) and 30°C (UTT) which are very similar to the thresholds used in our study. They found that temperature had a significant impact on ALB development as the relationship between temperature and development was linear between the LTT and UTT. Such a relationship was not established in our study, but it is recommended that this be considered in future research. Duell et al. (2022) found that the extreme cold tolerance in Winnipeg EAB individuals is most likely due to phenotypic plasticity rather than genetic adaptation which allows the beetle to survive the harsh winter climate.

Poland et al. (2011) related the number of EAB captured (artificial traps) with GDD accumulations for various field sites in Michigan. GDD were calculated with an LTT of 10°C (DD_{10}) in 2006-2008 to make recommendations for operational survey and trap program initiation to predict and manage EAB emergence and peak flight activities. McCullough et al. (2009b) studied how EAB attraction differs between girdled, wounded, or herbicide treated trees in Michigan. Cumulative GDD corresponding to the period of peak EAB activity were generally similar in each year (McCullough et al., 2009b). These studies demonstrated the usefulness of using GDD to predict EAB life cycle activities, and how the results can be used to assist EAB control and management measures.

2.4.2 1 vs 2-year life cycle

The results of this study summarize GDD accumulations in each year and do not consider the possibility of EAB larvae carrying accumulated GDD into a second year of development. Therefore, the results of our study are reflective of a one-year developmental life cycle for EAB in Winnipeg. Currently, it is unknown if EAB has a one or two-year life cycle in southern Manitoba. Given the high level of winter cold tolerance by EAB in Manitoba (Duell et al., 2022), it will be important to determine the life cycle duration of this species in Winnipeg. To determine the probability of a two-year life cycle, detailed sampling of infested trees is required over several years to understand how the immature stages are proportionally distributed within the population which was beyond the scope of my study. The duration of development varies from one to two years according to climatic conditions with most EAB developing in one year in regions with a warmer climate; developing in two years in regions with a colder climate; and in regions with an intermediate climate, a part of the population has a one-year life cycle and another part has a two-year life cycle (Duell et al., 2022; Orlova-Bienkowskaja & Bieńkowski, 2016). Ultimately, the speed of larval development is largely influenced by climate, primarily the duration of the warm period and the amount of heat that larvae receive in one season (Orlova-Bienkowskaja & Bieńkowski, 2016). In the southern part of its native range in China, EAB has a one-year life cycle (Liu et al., 2007) with few larvae taking two years to complete development (Wang et al., 2010). In northern China, EAB's life cycle is almost always two years and larvae overwinter twice (Liu et al., 2007; Wei et al., 2007). In some locations, EAB populations may experience both one and two-year life cycles such as Michigan (Cappaert et al., 2005). However, a two-year cycle also appears to be more common in low-density EAB populations (Herms & McCullough, 2014; Orlova-Bienkowskaja & Bieńkowski, 2016).

Should evidence of a two-year life cycle in Winnipeg be reported, the adult emergence and peak activity dates could differ from the results of this study. Overwintering larvae that require a second year of development will have already accumulated some GDD in their first year of development (Villari et al., 2016; Wang et al., 2010); and it is difficult to extrapolate the analysis to a second year without having local emergence and peak activity measurements to build upon. A two-year life cycle may also have implications on how EAB management is carried out (Tluczek et al., 2011). The management approaches themselves would not change but rather the

timelines for implementation would need to be adjusted as a two-year cycle could result in different emergence and peak activity dates compared to our one-year estimates.

2.4.3 Limitations

Our study estimated GDD in a single calendar year. The analyses and models estimated when the adult emergence and peak activity thresholds occur but did not estimate full life cycle GDD accumulation or within various developmental stages. Further research should concentrate on determining developmental thresholds and life stage GDD accumulations as well as determine life cycle length and possible proportion of the population that may take two years to develop to maturity which was beyond the scope of our study. A potential limitation to this study is it does not consider the impacts of winter minimums on EAB development and how extreme cold temperatures might influence the life cycle of EAB in Winnipeg. EAB has several mechanisms to cope with cold temperatures such as antifreeze agents, cuticular waxes, high concentrations of glycerol, resistance to external ice, and they do not dehydrate from the cold (Duell et al., 2022; Crosthwaite et al., 2011). EAB is a freeze avoidant insect meaning that it is killed by internal ice formation by temperatures around - 30°C (Crosthwaite et al., 2011). A recent study found that complete (99%) mortality of EAB prepupae was predicted for temperatures at or colder than -35.4°C while 75% mortality at - 30.6°C (Cuddington et al., 2018). Additionally, the lowest underbark temperatures recorded for the cities of Grand Rapids and St. Paul, Minnesota were -34°C and -26.3°C, respectively and the overwintering mortality for EAB larvae was 50% for Grand Rapids and 20% for St. Paul (Tussey et al., 2018). EAB is also found in Sault Ste. Marie, Ontario and Thunder Bay, Ontario (Canadian Food Inspection Agency, 2021) where winter minimums have reached below - 30°C (Government of Canada, 2019, 2021). Duell et al. (2022) conclude that increased cold tolerance is sufficient to allow EAB to survive extreme winter events in locations that previous research suggested they could not. However, areas with regular exposure to temperatures below −35°C may allow for the local persistence of native ash stands (Christianson & Venette, 2018). A key question for future research is whether EAB overwintering mortality events are sufficient to reduce the death rates of ash trees. There are other variables that may affect how EAB accumulates GDD in cold climates including snow cover, sun exposure, and underbark microclimate. Snow cover may provide insulation acting as a buffer for larvae (DeSantis et al., 2013); larvae found on the south side of trees will be exposed to more sunlight/heat accruing more GDD (Vermunt et al., 2012); and the underbark

microclimate experiences different temperatures than direct air temperature (Vermunt et al., 2012). These variables were not accounted for in this study and they may impact how EAB accumulates GDD in Winnipeg.

2.5 Conclusion

This study suggested that climate change in the Winnipeg region has not significantly impacted the date of first emergence for EAB; however, it has significantly impacted the date of peak activity (GDD 550 standard model). When comparing across the five decades, the earliest emergence and peak activity dates for each model-threshold combination occurred in the 2010 decade. Climatological data were not directly analyzed in this study to calculate the rate of change in temperatures and thus cannot compare to other published estimates. It is also unknown if the development rate thresholds used (LTT=10°C, UTT=37.8°C) are valid for the study region as these have not yet been verified for Winnipeg. Therefore, it is recommended that the development thresholds be determined for this region as well as further investigations of snow cover, sun exposure, and the underbark microclimate on EAB development in Winnipeg. The results of this study can better inform EAB management programs and decision-makers in Winnipeg and other Canadian cities with a similar climate to Winnipeg. It is recommended that EAB managers in Winnipeg (and areas with a similar climate) consider the results of all three models representing the range of days from (June 11 – June 15 for emergence; July 11 – July 13 for peak activity) when choosing a time to implement EAB control measures based on the temperature data from the 2010 decade. Understanding which areas of the city are most vulnerable to EAB could be considered in conjunction with the life cycle findings from this Chapter to inform management decisions. In Chapter 3, the potential susceptibility of neighbourhoods to EAB infestation across Winnipeg is analyzed by researching the effects of ash density (trees/ha), total ash count, and the influence of riverbanks.

2.6 Contributions of Authors

This Chapter was published as a peer-reviewed journal article; therefore, it is necessary to outline the contributions of each author. BM designed the study, performed statistical analyses, and wrote the manuscript. RB, RW, and DW assisted in conceiving the project and provided advice throughout. All authors contributed to the article and approved the submitted version.

2.7 References

Baek, S., Cho, K., Song, Y. H., & Lee, J. H. (2008). Degree-day based models for forecasting the flight activity of adult Helicoverpa assulta (Lepidoptera: Noctuidae) in hot pepper fields. *International Journal of Pest Management*, *54*(4), 295–300. https://doi.org/10.1080/09670870802203865

Bentz, B. J., Bracewell, R. R., Mock, K. E., & Pfrender, M. E. (2011). Genetic architecture and phenotypic plasticity of thermally-regulated traits in an eruptive species, Dendroctonus ponderosae. *Evolutionary Ecology*, *25*(6), 1269–1288. https://doi.org/10.1007/s10682-011-9474-x

Bracewell, R. R., Pfrender, M. E., Mock, K. E., & Bentz, B. J. (2013). Contrasting Geographic Patterns of Genetic Differentiation in Body Size and Development Time with Reproductive Isolation in Dendroctonus ponderosae (Coleoptera: Curculionidae, Scolytinae). *Annals of the Entomological Society of America*, *106*(3), 385–391. https://doi.org/10.1603/AN12133

Brown-Rytlewski, D., and Wilson, M. (2004). "Tracking the emergence of emerald ash borer adults," in *Emerald Ash Borer Research and Technology Development Meeting*, eds V. Mastro and R. Reardon (USDA – Forest Health Technology Enterprise Team), 13–14. https://www.invasive.org/eab/ eab2004.pdf

Buermann, W., Bikash, P. R., Jung, M., Burn, D. H., & Reichstein, M. (2013). Earlier springs decrease peak summer productivity in North American boreal forests. *Environmental Research Letters*, *8*(2), 024027. https://doi.org/10.1088/1748-9326/8/2/024027

Canadian Food Inspection Agency. (2021). *Areas regulated for the emerald ash borer*. https://inspection.canada.ca/plant-health/invasive-species/insects/emerald-ash-borer/areas-regulated/eng/1347625322705/1367860339942

Cappaert, D., Mccullough, D. G., Poland, T. M., & Siegert, N. W. (2005). Emerald Ash Borer in North America: A Research and Regulatory Challenge. *American Entomologist*, *51*(3), 152–165. https://doi.org/10.1093/ae/51.3.152

Christianson, L., & Venette, R. (2018). Modest Effects of Host on the Cold Hardiness of Emerald Ash Borer. *Forests*, *9*(6), 346. https://doi.org/10.3390/f9060346

Climate Atlas of Canada. (2019b). *Municipality: London*. https://climateatlas.ca/data/city/452/plus30_2030_85/line

Climate Atlas of Canada. (2019a). *Municipality: Winnipeg*. https://climateatlas.ca/data/city/465/plus30_2030_85/line

Crosthwaite, J. C., Sobek, S., Lyons, D. B., Bernards, M. A., & Sinclair, B. J. (2011). The overwintering physiology of the emerald ash borer, Agrilus planipennis Fairmaire (Coleoptera: Buprestidae). *Journal of Insect Physiology*, *51*(1), 166–173. https://doi.org/10.1016/j.jinsphys.2010.11.003

Cuddington, K., Sobek-Swant, S., Crosthwaite, J. C., Lyons, D. B., & Sinclair, B. J. (2018). Probability of emerald ash borer impact for Canadian cities and North America: A mechanistic model. *Biological Invasions*, *20*(9), 2661–2677. https://doi.org/10.1007/s10530-018-1725-0

Dearborn, K., & Westwood, R. (2014). Predicting adult emergence of Dakota skipper and Poweshiek skipperling (Lepidoptera: Hesperiidae) in Canada. *Journal of Insect Conservation*, *18*(5), 875–884. https://doi.org/10.1007/s10841-014-9695-8

Duell, M. E., Gray, M. T., Roe, A. D., MacQuarrie, C. J. K., and Sinclair, B. J. (2022). Plasticity drives extreme cold tolerance of emerald ash borer (*Agrilus planipennis*) during a polar vortex. *Current Research in Insect Science.* 2:100031. https://doi.org/10.1016/j.cris.2022.100031

Dytham, C. (2011). *Choosing and Using Statistics: A Biologist's Guide, 3rd Edn.* Chichester; West Sussex: John Wiley and Sons Inc.

GLISA (2017). *Historical Climatology: Detroit, Michigan. Great Lakes Integrated Sciences and Assessments Team, Michigan.* https://detroitenvironmentaljustice.org/wp-content/uploads/2017/10/2016-Detroit_MI_Climatology-3.pdf

Gould, J. S., Bauer, L. S., Duan, J. J., & Petrice, T. R. (2016). Emerald ash borer biological control release and recovery guidelines. *USDA–APHIS–ARS-FS, Riverdale, Maryland.* http://treesearch.fs.fed.us/pubs/40545

Government of Canada. (2019). *Daily Temperature Data for Sault Ste Marie, Ontario*. https://climate.weather.gc.ca/climate_data/daily_data_e.html?hlyRange=2012-03-20%7C2021-12-29&dlyRange=2012-03-20%7C2021-12-

29&mlyRange=%7C&StationID=50092&Prov=ON&urlExtension=_e.html&searchType=stnName&optLimit=yearRange&StartYear=1840&EndYear=2021&selRowPerPage=25&Line=2&searchMethod=contains&txtStationName=sault+ste+marie&timeframe=2&time=LST&Day=29&Year=2019&Month=1#

Government of Canada. (2021). *Daily Temperature Data for Thunder Bay, Ontario*. https://climate.weather.gc.ca/climate_data/daily_data_e.html?hlyRange=2012-04-12%7C2021-12-29&dlyRange=2018-10-30%7C2021-12-29&mlyRange=%7C&StationID=50132&Prov=ON&urlExtension=_e.html&searchType=stnName&optLimit=yearRange&StartYear=1840&EndYear=2021&selRowPerPage=25&Line=1&searchMethod=contains&txtStationName=thunder+bay&timeframe=2&time=LST&Day=29&Year=2021&Month=2#

Herms, D., (2004). "Using degree-days and plant phenology to predict pest activity," in *IPM (Integrated Pest Management) of Midwest Landscapes*, eds V. Krischik, and J. Davidson (Regents of the University of Minnesota. Minnesota Agricultural Experiment Station Publication SB-07645), 49–59.

Herms, D., & McCullough, D. (2014). Emerald Ash Borer Invasion of North America: History, Biology, Ecology, Impacts, and Management. *Annual Review of Entomology*, *59*, 13–30. https://doi.org/10.1146/annurev-ento-011613-162051

Herms, D., Mccullough, D., Smitley, D., Clifford, C., & Cranshaw, W. (2019). Insecticide Options for Protecting Ash Trees from Emerald Ash Borer Insecticide, 3rd ed. *North Central Center Bulletin*, 1–16. http://www.emeraldashborer.info/documents/Multistate_EAB_Insecticide_Fact_Sheet.pdf

Johansen, N. S. (1997). Influence of temperature on development, fecundity and survival of the cabbage moth Mamestra brassicae (L.) (Lep., Noctuidae) in relation to the improvement of forecasting and control methods. *Journal of Applied Entomology*, *121*(1–5), 81–88. https://doi.org/10.1111/j.1439-0418.1997.tb01375.x

Kappel, A. P., Trotter, R. T., Keena, M. A., Rogan, J., and Williams, C. A. (2017). Mapping of the Asian longhorned beetle's time to maturity and risk to invasion at contiguous United States extent. *Biological Invasions, 19*, 1999–2013. https://doi.org/10.1007/s10530-017-1398-0

Keena, M. A., and Moore, P. M. (2010). Effects of temperature on *Anoplophora glabripennis* (Coleoptera: Cerambycidae) Larvae and Pupae. *Environmental Entomologist, 39*, 1323–1335. https://doi.org/10.1603/EN09369

Liang, L., & Fei, S. (2014). Divergence of the potential invasion range of emerald ash borer and its host distribution in North America under climate change. *Climatic Change*, *122*(4), 735–746. https://doi.org/10.1007/s10584-013-1024-9

Liu, H. (2018). Under Siege: Ash management in the wake of the emerald ash borer. *Journal of Integrated Pest Management*, *9*(1). https://doi.org/10.1093/jipm/pmx029

Liu, H., Bauer, L. S., Miller, D. L., Zhao, T., Gao, R., Song, L., Luan, Q., Jin, R., & Gao, C. (2007). Seasonal abundance of Agrilus planipennis (Coleoptera: Buprestidae) and its natural enemies Oobius agrili (Hymenoptera: Encyrtidae) and Tetrastichus planipennisi (Hymenoptera: Eulophidae) in China. *Biological Control*, *42*(1), 61–71. https://doi.org/10.1016/j.biocontrol.2007.03.011

McCullough, D. G., Poland, T., & Cappaert, D. (2009b). Attraction of the emerald ash borer to ash trees stressed by girdling, herbicide treatment, or wounding. *Canadian Journal of Forest Research*, *39*(7), 1331–1345. https://doi.org/10.1139/X09-057

McCullough, D. G., Poland, T. M., Anulewicz, A. C., & Cappaert, D. (2009a). Emerald Ash Borer (Coleoptera: Buprestidae) Attraction to Stressed or Baited Ash Trees. *Environmental Entomology*, *38*(6), 1668–1679. https://doi.org/10.1603/022.038.0620

Minnesota Department of Health. (2021). *Climate & Health in Minnesota*. https://www.health.state.mn.us/communities/environment/climate/climate101.html

Minnesota Pollution Control Agency. (2021). *Effects of climate change in Minnesota*. https://www.pca.state.mn.us/air/effects-climate-change-minnesota

Mironidis, G. K., Stamopoulos, D. C., & Savopoulou-Soultani, M. (2010). Overwintering Survival and Spring Emergence of Helicoverpa armigera (Lepidoptera: Noctuidae) in Northern Greece. *Environmental Entomology*, *39*(4), 1068–1084. https://doi.org/10.1603/EN09148

Mitton, J. B., & Ferrenberg, S. M. (2012). Mountain Pine Beetle Develops an Unprecedented Summer Generation in Response to Climate Warming. *The American Naturalist*, *179*(5), 163–171. https://doi.org/10.1086/665007

Murray, M. (2008). Using Degree Days to Time Treatments for Insect Pests. Utah State University Extension and Utah Plant Pest Diagnostic Laboratory. https://climate.usu.edu/includes/pestFactSheets/degree-days08.pdf

O'Neal, M. J., Headrick, D. H., Montez, G. H., & Grafton-Cardwell, E. E. (2011). Temperature Thresholds and Degree-Day Model for Marmara gulosa (Lepidoptera: Gracillariidae). *Journal of Economic Entomology*, *104*(4), 1286–1293. https://doi.org/10.1603/EC10438

Orlova-Bienkowskaja, M. J., & Bieńkowski, A. O. (2016). The life cycle of the emerald ash borer Agrilus planipennis in European Russia and comparisons with its life cycles in Asia and North America. *Agricultural and Forest Entomology*, *18*(2), 182–188. https://doi.org/10.1111/afe.12140

Pest Prophet. (2021). *The Complete Guide to Emerald Ash Borer*. ://blog.pestprophet.com/emerald-ash-borers/

Poland, T. M., McCullough, D. G., & Anulewicz, A. C. (2011). Evaluation of Double-Decker Traps for Emerald Ash Borer (Coleoptera: Buprestidae). *Journal of Economic Entomology*, *104*(2), 517–531. https://doi.org/10.1603/EC10254

Prairie Climate Centre (2018). *Custom Climate Change Reports for Your Community: Municipality: Winnipeg. University of Winnipeg.* https://prairieclimatecentre.ca/2018/05/custom-climate-change-reports-for-your-community/

Régnière, J., Powell, J., Bentz, B., & Nealis, V. (2012). Effects of temperature on development, survival and reproduction of insects: Experimental design, data analysis and modeling. *Journal of Insect Physiology*, *58*(5), 634–647. https://doi.org/10.1016/j.jinsphys.2012.01.010

Son, Y., Nadel, H., Baek, S., Johnson, M. W., & Morgan, D. J. W. (2012). Estimation of developmental parameters for adult emergence of Gonatocerus morgani, a novel egg parasitoid of the glassy-winged sharpshooter, and development of a degree-day model. *Biological Control*, *60*(3), 233–240. https://doi.org/10.1016/j.biocontrol.2011.04.008

SPSS (2017). IBM SPSS Statistics for Windows, Version 25.0. IBM Corp. Released 2017. Armonk, NY.

Thöming, G., & Saucke, H. (2011). Key factors affecting the spring emergence of pea moth (Cydia nigricana). *Bulletin of Entomological Research*, *101*(2), 127–133. https://doi.org/10.1017/S0007485309990642

Tluczek, A. R., Mccullough, D. G., & Poland, T. M. (2011). Influence of Host Stress on Emerald Ash Borer (Coleoptera: Buprestidae) Adult Density, Development, and Distribution in Fraxinus pennsylvanica Trees. *Environmental Entomology*, *40*(2), 357–366. https://doi.org/10.1603/EN10219

Tussey, D. A., Aukema, B. H., Charvoz, A. M., & Venette, R. C. (2018). Effects of Adult Feeding and Overwintering Conditions on Energy Reserves and Flight Performance of Emerald Ash Borer (Coleoptera: Buprestidae). *Environmental Entomology*, *47*(3), 755–763. https://doi.org/10.1093/ee/nvy040

University of California. (2016). *About Degree-Days. University of California Agriculture and Natural Resources – Statewide Integrated Pest Management Program.* http://ipm.ucanr.edu/WEATHER/ddconcepts.html

Vermunt, B., Cuddington, K., Sobek-Swant, S., Crosthwaite, J. C., Barry Lyons, D., and Sinclair, B. J. (2012). Temperatures experienced by wood-boring beetles in the under-bark microclimate. *Forest Ecology and Management, 269*, 149–157. https://doi.org/10.1016/j.foreco.2011.12.019

Villari, C., Herms, D. A., Whitehill, J. G. A., Cipollini, D., & Bonello, P. (2016). Progress and gaps in understanding mechanisms of ash tree resistance to emerald ash borer, a model for wood-boring insects that kill angiosperms. *New Phytologist*, *209*(1), 63–79. https://doi.org/10.1111/nph.13604

Wang, X., Yang, Z.-Q., Gould, J. R., Zhang, Y.-N., Liu, G.-J., & Liu, E. (2010). The Biology and Ecology of the Emerald Ash Borer, Agrilus planipennis , in China. *Journal of Insect Science*, *10*(128), 1–23. https://doi.org/10.1673/031.010.12801

Wei, X., Wu, Y., Reardon, R., Sun, T.-H., Lu, M., & Sun, J.-H. (2007). Biology and damage traits of emerald ash borer (Agrilus planipennis Fairmaire) in China. *Insect Science*, *14*(5), 367–373. https://doi.org/10.1111/j.1744-7917.2007.00163.x

Westwood, A. R., and Blair, D. (2010). Effect of regional climate warming on the phenology of butterflies in boreal forests in Manitoba, Canada. *Environmental Entomology, 39*, 1122–1133. https://doi.org/10.1603/EN09143

Chapter 3: Predicting the Potential Spread of Emerald Ash Borer in Winnipeg, Manitoba, Canada using Spatial Models

3.1 Introduction

Dispersal of invasive species is often characterized by stratified dispersal processes including a combination of short and long-distance dispersal events (Liebhold & Tobin, 2008; Shigesada & Kawasaki, 1997). Like many invasive species, the spread of EAB is characterised by both short-distance and long-distance movements (Liebhold & Tobin, 2008; Mercader et al., 2011a, 2012). Long-distance dispersal of EAB is facilitated by human activity, particularly the movement of infested ash material such as firewood (BenDor et al., 2006; Prasad et al., 2010; Siegert et al., 2014; Mercader et al., 2016) resulting in the establishment of localized satellite populations that are geographically disjunct from the original infestation (Mercader et al., 2011a; Shigesada & Kawasaki, 1997). Anthropogenic movement of ash material infested with EAB larvae has resulted in the establishment of new populations hundreds of kilometres beyond the source infestation (Herms & McCullough, 2014). These long-distance dispersal events establish isolated satellite infestations (Siegert et al., 2015) that will eventually combine with each other and the original infestation site (Herms & McCullough, 2014). Short-distance movement primarily reflects natural dispersal through the flight by adult beetles (Cappaert et al., 2005; Herms & McCullough, 2014). Understanding the tendencies of adult EAB spread and dispersal have practical implications for the surveying, monitoring, and management of EAB infestations (Siegert et al., 2015). Quantifying invasive spread and dispersal patterns can provide resource managers with information for designing and implementing management programs (Liebhold & Kean, 2019; Sadof et al., 2017). Predictive models of range expansion can improve the efficacy of detection, delimitation, eradication, and barrier-zone management (Liebhold et al., 2016) while providing insight into underlying drivers of invasion (Ward et al., 2020). Currently, most information regarding EAB spread and dispersal was acquired in the US states and Canadian provinces bordering the Great Lakes (Siegert et al., 2015); therefore, there could be differences between the Winnipeg region and other infestation sites such as climate, host quality, and other variables that may impact EAB dispersal patterns.

Adult EAB are highly capable fliers and can naturally disperse without the aid of people. Estimates from flight mill and laboratory tests showed that mature females were physiologically

capable of flying at least 3km indicating a strong physiological potential for flight (Taylor et al., 2007, 2010). Long-distance movement of EAB is usually addressed only in regional models where pathways of potential spread may be weighted by demographic or anthropogenic factors (Siegert et al., 2015). While long-distance transport of EAB has clearly played a major role in the current EAB distribution in North America, our ability to accurately predict such events is minimal (Prasad et al., 2010). Although EAB adults are capable of flying such distances, field studies have shown that when hosts are readily available, EAB females lay the majority of their eggs within 100m of their emergence point and lay over 90% of their eggs within 500m (Mercader et al., 2009; Siegert et al., 2010). Further to this, Mercader et al. (2009) found that EAB larval densities rapidly declined with distance and that most larvae (88.9-90.3%) were on trees within 100m of the emergence point of the adults at each study site. Field studies indicate EAB dispersal was directed toward areas where ash was relatively abundant within 200m of the origin, but beyond 200m, the abundance of ash had little influence on adult dispersal or host selection (Siegert et al., 2010, 2015). Within 200m of the origin, beetles were most likely to colonize trees growing in areas with abundant ash, but beyond 200m, colonization was not affected by ash abundance (McCullough et al., 2009a; McCullough et al., 2009b; Siegert et al., 2010). Large amounts of ash at longer distances did not lead to a high probability of infestation suggesting that EAB is inclined to colonize nearby trees in areas where ash is abundant (Siegert et al., 2010). A small fraction of larvae; however, have been observed in trees more than 700m from the emergence point of the adults (Mercader et al., 2009; Siegert et al., 2010). This natural dispersal contributes to the spread of established populations, but factors that trigger dispersal and affect the proportion of females that engage in long-distance flights remains unknown (McCullough & Mercader, 2012).

The objective of this chapter is to investigate the distribution of host trees in the City of Winnipeg and determine the susceptibility of neighbourhoods to short distance movements of adult beetles. This was done by 1) examining patterns of host tree densities in neighbourhoods in Winnipeg, 2) determining potential movement corridors, especially along riverbanks, and 3) examining local patterns of spatial autocorrelation. To better understand management implications, patterns were examined based on status and species of host trees. The status of trees was classified as being either public (trees on City owned properties such as boulevards, golf courses, cemeteries, parks, and natural areas) or private (trees on privately owned lots). The

species of tree was classified as being either green (*F. pensylvanica*) or black (*F. nigra*). Neighbourhoods were derived from a census boundary map which designates the area and boundaries of each neighbourhood in Winnipeg (Figure 3.1).

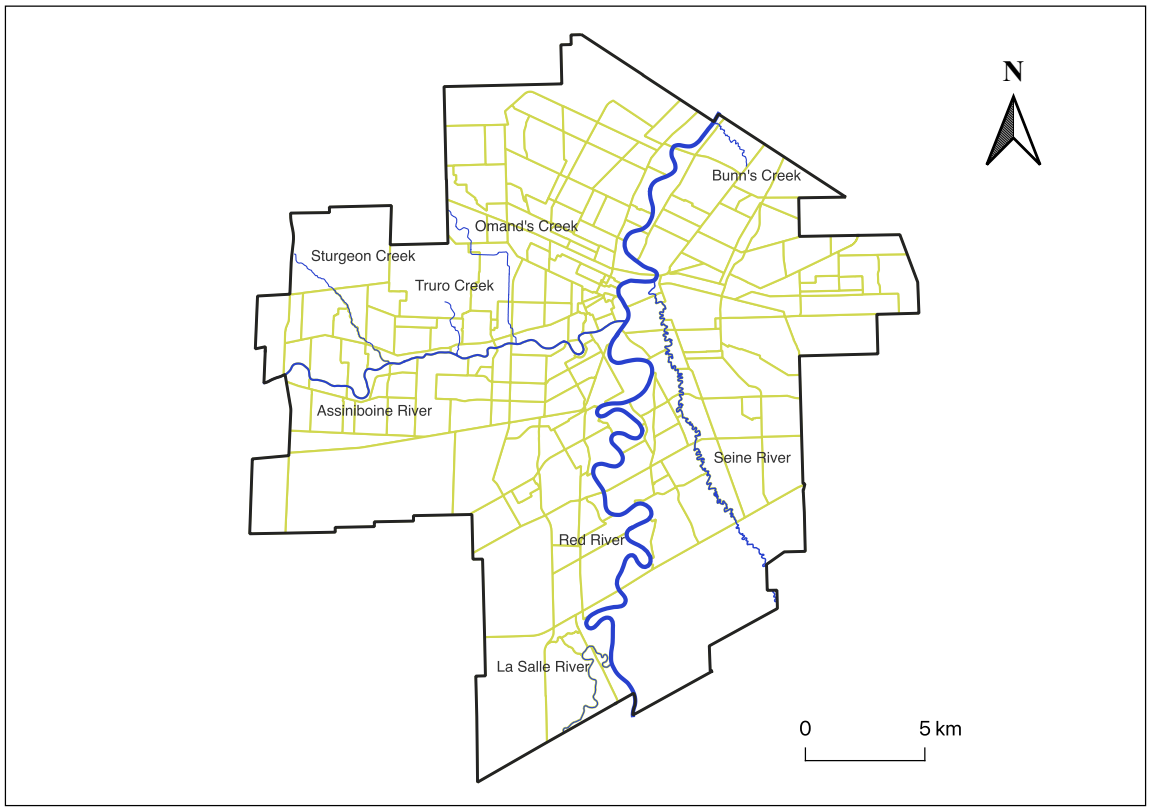

Figure 3.1. Census boundary map showing the polygons of each neighbourhood and river/creek for the City of Winnipeg.

It is relatively unknown how the ash inventory in Winnipeg is dispersed and the differences that tree ownership (public or private) and tree species (green or black) may have on management. Additionally, it is currently unknown how EAB might spread throughout Winnipeg and the potential corridors that might facilitate beetle movement. The models and analyses developed in this Chapter should allow for a better understanding of potential EAB dispersal patterns and neighbourhood-level susceptibility in Winnipeg.

3.2 Methodology

3.2.1 Ash Density Maps

Public and private ash tree inventories as well as a census boundary GIS layer containing the neighbourhoods of Winnipeg were provided by the City of Winnipeg Urban Forestry Branch. Using the public and private ash tree inventories and city neighbourhoods (n= 230 polygons), neighbourhood ash densities were calculated. Nine ash inventories and combinations were examined: green ash on private property (hereafter referred to as 'private'), green ash on public property (hereafter referred to as 'public'), black ash private, black ash public, and combined by species as all green ash, all black ash, and combined by status as all private ash, all public ash, and finally as all ash. For each of these inventories and combinations, the total number of trees were counted for each city neighbourhood using the 'Count Points in Polygon' tool in QGIS (QGIS Development Team, 2022). The area in hectares was also calculated for each neighbourhood, and the counts expressed as density using the QGIS Field Calculator. Ash density maps were created by using the total number of points (trees) and dividing by the area in hectares for each neighbourhood. The symbology of these maps was selected to be graduated and the value that the maps were based on was the number of points per area (trees/ha). This resulted in each polygon (neighbourhood) receiving a density value based on how many trees are within that neighbourhood's total area in hectares. Five categories (very low, low, moderate, high, very high) represented by an appropriate colour ramp was then selected to visualize neighbourhood densities across the city. An equal count (quantile) mode was selected to make comparisons between species-status combinations consistent as each category would have the same number of neighbourhoods (n= 46). All layers and maps used the NAD83/ UTM zone 14N EPSG:26914 coordinate reference system.

3.2.2 Riverbanks

Riverbanks (rivers and creeks) were analyzed to determine the influence they have on ash distribution and densities in Winnipeg. Using the public and private ash tree inventories and a river layer provided by the City of Winnipeg Urban Forestry Department, the proportion of ash located near riverbanks was calculated and hotspot density maps were created. The proportion of ash located near riverbanks was calculated by using the 'Buffer' tool in QGIS. A buffer of 100m (50m on each side) was applied to the river layer which contained eight rivers and creeks in

Winnipeg (Assiniboine River, Bunn's Creek, La Salle River, Omand's Creek, Red River, Seine River, Sturgeon Creek, and Truro Creek). Each river and creek buffer became its own attribute (i.e., Red River Buffer) so that trees located within those buffers could be categorized with that attribute. Additionally, a ninth option was created which was called 'No River' for trees that did not fall within a 100m buffer. Using the 'Join' function in QGIS, the point layer containing all ash trees was spatially joined to the buffer layer so that every tree could be assigned to one of the nine buffer possibilities. For trees that intersected the buffer area of two rivers/creeks, those trees were counted in the larger river/creek's buffer. For example, trees that intersected the buffers of Sturgeon Creek and the Assiniboine River were part of the Assiniboine River's buffer. Trees were always part of the Red River's buffer when two rivers met (Red and Assiniboine, Red and Seine, Red and La Salle). Using the 'GroupStats' plugin on the spatially joined layer, the exact number of trees (along with status and species indicators) located within each buffer was determined.

Hotspot maps were created for the all ash, private ash, and public ash inventories, and then compared to the proximity of riverbanks. The term hotspot refers to areas of the city that have high ash densities. Using the 'Create Grid' vector tool in QGIS, a 50x50 metre grid was created for each of these three inventories using the census boundary layer as the base layer. Then using the 'Join' function, the point layers containing all ash, private ash, and public ash were spatially joined to their respective grid layers. Each cell (n= 188,721) in the grid was configured to display its density (trees/hectare) value. A natural breaks (Jenks) mode was selected to best group similar values together and maximize the difference between classes.

3.2.3 Spatial Autocorrelation

Using the public and private ash tree inventories and city neighbourhoods (n= 230 polygons) provided by the City of Winnipeg Urban Forestry Branch, spatial autocorrelation was tested. Seven ash inventories and combinations were examined: green ash private, green ash public, black ash private, black ash public, and combined by species as all green ash, all black ash, and finally as all ash. For each of these inventories and combinations, the total number of trees were counted for each city neighbourhood using the 'Count Points in Polygon' tool in QGIS. The area in hectares was also calculated for each neighbourhood, and the counts expressed as density

using the QGIS Field Calculator. All spatial analyses were performed on the density per hectare expressed as log+1 as the distributions of observed densities were strongly log-normal.

Spatial analyses including Moran plots and correlograms were run for each of these inventories based on densities in neighbourhood polygons in comparison with their neighbours. Note that because the polygon layer used in this study is a city neighbourhood layer, and in spatial analysis 'neighbourhood' is used to refer to a local collection of (often adjacent) polygons, to avoid confusion the term 'neighbourhood' will only refer to a single polygon (the city neighbourhood), and 'neighbours' will refer to local adjacent polygons. For all analyses, adjacency was defined as a shared edge between neighbourhood polygons and neighbours identified in this way were equally weighted using the package spdep (Bivand & Wong, 2018) in CRAN R (R Core Team, 2022). Adjacencies used in this analysis are provided in Figure 3.2.

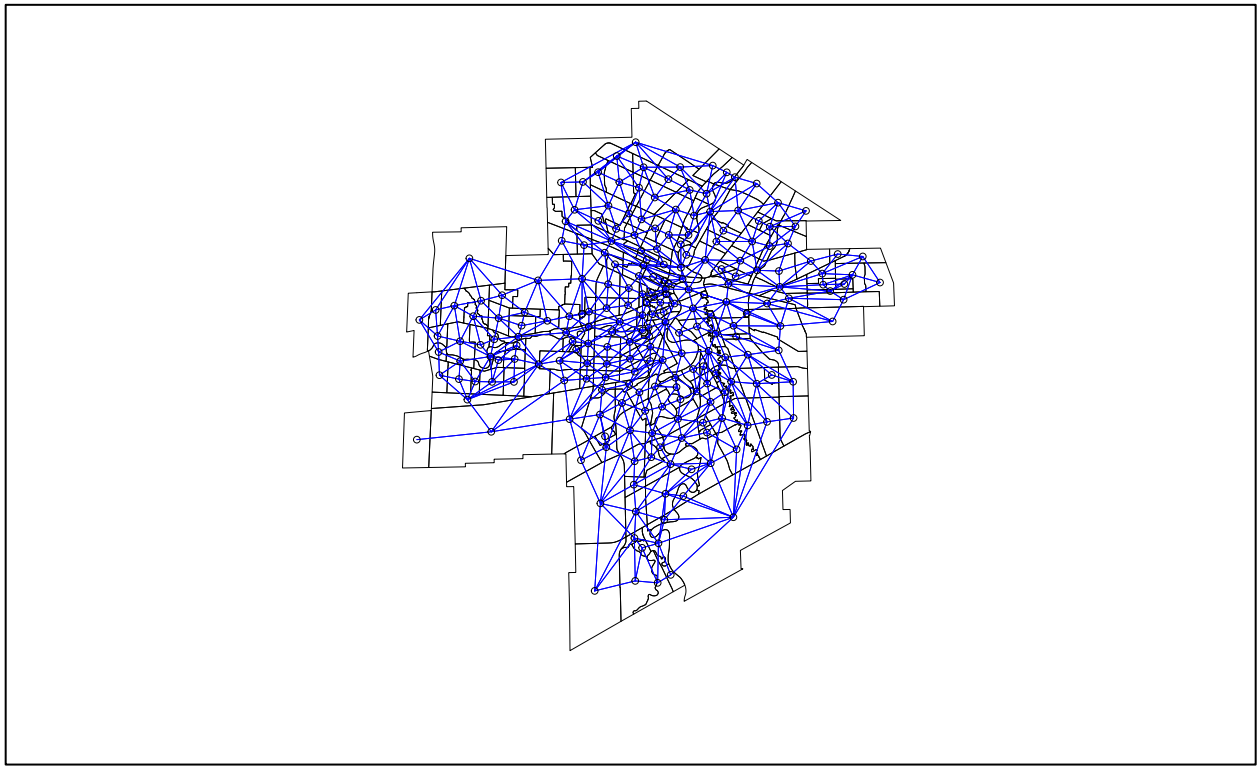

Figure 3.2. The neighbourhoods of Winnipeg represented in ash/hectare being tested for spatial autocorrelation with adjacent neighbours.

Moran plots were constructed from ash densities for each neighbourhood (x-axis), and tested against the spatial lag of its neighbours (y-axis) using the function moran.plot in package spdep in CRAN R. The Moran plot is a LISA-based (local indicators of spatial association) method

(Anselin, 1995) that provides a hot-cold spot analysis and of patterns of spatial autocorrelation. The plot is divided into four quadrants with each quadrant representing different local patterns of autocorrelation, the interpretation of this plot is provided (Figure 3.3).

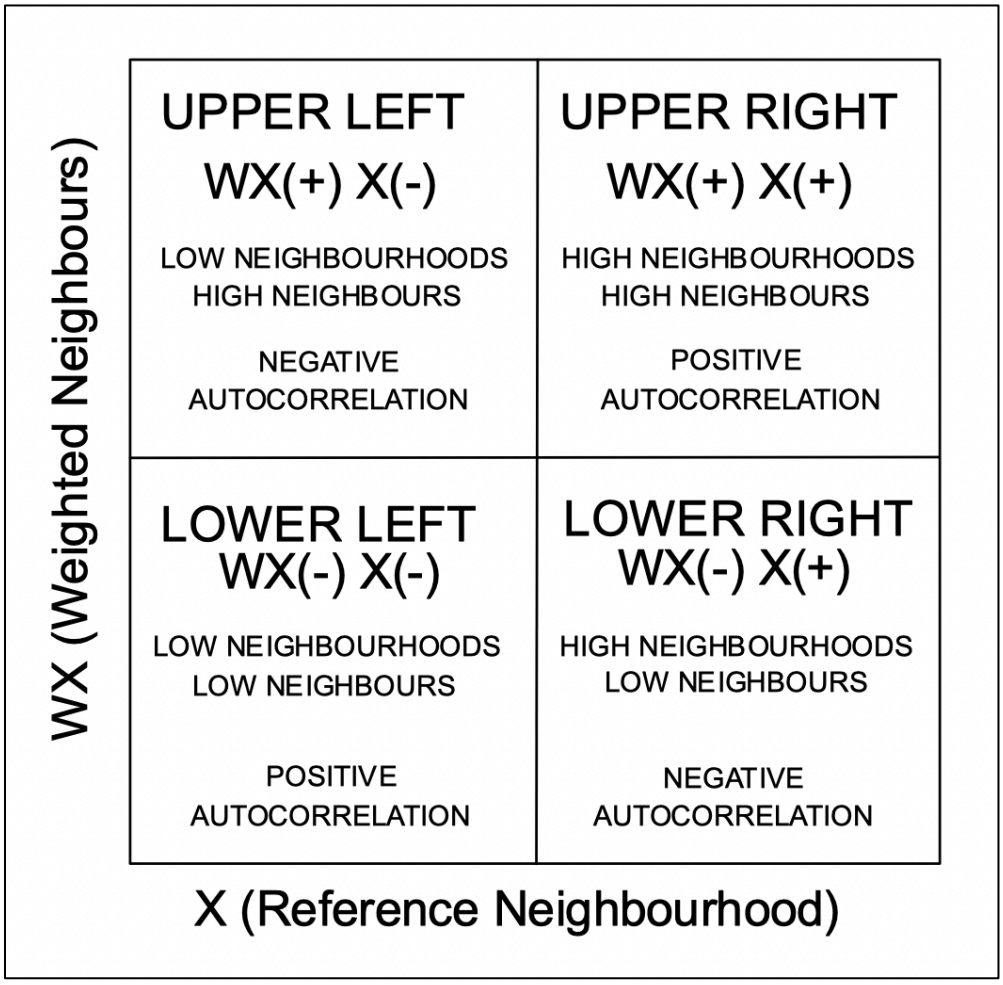

Figure 3.3. The interpretation of a Moran plot illustrating the four quadrants with 'X' referring to ash densities of each neighbourhood and 'WX' referring to the spatial lag of neighbours.

The upper-right quadrant (Q1) contains high ash density neighbourhoods (x) who's neighbours also have high ash densities (wx); the lower-right quadrant (Q2) contains high neighbourhoods (x) and low neighbours (wx); the lower-left quadrant (Q3) contains low neighbourhoods (x) and low neighbours (wx); and the upper-left quadrant (Q4) contains low neighbourhoods (x) and high neighbours (wx). Pearson's product-moment correlation was used to test for association between the paired samples (ash density vs lagged ash density).

Correlograms were constructed to examine patterns of spatial autocorrelation over distance (lag) using Moran's I in the function sp.correlogram in package spdep in CRAN R. For this analysis the maximal lag used was eight.

3.3 Results

3.3.1 Ash Densities

Considering all ash trees (n= 341,059) in Winnipeg, the neighbourhoods with the highest ash densities were Perrault (44.5 ash/ha), Cloutier Drive (42.9 ash/ha), and Royalwood (37.2 ash/ha). Appendix B provides a map and table with the indexed numbers of neighbourhood names for reference. The neighbourhoods containing the highest counts of ash trees were St. Vital Perimeter South (n= 49,389), Royalwood (n= 10,709), and Perrault (n= 8,734). The city-wide all ash density map can be seen in Figure 3.4 and the top ten neighbourhoods in all ash tree count and all ash density in Table 3.1. Ash densities differed by status (public or private) and species (green or black) across the neighbourhoods of Winnipeg. The neighbourhoods with the highest public ash (n= 93,675) densities were Kildonan Park (13.2 ash/ha), Exchange District (10.5 ash/ha), and Manadalay West (10.1 ash/ha). The neighbourhoods containing the highest counts of public trees were River Park South (n= 2,724), Dakota Crossing (n= 2,450), and Tyndall Park (n= 2,369). The neighbourhoods with the highest private ash densities were Perrault (44.4 ash/ha), Cloutier Drive (42.6 ash/ha), and St. Norbert (35.1 ash/ha). The neighbourhoods containing the highest counts of private trees (n= 247,384) were St. Vital Perimeter South (n= 49,299), Royalwood (n= 9,531), and Perrault (n= 8,727). The city-wide density maps of public ash and private ash can be seen in Figures 3.5 and 3.6 respectively. The top ten neighbourhoods in public ash tree count and public ash density can be seen in Table 3.2 and private trees in Table 3.3.

The neighbourhoods with the highest green ash (n= 325,855) densities were Perrault (44.0 ash/ha), Cloutier Drive, (40.1 ash/ha), and Niakwa Park (36.3 ash/ha). The neighbourhoods containing the highest counts of green ash were St. Vital Perimeter South (n= 48,677), Royalwood (n= 10,024), and Perrault (n= 8,642). The neighbourhoods with the highest black ash densities were Royalwood (2.4 ash/ha), Radisson (2.2 ash/ha), and Cloutier Drive (2.2 ash/ha). The neighbourhoods containing the highest counts of black ash (n= 15,204) were Island Lakes (n= 894), St. Vital Perimeter South (n= 712), and Royalwood (n= 685). The city-wide density maps of green ash and black ash can be seen in Figures 3.7 and 3.8 respectively. The top ten neighbourhoods in green ash tree count and green ash density can be seen in Table 3.4 and black ash in Table 3.5.

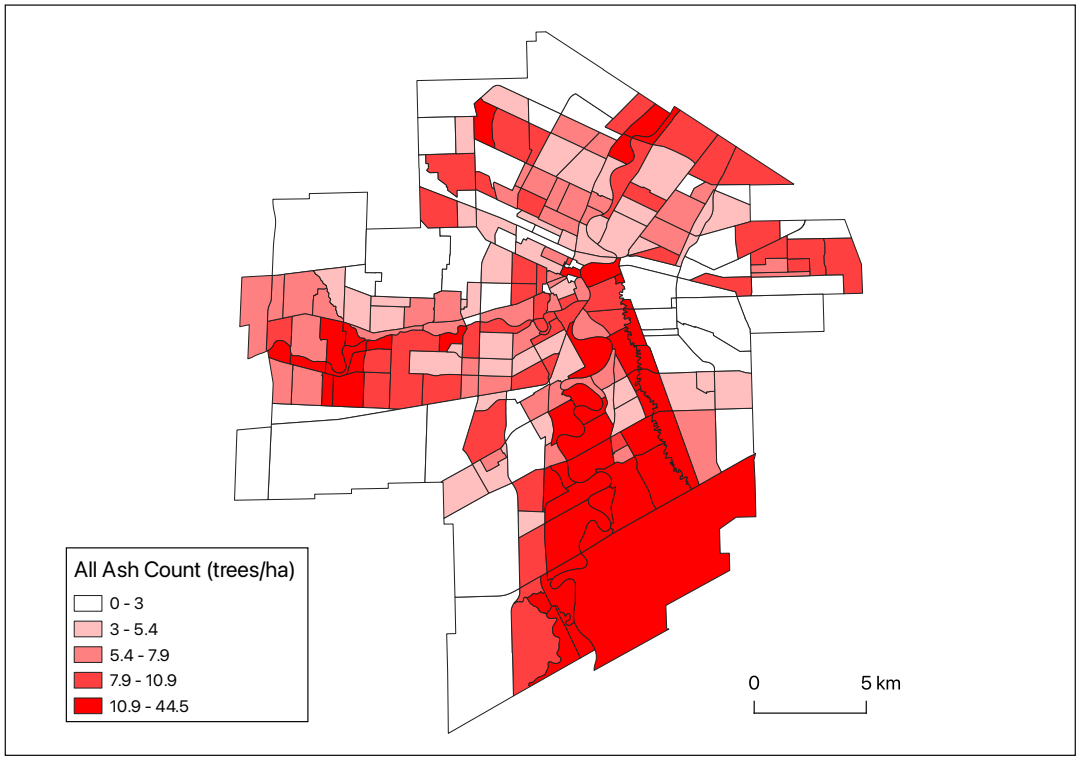

Figure 3.4. The density of the total ash count (trees/hectare) across the neighbourhoods in the City of Winnipeg.

Table 3.1. The top ten neighbourhoods in all ash tree count and all ash density. (Bolded neighbourhoods are found in both lists).

Ash Tree Count			Ash Density (trees/ha)		
Rank	Neighbourhood	Count	Rank	Neighbourhood	Density
1	St. Vital Perimeter South	49,389	1	**Perrault**	44.5
2	**Royalwood**	10,709	2	Cloutier Drive	42.9
3	**Perrault**	8,734	3	**Royalwood**	37.2
4	Fort Richmond	7,939	4	Niakwa Park	36.7
5	**St. Norbert**	6,498	5	**St. Norbert**	35.9
6	River Park South	6,230	6	Archwood	35.5
7	Pulberry	5,802	7	Wildwood	35.3
8	Dakota Crossing	5,605	8	Marlton	31.2
9	Trappistes	5,321	9	Victoria Crescent	30.3
10	**Niakwa Place**	5,003	10	**Niakwa Place**	29.6

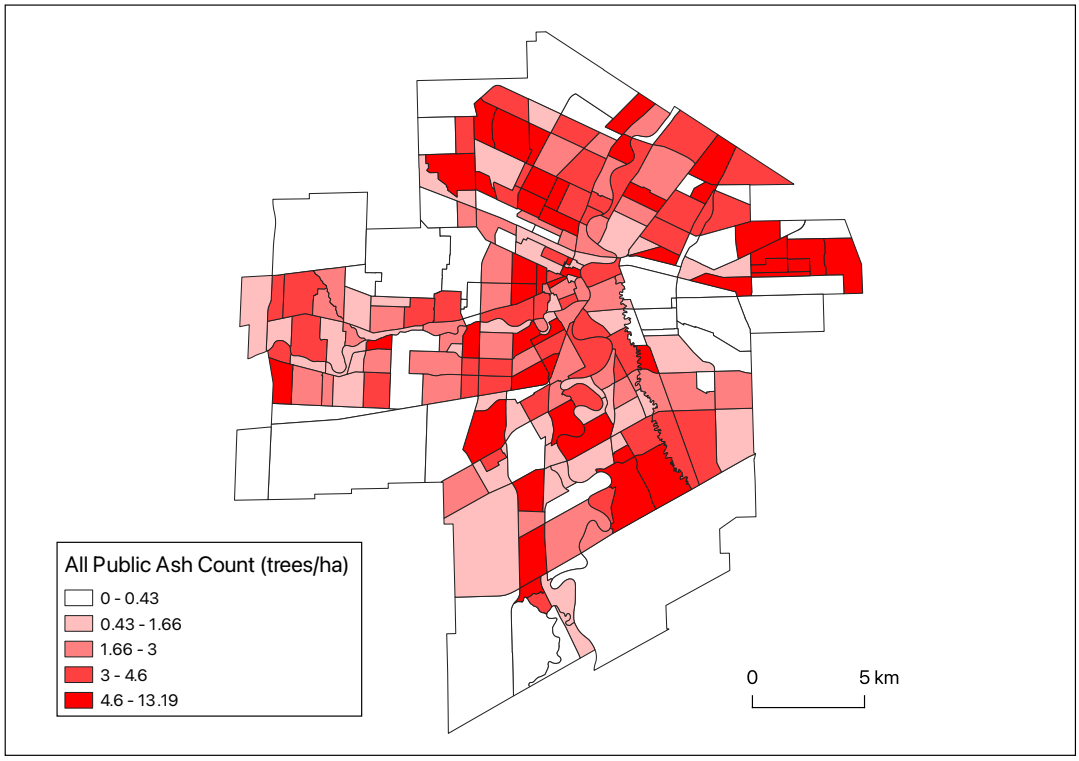

Figure 3.5. The density of the public ash count (trees/hectare) across the neighbourhoods in the City of Winnipeg.

Table 3.2. The top ten neighbourhoods in public ash tree count and public ash density. (Bolded neighbourhoods are found in both lists).

Ash Tree Count			Ash Density (area/ha)		
Rank	Neighbourhood	Public Ash	Rank	Neighbourhood	Density
1	River Park South	2,724	1	Kildonan Park	13.2
2	Dakota Crossing	2,450	2	Exchange District	10.5
3	**Tyndall Park**	2,369	3	Mandalay West	10.1
4	**Richmond West**	2,348	4	East Elmwood	9.1
5	Linden Woods	2,268	5	**Richmond West**	8.8
6	The Maples	2,167	6	Daniel Mcintyre	8.7
7	Canterbury Park	2,027	7	**Kildare-redonda**	8.2
8	Island Lakes	2,015	8	Burrows Central	8.1
9	Meadows	1,747	9	Riverbend	8.0
10	**Kildare-redonda**	1,638	10	**Tyndall Park**	7.9

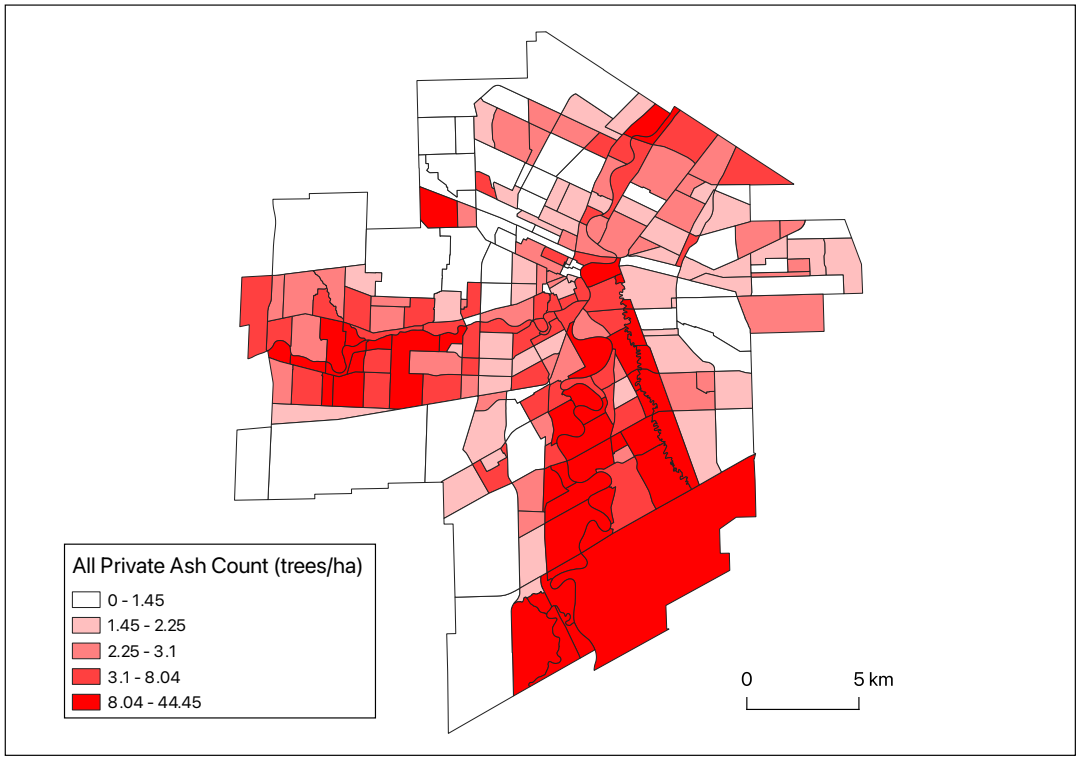

Figure 3.6. The density of the private ash count (trees/hectare) across the neighbourhoods in the City of Winnipeg.

Table 3.3. The top ten neighbourhoods in private ash tree count and private ash density. (Bolded neighbourhoods are found in both lists).

Ash Tree Count			Ash Density (area/ha)		
Rank	Neighbourhood	Private Ash	Rank	Neighbourhood	Density
1	St. Vital Perimeter South	49,299	1	**Perrault**	44.4
2	**Royalwood**	9,531	2	Cloutier Drive	42.6
3	**Perrault**	8,727	3	**St. Norbert**	35.1
4	Fort Richmond	6,558	4	Archwood	35.1
5	**St. Norbert**	6,363	5	**Royalwood**	33.1
6	Trappistes	5,320	6	Niakwa Park	32.1
7	Assiniboine Park	4,914	7	**Wildwood**	31.9
8	**Niakwa Place**	4,679	8	Marlton	29.7
9	Pulberry	4,304	9	Victoria Crescent	28.7
10	**Wildwood**	4,070	10	**Niakwa Place**	27.7

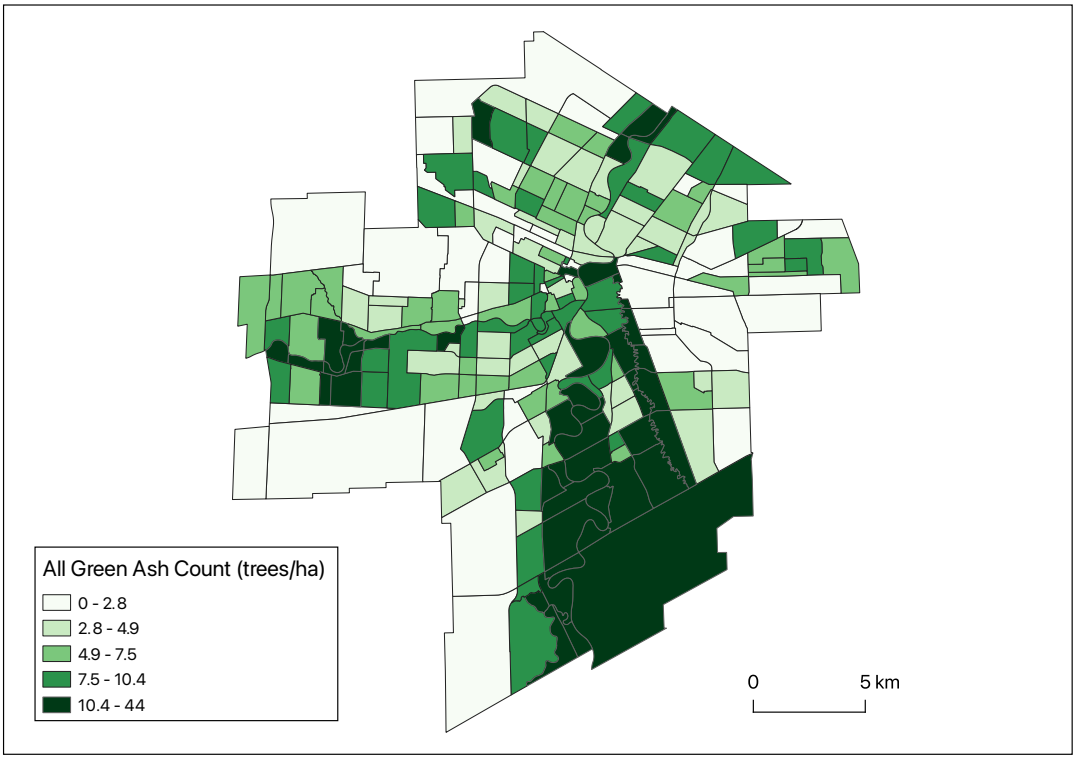

Figure 3.7. The density of the green ash count (trees/hectare) across the neighbourhoods in the City of Winnipeg.

Table 3.4. The top ten neighbourhoods in green ash tree count and green ash density. (Bolded neighbourhoods are found in both lists).

Ash Tree Count			Ash Density (area/ha)		
Rank	Neighbourhood	Green Ash	Rank	Neighbourhood	Density
1	St. Vital Perimeter South	48,677	1	**Perrault**	44.0
2	**Royalwood**	10,024	2	Cloutier Drive	40.1
3	**Perrault**	8,642	3	Niakwa Park	36.3
4	Fort Richmond	7,690	4	**St. Norbert**	34.9
5	**St. Norbert**	6,315	5	**Royalwood**	34.8
6	River Park South	5,907	6	Archwood	34.5
7	Pulberry	5,702	7	Wildwood	34.4
8	Dakota Crossing	5,405	8	Marlton	30.9
9	Trappistes	5,261	9	Victoria Crescent	30.0
10	Assiniboine Park	4,896	10	Niakwa Place	28.9

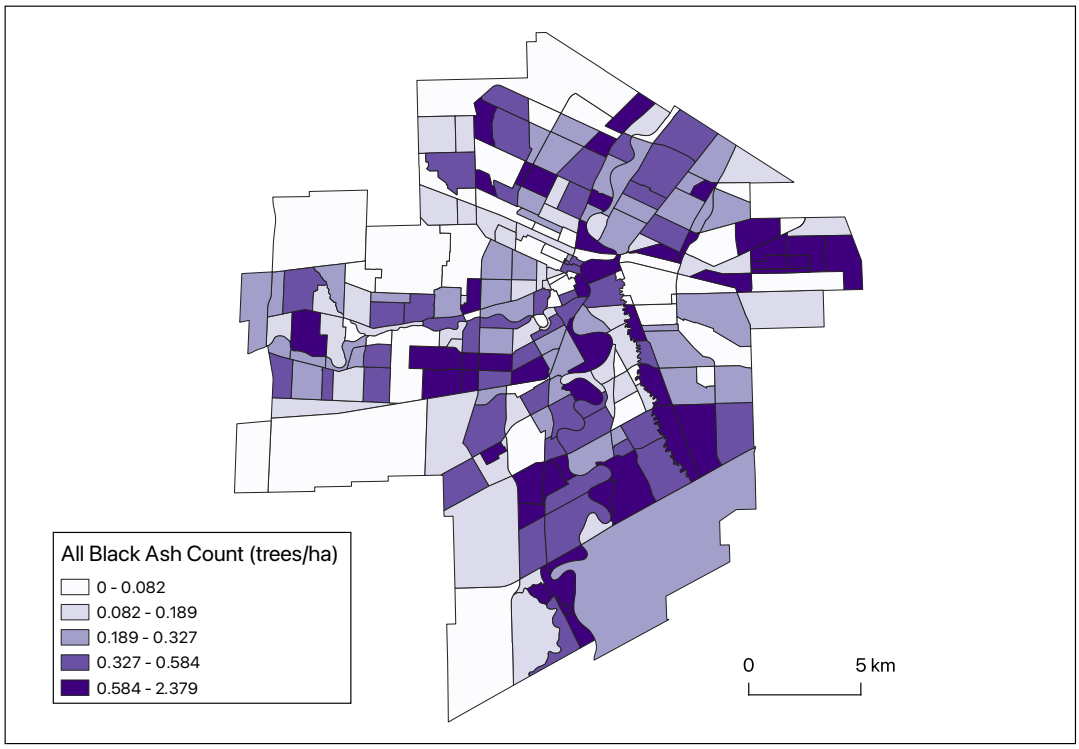

Figure 3.8. The density of the black ash count (trees/hectare) across the neighbourhoods in the City of Winnipeg.

Table 3.5. The top ten neighbourhoods in black ash tree count and black ash density. (Bolded neighbourhoods are found in both lists).

Ash Tree Count			Ash Density (area/ha)		
Rank	Neighbourhood	Black Ash	Rank	Neighbourhood	Density
1	**Island Lakes**	894	1	**Royalwood**	2.4
2	St. Vital Perimeter South	712	2	**Radisson**	2.2
3	**Royalwood**	685	3	Cloutier Drive	2.2
4	**Westwood**	441	4	**Island Lakes**	2.0
5	River Park South	323	5	**Robertson**	1.9
6	Waverley Heights	272	6	Linden Ridge	1.7
7	**Radisson**	265	7	Melrose	1.6
8	Kildare-redonda	258	8	**Westwood**	1,6
9	**Robertson**	256	9	Fairfield Park	1.6
10	Fort Richmond	249	10	East Elmwood	1.5

The various status and species combinations (private green, public green, private black, public black) were analyzed to determine if there were any noticeable differences when compared to the stand-alone results (non-combinations). The neighbourhoods with the highest private green ash (n= 240,851) densities were Perrault (44.0 ash/ha), Cloutier Drive (40.4 ash/ha), and St. Norbert (34.3 ash/ha). The neighbourhoods containing the highest counts of private green ash trees were St. Vital Perimeter South (n= 48,587), Royalwood (n= 9,420), and Perrault (n= 8,642). The neighbourhoods with the highest public green ash densities were Kildonan Park (12.8 ash/ha), Exchange District (10.1 ash/ha), and Mandalay West (8.9 ash/ha). The neighbourhoods containing the highest counts of public green ash trees (n= 85,004) were River Park South (n= 2,567), Dakota Crossing (n= 2,405), and Tyndall Park (n= 2,274). The city-wide density maps of private green ash and public green ash can be seen in Figures 3.9 and 3.11 respectively. The top ten neighbourhoods in private green ash tree count and private green ash density can be seen in Table 3.6 and public green ash in Table 3.8.

The neighbourhoods with the highest private black ash (n= 6,533) densities were Cloutier Drive (2.2 ash/ha), Montcalm (1.1 ash/ha), and Archwood (1.0 ash/ha). The neighbourhoods containing the highest counts of private black ash trees were St. Vital Perimeter South (n= 712), Fort Richmond (n= 216), and Cloutier Drive (n= 179). The neighbourhoods with the highest public black ash densities were Radisson (2.0 ash/ha), Royalwood (2.0 ash/ha), and Robertson (1.8 ash/ha). The neighbourhoods containing the highest counts of public black ash trees (n= 8,671) were Island Lakes (n= 765), Royalwood (n= 574), and Westwood (n= 386). The city-wide density maps of private black ash and public black ash can be seen in Figures 3.10 and 3.12 respectively. The top ten neighbourhoods in private black ash tree count and private black ash density can be seen in Table 3.7 and public black ash in Table 3.9.

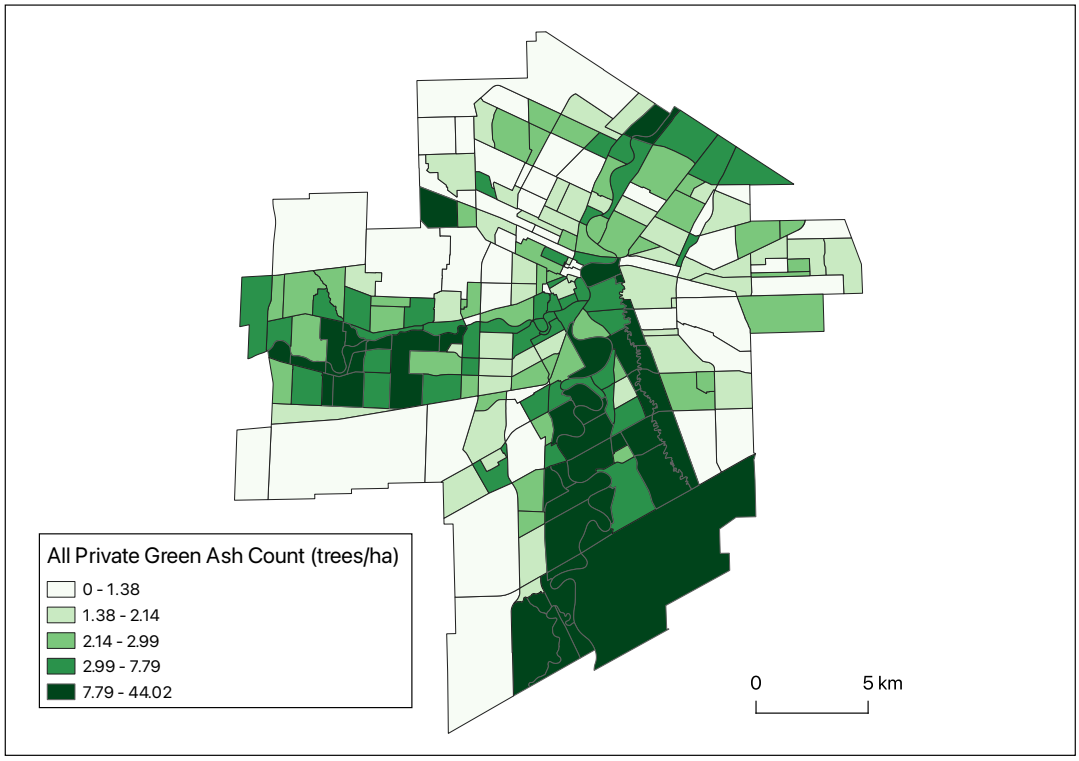

Figure 3.9. The density of the private green ash count (trees/hectare) across the neighbourhoods in the City of Winnipeg.

Table 3.6. The top ten neighbourhoods in private green ash tree count and private green ash density. (Bolded neighbourhoods are found in both lists).

Ash Tree Count			Ash Density (area/ha)		
Rank	Neighbourhood	Count	Rank	Neighbourhood	Density
1	St. Vital Perimeter South	48,587	1	**Perrault**	44.0
2	**Royalwood**	9,420	2	Cloutier Drive	40.4
3	**Perrault**	8,642	3	**St. Norbert**	34.3
4	Fort Richmond	6,342	4	Archwood	34.1
5	**St. Norbert**	6,210	5	**Royalwood**	32.7
6	Trappistes	5,260	6	Niakwa Park	31.8
7	Assiniboine Park	4,894	7	**Wildwood**	31.1
8	**Niakwa Place**	4,582	8	Marlton	29.7
9	Pulberry	4,237	9	Victoria Crescent	28.4
10	**Wildwood**	3,971	10	**Niakwa Place**	27.1

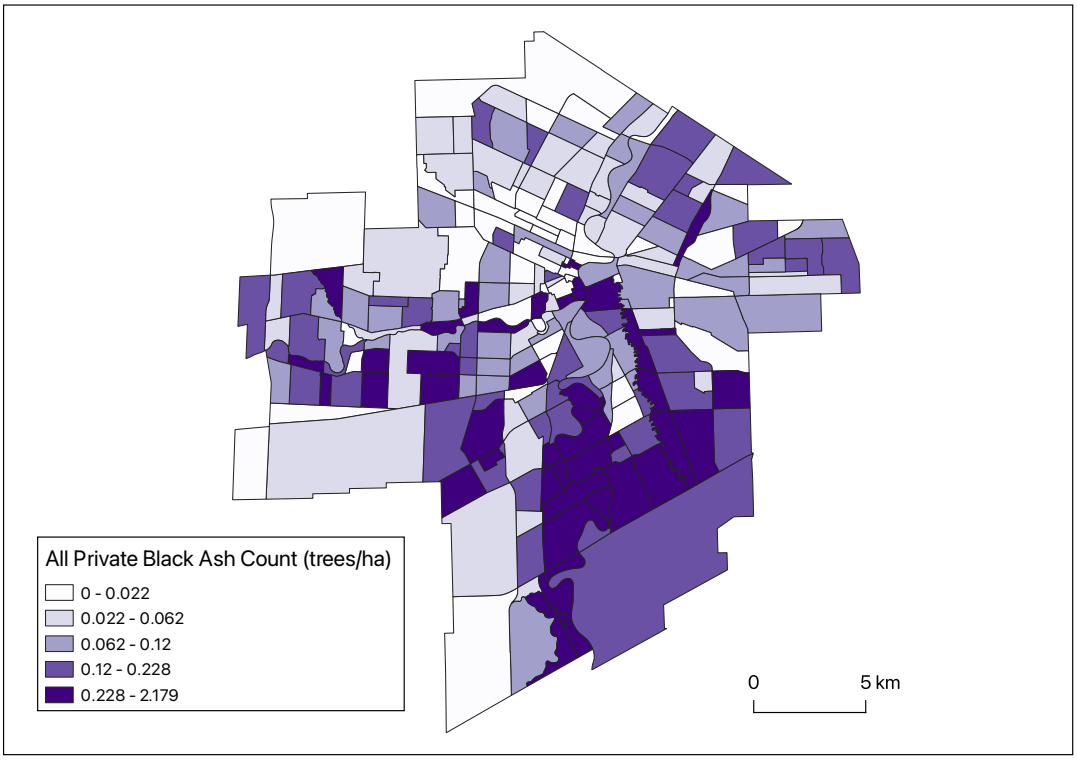

Figure 3.10. The density of the private black ash count (trees/hectare) across the neighbourhoods in the City of Winnipeg.

Table 3.7. The top ten neighbourhoods in private black ash tree count and private black ash density. (Bolded neighbourhoods are found in both lists).

Ash Tree Count			Ash Density (area/ha)		
Rank	Neighbourhood	Count	Rank	Neighbourhood	Density
1	St. Vital Perimeter South	712	1	**Cloutier Drive**	2.2
2	Fort Richmond	216	2	**Montcalm**	1.1
3	**Cloutier Drive**	179	3	Archwood	1.0
4	River Park South	166	4	Normand Park	1.0
5	Dakota Crossing	155	5	**St. Norbert**	0.8
6	**St. Norbert**	153	6	Wildwood	0.8
7	South Tuxedo	134	7	Polo Park	0.8
8	Linden Woods	130	8	The Forks	0.7
9	Island Lakes	129	9	Turnbull Drive	0.7
10	**Montcalm**	126	10	Kildonan Crossing	0.7

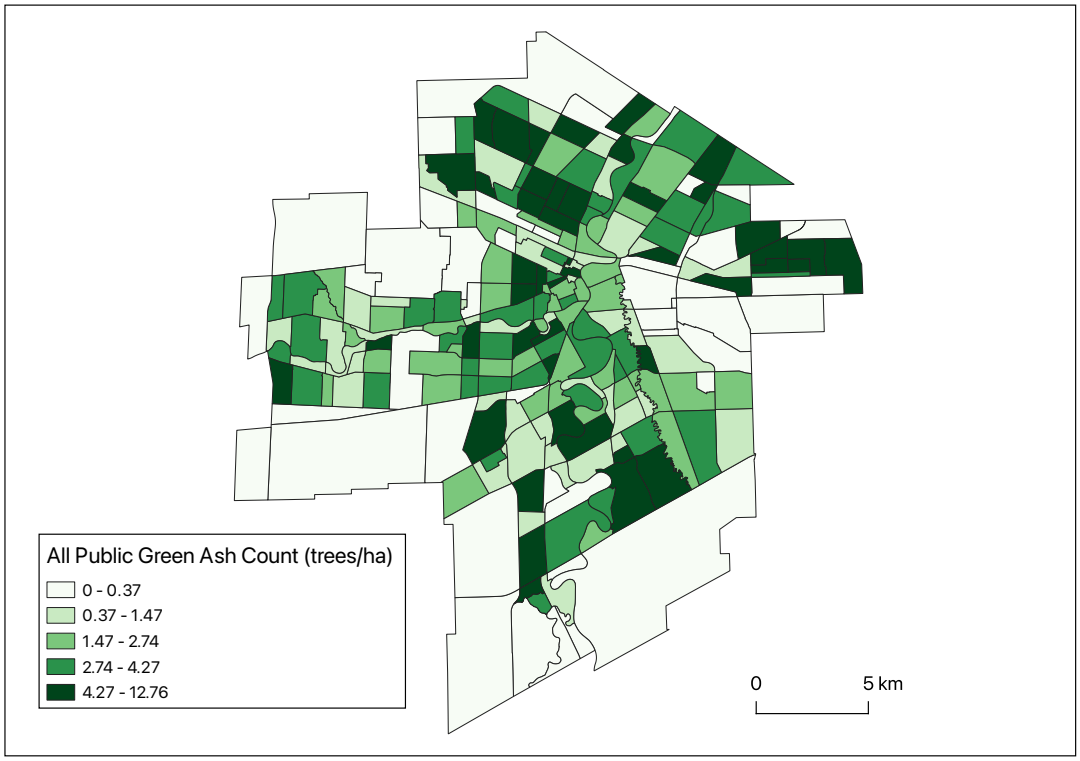

Figure 3.11. The density of the public green ash count (trees/hectare) across the neighbourhoods in the City of Winnipeg.

Table 3.8. The top ten neighbourhoods in public green ash tree count and public green ash density. (Bolded neighbourhoods are found in both lists).

Ash Tree Count			Ash Density (area/ha)		
Rank	Neighbourhood	Count	Rank	Neighbourhood	Density
1	River Park South	2,567	1	Kildonan Park	12.8
2	Dakota Crossing	2,405	2	Exchange District	10.1
3	**Tyndall Park**	2,274	3	Mandalay West	8.9
4	**Richmond West**	2,256	4	**Richmond West**	8.5
5	Linden Woods	2,218	5	Daniel Mcintyre	8.4
6	The Maples	2,058	6	Burrows Central	8.0
7	Canterbury Park	1,846	7	East Elmwood	7.6
8	Meadows	1,544	8	**Tyndall Park**	7.6
9	Springfield North	1,515	9	Ebby-wentworth	7.2
10	Pulberry	1,465	10	Kildare-redonda	7.1

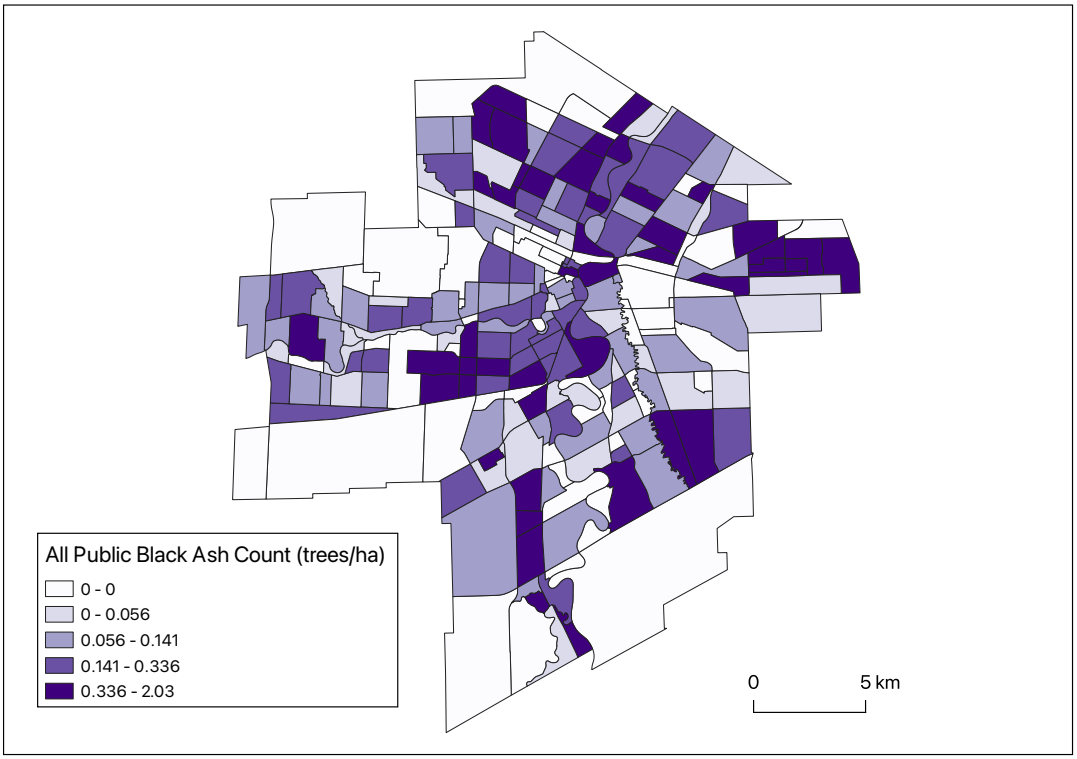

Figure 3.12. The density of the public black ash count (trees/hectare) across the neighbourhoods in the City of Winnipeg.

Table 3.9. The top ten neighbourhoods in public black ash tree count and public black ash density. (Bolded neighbourhoods are found in both lists).

Ash Tree Count			Ash Density (area/ha)		
Rank	Neighbourhood	Count	Rank	Neighbourhood	Density
1	**Island Lakes**	765	1	**Radisson**	2.0
2	**Royalwood**	574	2	**Royalwood**	2.0
3	**Westwood**	386	3	**Robertson**	1.8
4	**Robertson**	253	4	**Island Lakes**	1.7
5	**Radisson**	246	5	Melrose	16
6	Waverley Heights	245	6	Fairfield Park	1.5
7	Kildare-redonda	215	7	East Elmwood	1.4
8	Meadows	203	8	**Westwood**	1,4
9	Riverbend	187	9	Mathers	1.3
10	Canterbury Park	181	10	Linden Ridge	1.2

3.3.2 Riverbanks

A 100m buffer was created (50m on each side) for all rivers and creeks in Winnipeg. The Assiniboine River's buffer contained 1.36% (n= 4,637) of the all ash inventory (n= 341,059). Bunn's Creek's buffer contained 0.22% (n=739) of the all ash inventory. The La Salle River's buffer contained 2.23% (n= 7,604) of the all ash inventory. Omand Creek's buffer contained 0.16% (n= 566) of the all ash inventory. The Red River's buffer contained 6.60% (n= 22,477) of the all ash inventory. The Seine River's buffer contained 9.39% (n= 32,027) of the all ash inventory. Sturgeon Creek's buffer contained 0.07% (n= 256) of the all ash inventory. Truro Creek's buffer contained 0.04% (n= 141) of the all ash inventory. The 'No River' category contained 79.93% (n= 272,612) of the all ash inventory meaning that 79.93% of the ash trees in Winnipeg are not within 50m of a river or creek. Table 3.10 shows the breakdown via buffer, species, status, ash count, and percentage of the all ash inventory.

The total area that the buffer makes up in Winnipeg was calculated and represented as a percentage of the city's total area. This was done by taking the total area of the buffer (2035.51 hectares) and dividing it by the total area of Winnipeg (47539.39 hectares) and multiplying by 100 to represent it as a percentage. The result of this calculation was 4.28% meaning that all creeks and rivers with a 100m buffer represents 4.28% of Winnipeg's total area. It was then determined that 20.07% (100% - 79.93%) of the all ash inventory is located within 4.28% of Winnipeg's total area.

Table 3.10. Number of ash trees by species, status, and percentage of the all ash inventory within each river buffer.

River/Creek Name	Tree Species	Status	Count	% of All Ash Inventory
Assiniboine River	Black Ash	Private	22	0.01
Assiniboine River	Black Ash	Public	5	< 0.01
Assiniboine River	Green Ash	Private	4263	1.25
Assiniboine River	Green Ash	Public	347	0.10
Bunn's Creek	Black Ash	Private	5	< 0.01
Bunn's Creek	Black Ash	Public	8	< 0.01
Bunn's Creek	Green Ash	Private	566	0.17
Bunn's Creek	Green Ash	Public	160	0.05
La Salle River	Black Ash	Private	161	0.05
La Salle River	Black Ash	Public	42	0.01
La Salle River	Green Ash	Private	7394	2.17
La Salle River	Green Ash	Public	7	< 0.01
No River	Black Ash	Private	5739	1.68
No River	Black Ash	Public	8586	2.52
No River	Green Ash	Private	175501	51.46
No River	Green Ash	Public	82786	24.27
Omand's Creek	Black Ash	Private	49	0.01
Omand's Creek	Black Ash	Public	3	< 0.01
Omand's Creek	Green Ash	Private	491	0.14
Omand's Creek	Green Ash	Public	23	0.01
Red River	Black Ash	Private	363	0.11
Red River	Black Ash	Public	18	0.01
Red River	Green Ash	Private	20966	6.15
Red River	Green Ash	Public	1130	0.33
Seine River	Black Ash	Private	186	0.05
Seine River	Black Ash	Public	4	< 0.01
Seine River	Green Ash	Private	31514	9.24

Seine River	Green Ash	Public	323	0.09
Sturgeon Creek	Black Ash	Private	6	< 0.01
Sturgeon Creek	Black Ash	Public	5	< 0.01
Sturgeon Creek	Green Ash	Private	109	0.03
Sturgeon Creek	Green Ash	Public	136	0.04
Truro Creek	Black Ash	Private	2	< 0.01
Truro Creek	Black Ash	Public	0	0
Truro Creek	Green Ash	Private	47	0.01
Truro Creek	Green Ash	Public	92	0.03

The all ash hotspot map (Figure 3.13) shows the spatial distribution of all ash trees in the city. The highest densities occur near riverbanks, most notably the Seine River and the southern portion of the Red River. The moderate density areas (lighter red) occur primarily within neighbourhoods and are not close to riverbanks. These areas are indicative of public ash likely along boulevards. The private ash hotspot map (Figure 3.14) shows the spatial distribution of all private trees in the city. The hotspots are almost exclusively along riverbanks, again most notably the Seine and Red Rivers. The public ash hotspot map (Figure 3.15) shows the spatial distribution of all public trees in the city. The hotspots are representative of where ash was planted as boulevard trees, especially in the newer (developed post-1975) suburban portions of the city. St.Vital Park and Kildonan Park also have high densities of public ash.

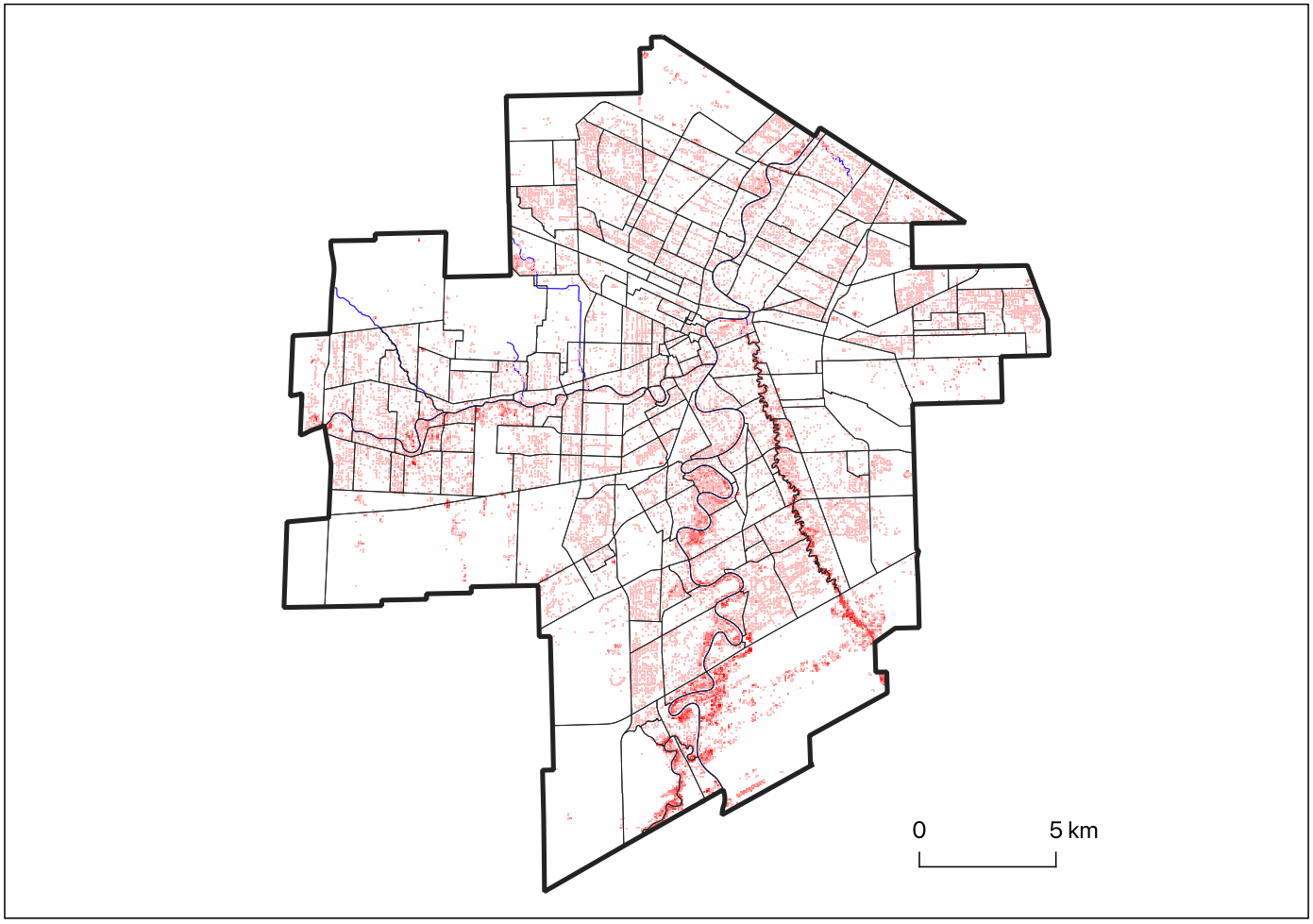

Figure 3.13. Hotspot analysis of the all ash inventory in Winnipeg using a 50mx50m grid to display densities (ash/ha) represented by shades of red in comparison to the proximity of rivers and creeks.

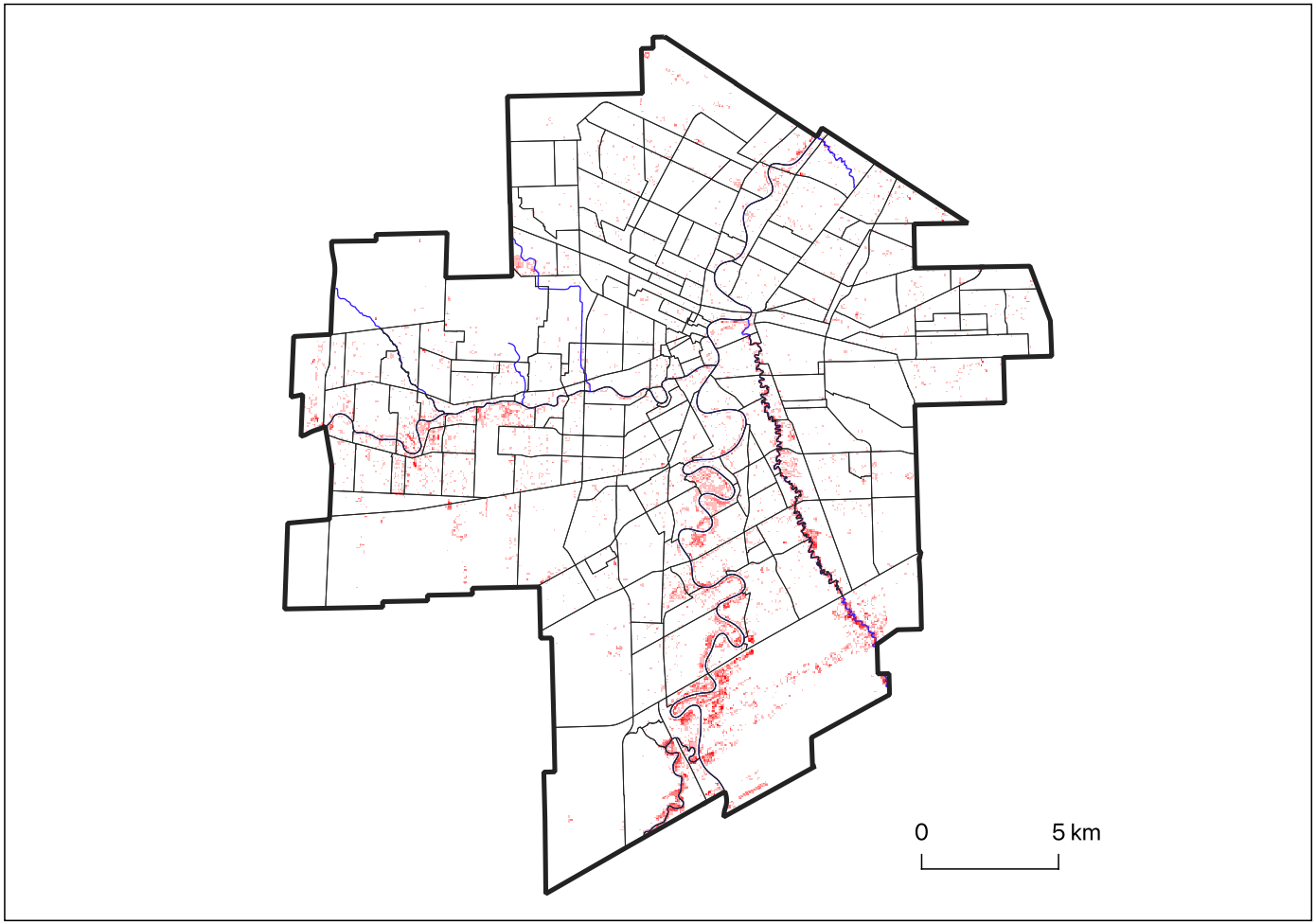

Figure 3.14. Hotspot analysis of the private ash inventory in Winnipeg using a 50mx50m grid to display densities (ash/ha) represented by shades of red in comparison to the proximity of rivers and creeks.

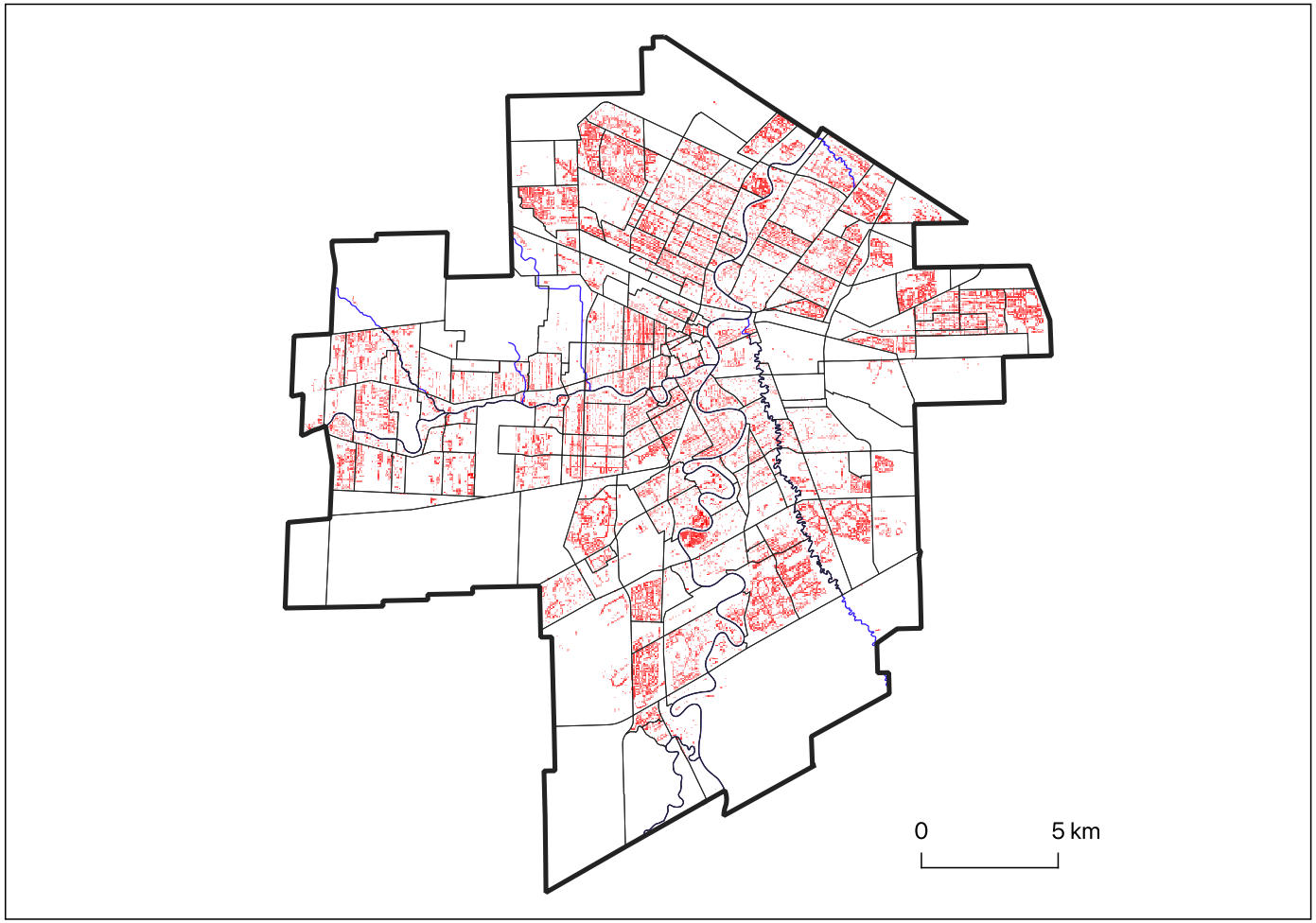

Figure 3.15. Hotspot analysis of the public ash inventory in Winnipeg using a 50mx50m grid to display densities (ash/ha) represented by shades of red in comparison to the proximity of rivers and creeks.

3.3.3 Spatial Autocorrelation

The spatial autocorrelation of ash inventories differed between species and status in the Moran plots and correlograms. The Moran plots also showed high influence points which are neighbourhoods that are the most influential areas in each respective quadrant. Only a few high influence points were highlighted in Figures 3.16-3.22, see Appendix C for the full list of high influence points for each ash inventory. For the all ash inventory, the Moran plot (Figure 3.16) showed that the high influence points in Q1 (high density-high neighbour density) included Perrault, Turnbull Drive, and Cloutier Drive; high influence points in Q2 (high density-low neighbour density) included Beaumont, Omand's Creek Industrial, and Linden Woods; and high influence points in Q3 (low density-low neighbour density) included Airport, Symington Yards, and West Perimeter South. Q4 (low density-high neighbour density) contained no high influence points for this inventory. Q1 contained 79 (34.3%) neighbourhoods; Q2 contained 46 (20.0%) neighbourhoods; Q3 contained 70 (30.4%) neighbourhoods; and Q4 contained 35 (15.2%) neighbourhoods. The correlogram showed that for one lag (neighbourhood) away from any given neighbourhood, there is a high likelihood (Moran's I = 0.4156) that the neighbouring polygon will have a similar ash density. Up to four lags away, positive spatial autocorrelation is still likely to occur (two lags - Moran's I = 0.1363; three lags - Moran's I = 0.0821; four lags - Moran's I = 0.0613). The sixth lag away shows total negative spatial autocorrelation (Moran's I = -0.0495) suggesting that a given neighbourhood will have a different ash density than neighbourhoods located six neighbourhood polygons away. The fifth, seventh, and eighth lags overlap zero and do not have any indication of spatial autocorrelation.

For the all green ash inventory, the Moran plot (Figure 3.17) showed that high influence points in Q1 included Perrault, Turnbull Drive, and Cloutier Drive; high influence points in Q2 included Beaumont, Omand's Creek Industrial, and Linden Woods; and high influence points in Q3 included Airport, Symington Yards, and West Perimeter South. Q4 contained no high influence points for this inventory. Q1 contained 79 (34.3%) neighbourhoods; Q2 contained 44 (19.1%) neighbourhoods; Q3 contained 74 (32.2%) neighbourhoods; and Q4 contained 33 (14.3%) neighbourhoods. The correlogram showed that for one lag away from any given neighbourhood, there is a high likelihood (Moran's I = 0.4212) that the neighbour will have a similar green ash density. Up to four lags away, positive spatial autocorrelation is still likely to occur (two lags - Moran's I = 0.1355; three lags - Moran's I = 0.0789; four lags - Moran's I = 0.0588). The sixth

lag away shows total negative spatial autocorrelation (Moran's I = -0.0537) suggesting that a given neighbourhood will have a different green ash density than neighbourhoods located six neighbourhood polygons away. The fifth, seventh, and eighth lags overlap zero and do not have any indication of spatial autocorrelation.

For the all black ash inventory, the Moran plot (Figure 3.18) showed that high influence points in Q1 included Victoria West, Kern Park, Royalwood, and Island Lakes; high influence points in Q2 included Linden Ridge, Grant park, Westwood, and East Elmwood; and high influence points in Q4 included St. Vital Perimeter South, Griffin, and Transcona North. Q3 contained no high influence points for this inventory. Q1 contained 48 (20.9%) neighbourhoods; Q2 contained 40 (17.4%) neighbourhoods; Q3 contained 85 (37.0%) neighbourhoods; and Q4 contained 57 (24.7%) neighbourhoods. The correlogram showed that there is positive spatial autocorrelation for the first three lags (one lag - Moran's I = 0.1251; two lags - Moran's I = 0.0560; three lags - Moran's I = 0.0356), although these are small indicators of autocorrelation. The other lags (4-8) overlap zero; therefore, they have no indication of spatial autocorrelation.

For the private green ash inventory, the Moran plot (Figure 3.19) showed that the high influence points in Q1 included Perrault, Turnbull Drive, Archwood, and Marlton; high influence points in Q2 included Omand's Creek Industrial, and Burrows-keewatin; the high influence point in Q3 was West Perimeter South; and the high influence points in Q4 included Island Lakes, St. George, and Vista. Q1 contained 69 (30.0%) neighbourhoods; Q2 contained 14 (6.1%) neighbourhoods; Q3 contained 122 (53.0%) neighbourhoods; and Q4 contained 25 (10.9%) neighbourhoods. The correlogram showed that for one lag away from any given neighbourhood, there is a high likelihood (Moran's I = 0.4594) that the neighbour will have a similar private green ash density. Up to four lags away, positive spatial autocorrelation is still likely to occur (two lags - Moran's I = 0.1706; three lags - Moran's I = 0.1060; four lags - Moran's I = 0.0726). The sixth lag away shows total negative spatial autocorrelation (Moran's I = -0.0434) suggesting that a given neighbourhood will have a different private green ash density than neighbourhoods located six neighbourhood polygons away. The seventh and eighth lags also show near total negative spatial autocorrelation (seven lags - Moran's I = -0.0344; eight lags - Moran's I = -0.0353). The fifth lag overlaps zero and does not have any indication of spatial autocorrelation.

For the public green ash inventory, the Moran plot (Figure 3.20) showed that the high influence points in Q1 were Daniel McIntyre, Exchange District, and Mandalay West; the high influence point in Q2 was Kildonan Park; the high influence points in Q3 were West Perimeter South, and Holden; and the high influence points in Q4 were North Transcona Yards, and Inkster Industrial Park. Q1 contained 76 (33.0%) neighbourhoods; Q2 contained 45 (19.6%) neighbourhoods; Q3 contained 61 (26.5%) neighbourhoods; and Q4 contained 48 (20.9%) neighbourhoods. The correlogram showed that there is positive spatial autocorrelation for the first lag (Moran's I = 0.0696), although this is a small indication of autocorrelation. The fifth lag is almost totally negatively autocorrelated (Moran's I = -0.0279) suggesting that a given neighbourhood will have a different public green ash density than neighbourhoods located five polygons away. The other lags (2-4 and 6-8) overlap zero; therefore, they have no indication of spatial autocorrelation.

For the private black ash inventory, the Moran plot (Figure 3.21) showed that the high influence points in Q1 included Cloutier Drive, Maple Grove Park, St. Norbert, and Normand Park; high influence points in Q2 included Polo Park, The Forks, and Grant Park; and the high influence point in Q4 was Fairfield Park. Q3 contained no high influence points for this inventory. Q1 contained 54 (23.5%) neighbourhoods; Q2 contained 29 (12.6%) neighbourhoods; Q3 contained 108 (47.0%) neighbourhoods; and Q4 contained 39 (17.0%) neighbourhoods. The correlogram showed that for one lag away from any given neighbourhood, there is a high likelihood (Moran's I = 0.2089) that the neighbour will have a similar private black ash density. Up to five lags away, positive spatial autocorrelation is still likely to occur (two lags - Moran's I = 0.1435; three lags - Moran's I = 0.1178; four lags - Moran's I = 0.0728; five lags – Moran's I = 0.0603). The eighth lag away shows total negative spatial autocorrelation (Moran's I = -0.0514) suggesting that a given neighbourhood will have a different private black ash density than neighbourhoods located eight neighbourhood polygons away. The sixth and seventh lags overlap zero and do not have any indication of spatial autocorrelation.

For the public black ash inventory, the Moran plot (Figure 3.22) showed that high influence points in Q1 included Victoria West, Kern Park, Kildare-redonda, and Radisson; high influence points in Q2 included Westwood, East Elmwood, and Linden Ridge; and high influence points in the Q4 included Transcona North, Griffin, and Transcona Yards. Q3 contained no high influence points for this inventory. Q1 contained 42 (18.3%) neighbourhoods; Q2 contained 31 (13.5%)

neighbourhoods; Q3 contained 99 (43.0%) neighbourhoods; and Q4 contained 58 (25.2%) neighbourhoods. The correlogram showed that for one lag away from any given neighbourhood, there is a high likelihood (Moran's I = 0.1118) that the neighbour will have a similar public black ash density. The fifth lag away shows total negative spatial autocorrelation (Moran's I = -0.0446) suggesting that a given neighbourhood will have a different public black ash density than neighbourhoods located five polygons away. The other lags overlap zero and do not have any indication of spatial autocorrelation.

Pearson's product-moment correlation was used to test for association between the paired samples (ash density vs lagged ash density) (Table 3.11). The results in Table 3.11 should only be interpreted for adjacent neighbourhoods (one lag away).

Table 3.11. Pearson's product-moment correlation results testing for association between ash density and lagged ash density (Moran plots) for the seven ash inventories.

Ash Inventory	p-value	Correlation coefficient	t-statistic	df	95 % CI lower bound	95% CI upper bound
All Ash	< 0.0001	0.673	13.752	228	0.596	0.738
All Green Ash	< 0.0001	0.678	13.94	228	0.602	0.743
All Black Ash	< 0.0001	0.263	4.1135	228	0.138	0.379
Private Green Ash	< 0.0001	0.715	15.425	228	0.645	0.773
Public Green Ash	0.0191	0.155	2.3613	228	0.026	0.278
Private Black Ash	< 0.0001	0.420	6.9816	228	0.307	0.521
Public Black Ash	0.0006	0.226	3.4999	228	0.099	0.345

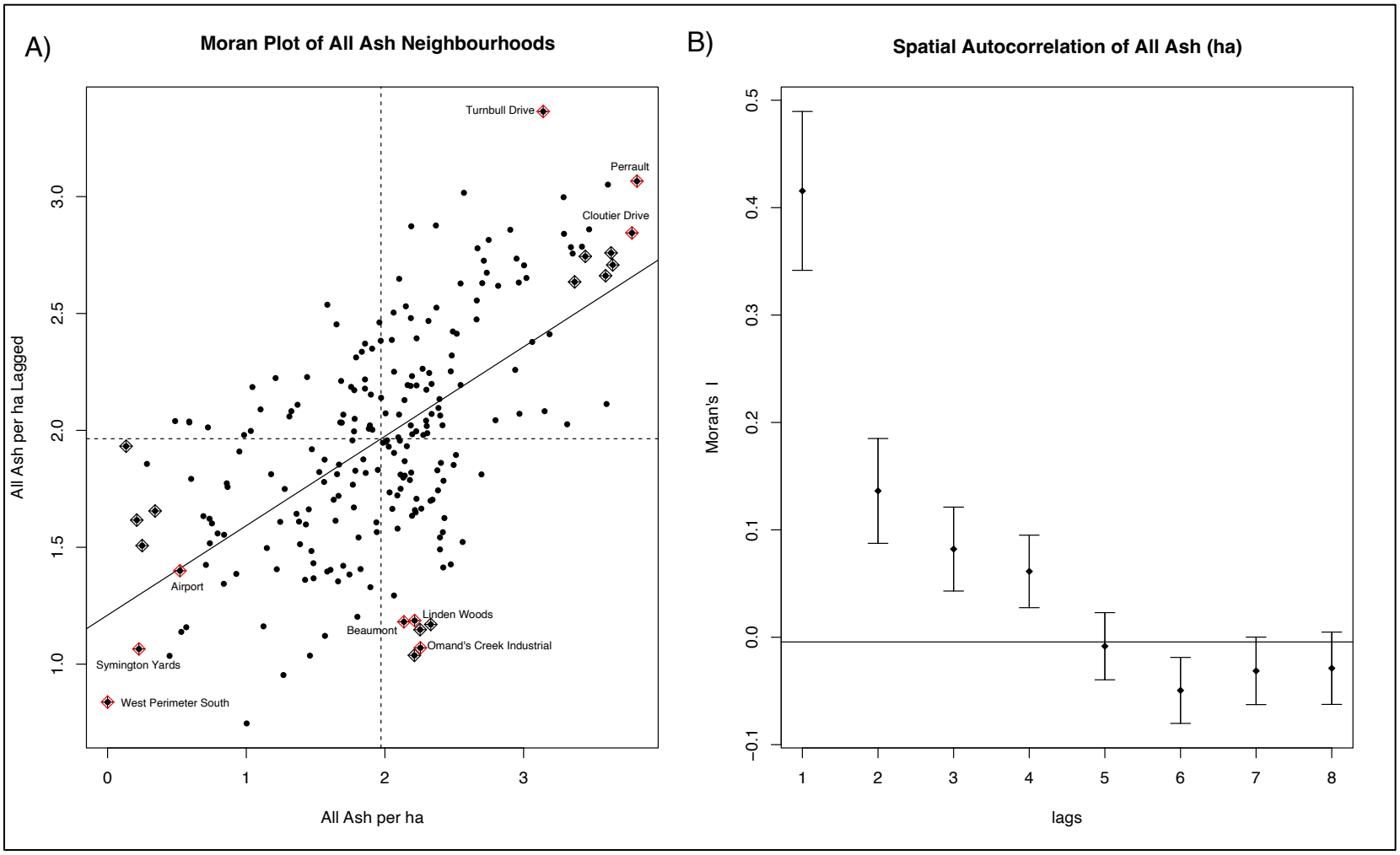

Figure 3.16. **(A)** Moran plot of all the neighbourhoods (n=230) in Winnipeg comparing all ash density per hectare (log+1) with the weighted lagged density (log+1) ($F = 133.2$, $df = 228$, $p = < 0.0001$, $r^2 = 0.366$). **(B)** Correlogram of the all ash inventory showing the spatial autocorrelation by lag.

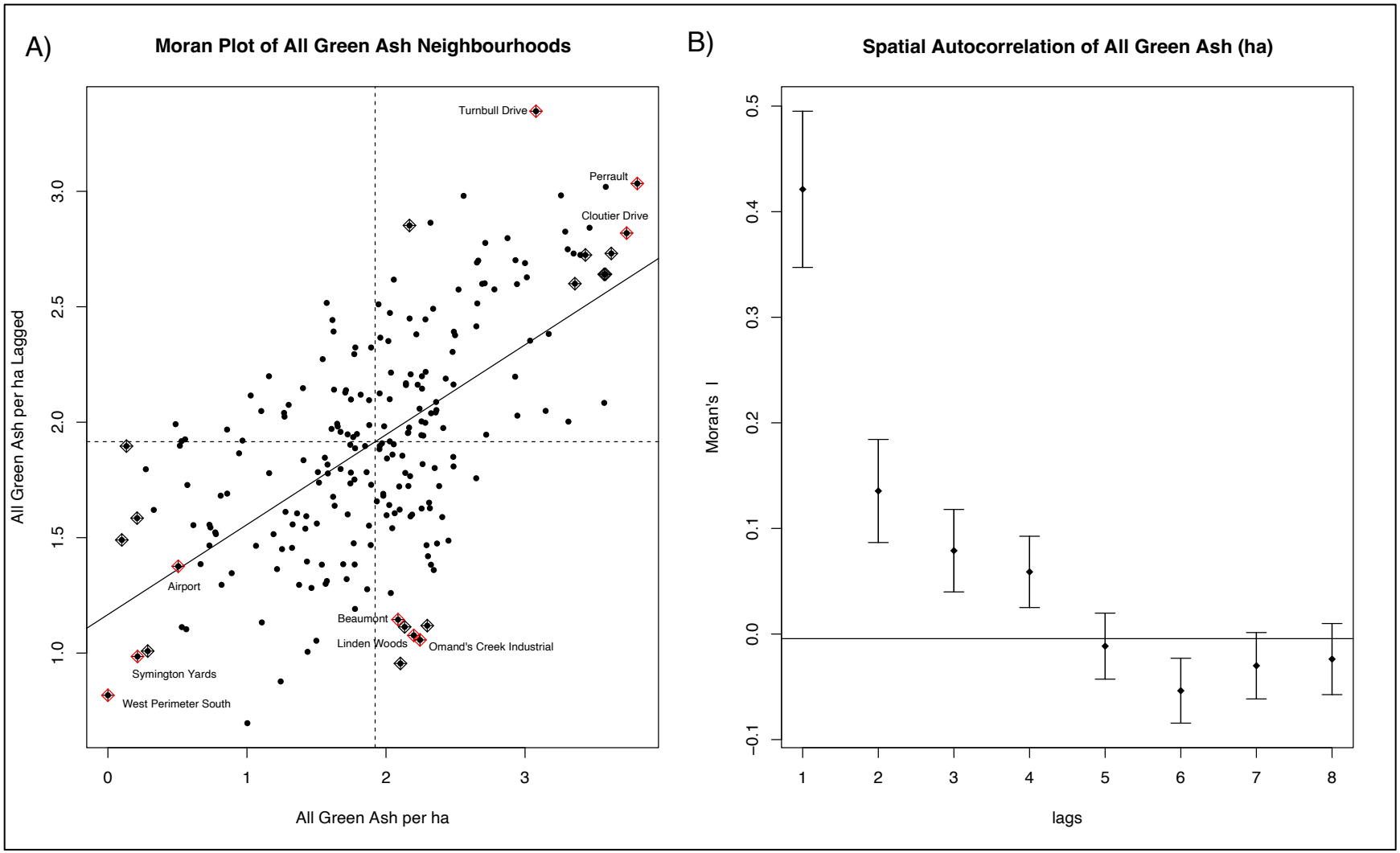

Figure 3.17. **(A)** Moran plot of all the neighbourhoods (n=230) in Winnipeg comparing all green ash density per hectare (log+1) with the weighted lagged density (log+1) (F = 138.1, df = 228, p = < 0.0001, r^2 = 0.375). **(B)**. Correlogram of the all green ash inventory showing the spatial autocorrelation by lag.

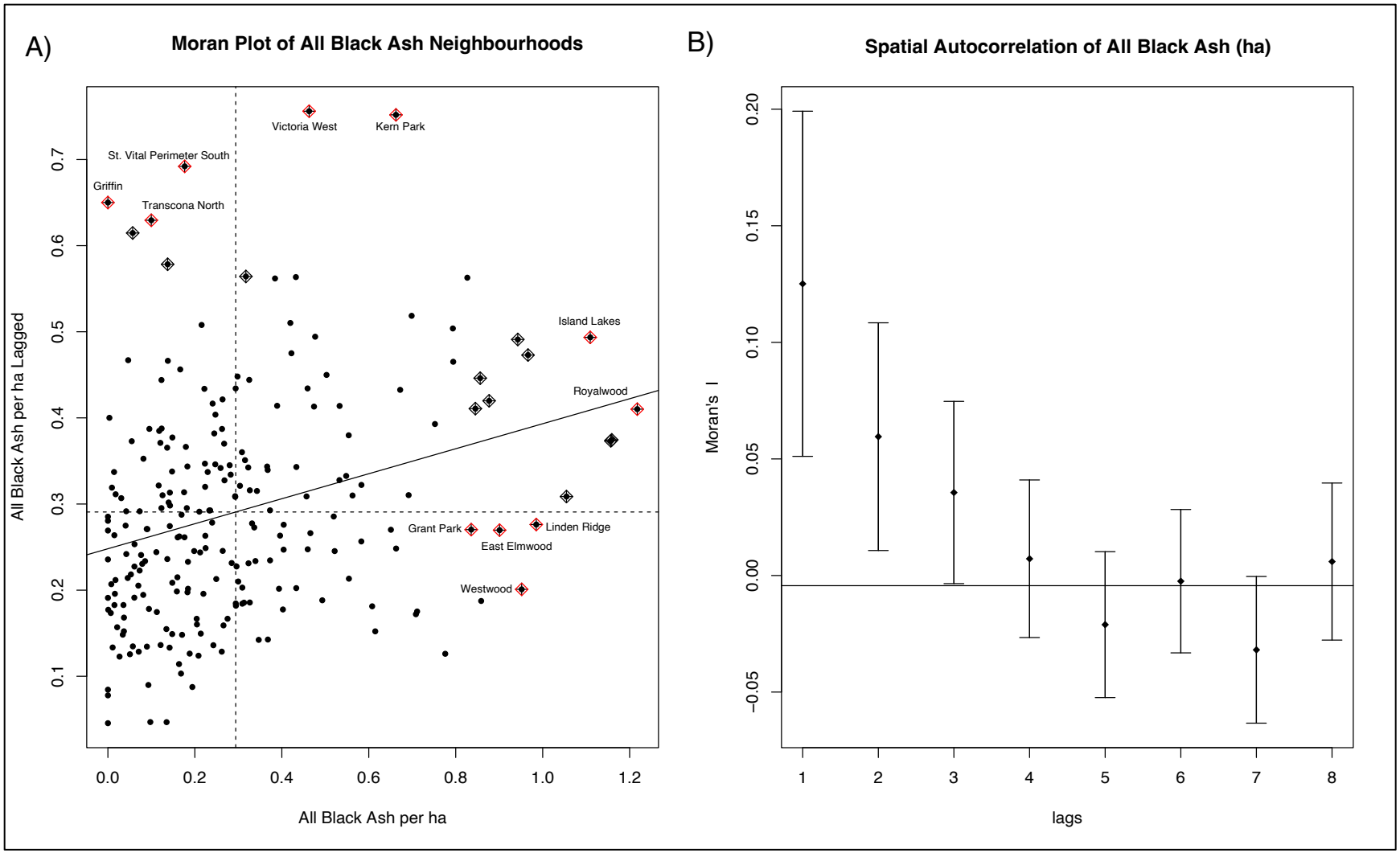

Figure 3.18. **(A)** Moran plot of all the neighbourhoods (n=230) in Winnipeg comparing all black ash density per hectare (log+1) with the weighted lagged density (log+1) ($F = 21.87$, $df = 228$, $p = < 0.0001$, $r^2 = 0.084$). **(B)**. Correlogram of the all black ash inventory showing the spatial autocorrelation by lag.

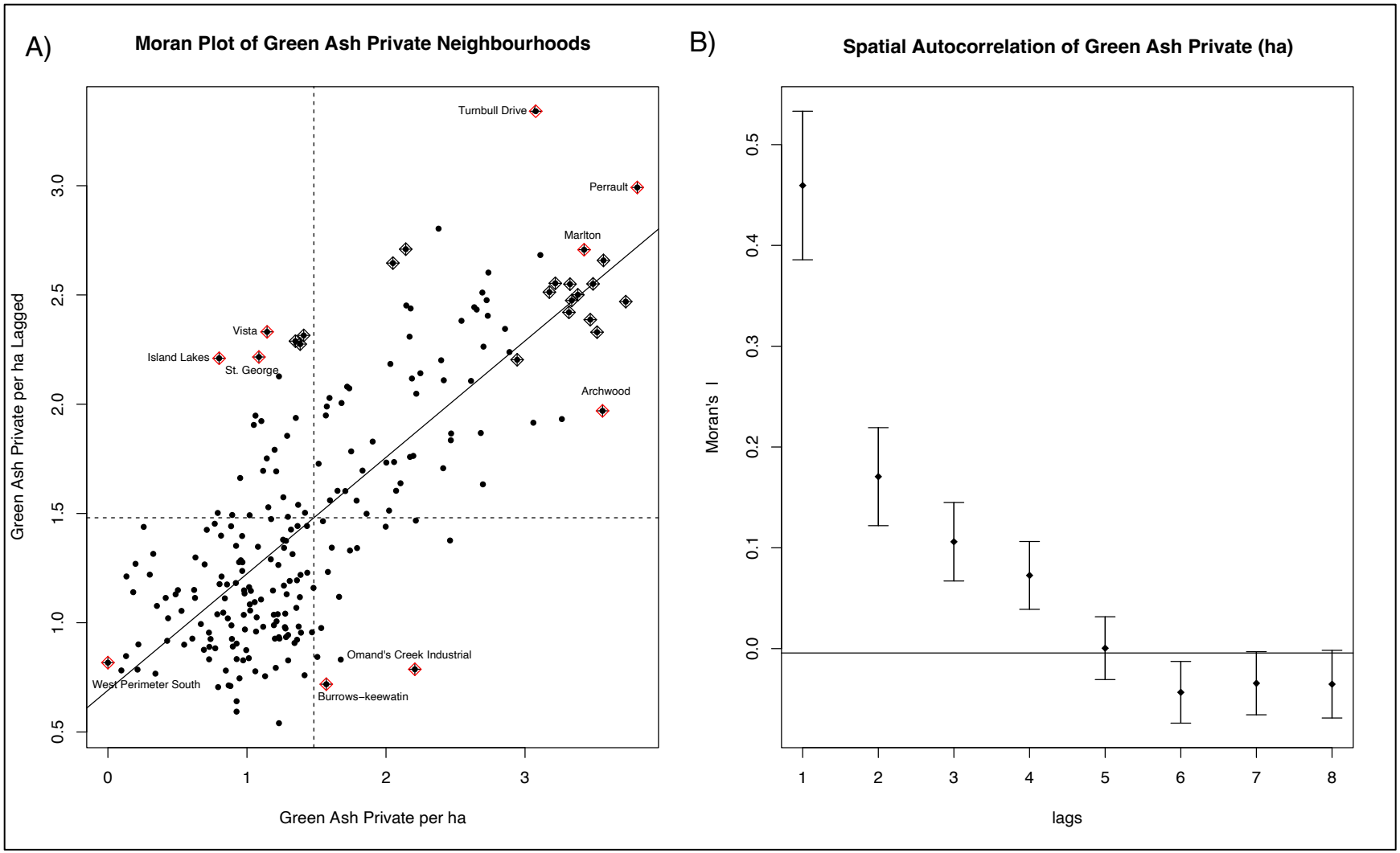

Figure 3.19. **(A)** Moran plot of all the neighbourhoods (n=230) in Winnipeg comparing private green ash density per hectare (log+1) with the weighted lagged density (log+1) (F = 309.8, df = 228, p = < 0.0001, r^2 = 0.574). **(B)**. Correlogram of the private green ash inventory showing the spatial autocorrelation by lag.

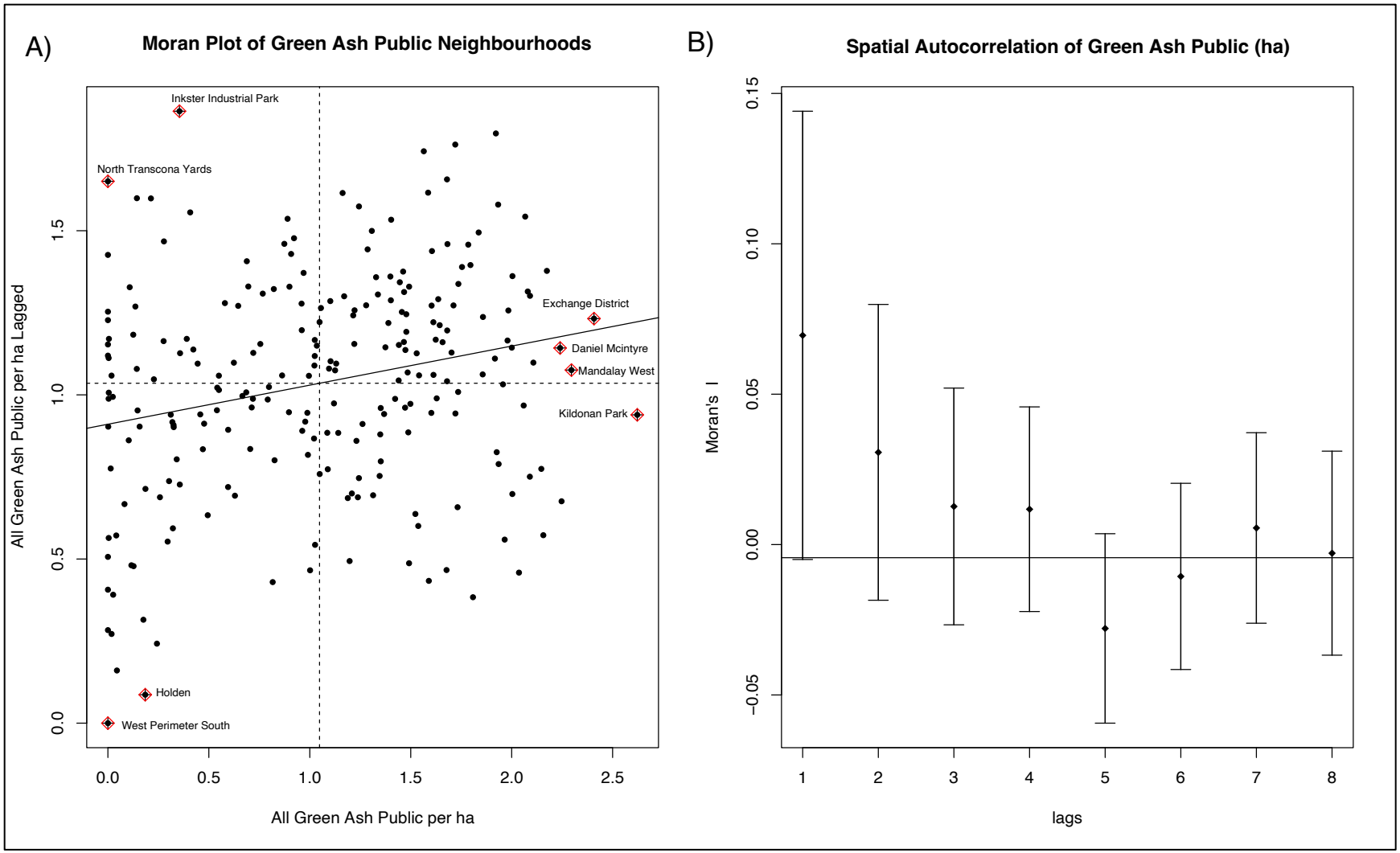

Figure 3.20. **(A)** Moran plot of all the neighbourhoods (n=230) in Winnipeg comparing public green ash density per hectare (log+1) with the weighted lagged density (log+1) (F = 13.25, df = 228, p = 0.0003, r^2 = 0.051). **(B)**. Correlogram of the public green ash inventory showing the spatial autocorrelation by lag.

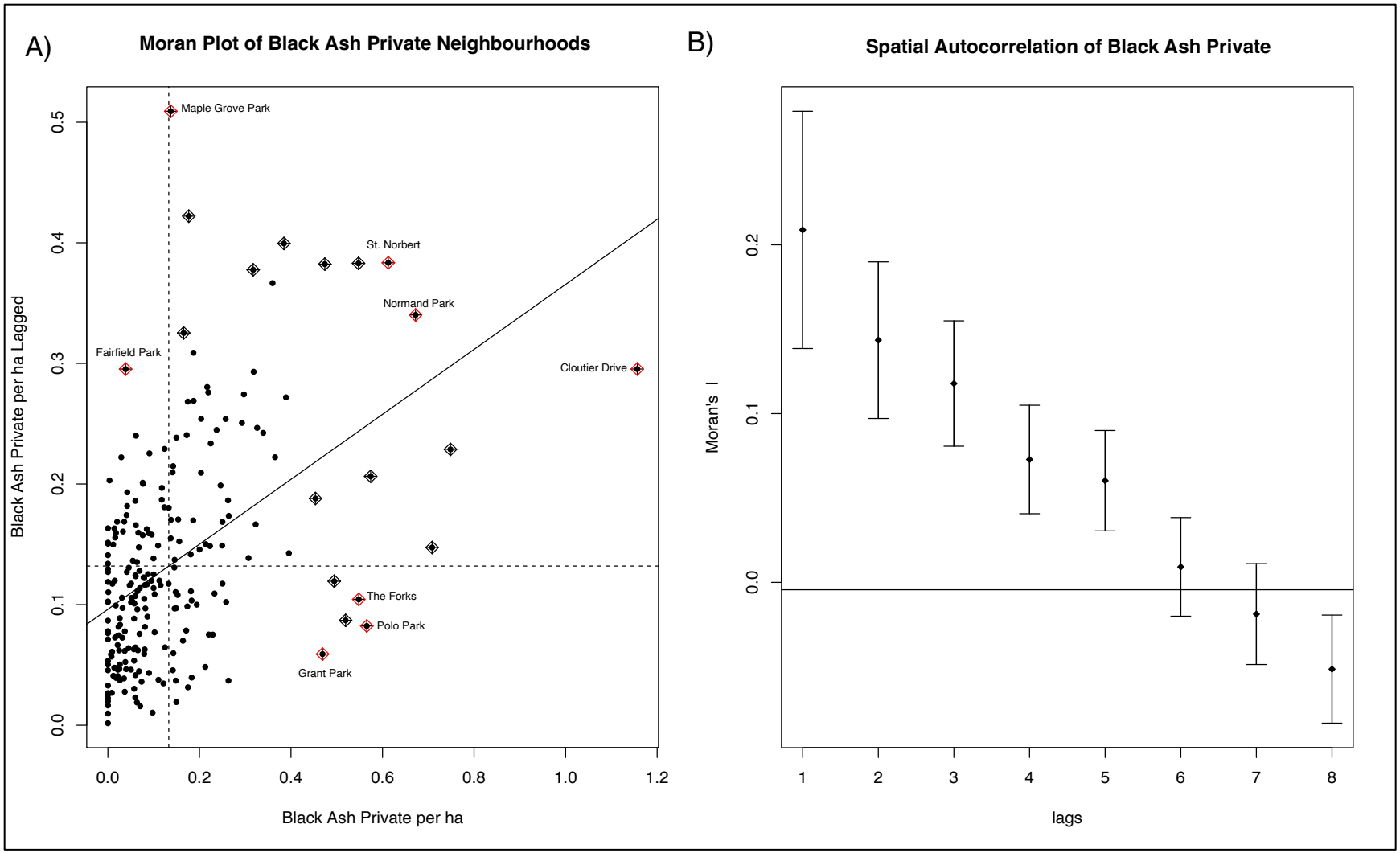

Figure 3.21. **(A)** Moran plot of all the neighbourhoods (n=230) in Winnipeg comparing private black ash density per hectare (log+1) with the weighted lagged density (log+1) (F = 69.72, df = 228, p = <0.0001, r^2 = 0.231). **(B)**. Correlogram of the private black ash inventory showing the spatial autocorrelation by lag.

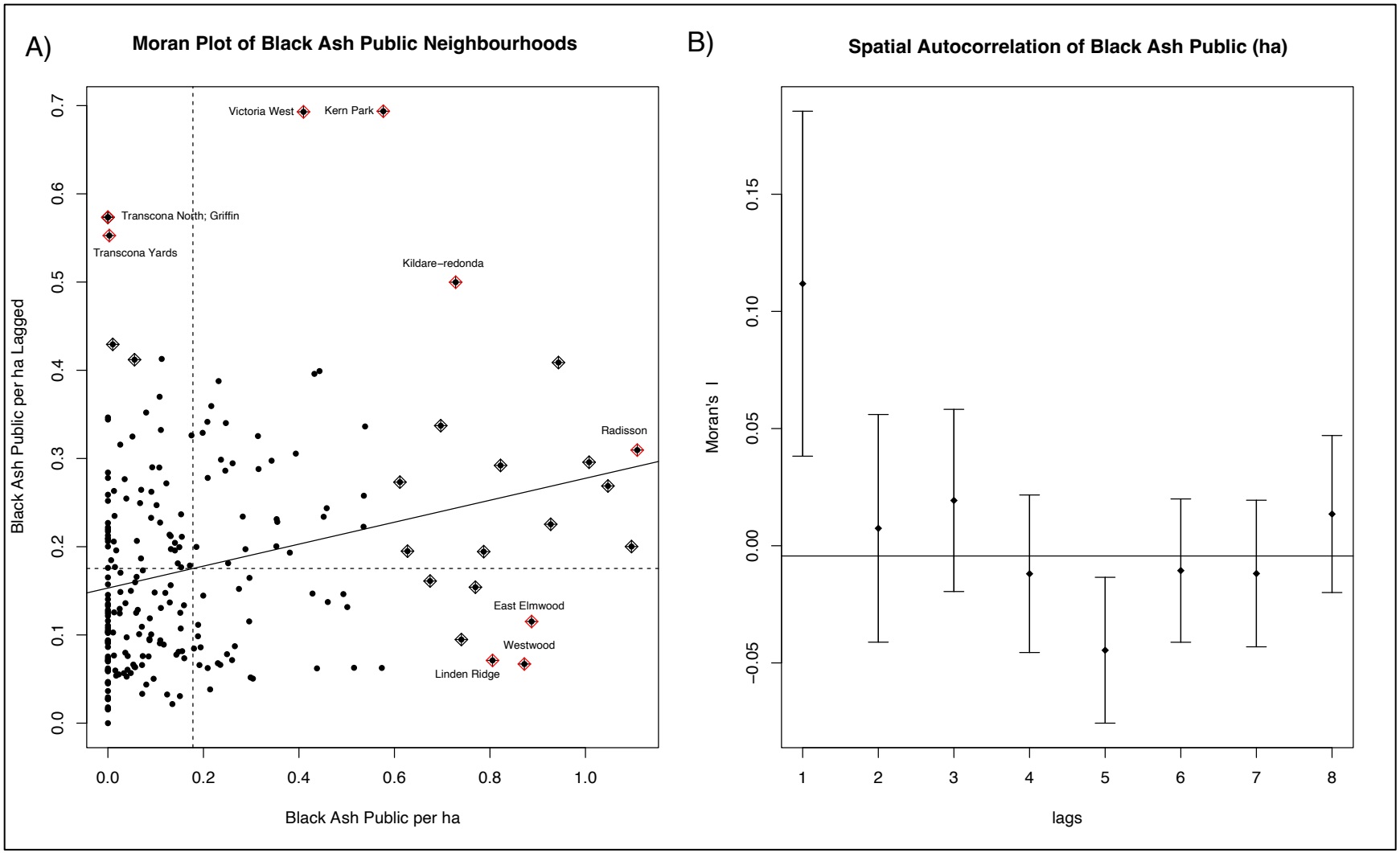

Figure 3.22. **(A)** Moran plot of all the neighbourhoods (n=230) in Winnipeg comparing public black ash density per hectare (log+1) with the weighted lagged density (log+1) (F = 15.01, df = 228, p = <0.0001, r^2 = 0.058). **(B)**. Correlogram of the public black ash inventory showing the spatial autocorrelation by lag

3.4 Discussion

3.4.1 Ash Densities

Using tree inventory data to derive ash densities for each neighbourhood will help guide logistical planning for a city wide EAB management program in Winnipeg. The results from this study are useful for examining ash as a whole or as a subset by status or species. Managers can use these results to determine which neighbourhoods and areas in Winnipeg contain the highest ash densities and thus allocate more resources and attention to those areas. The results also assist managers in determining management strategies based on the status (public or private) and species (green or black) of tree throughout the neighbourhoods of Winnipeg.

Considering the all ash inventory, neighbourhoods with the highest ash densities often occurred along riverbanks namely the Seine, Red, and La Salle Rivers. Neighbourhoods such as Perrault, Turnbull Drive, Royalwood, and Victoria Crescent are among the top ten densest neighbourhoods in the all ash inventory and all occur along those three rivers. The all ash inventory was largely influenced by private green ash trees as this is the most common type (status-species) of ash in Winnipeg. Private green ash trees also grow abundantly along riverbanks where densities can be high; therefore, it is not surprising to see such neighbourhoods as these among the densest when considering the all ash inventory. However, it is important to note that neighbourhoods with high all ash densities (and counts) that are along riverbanks may be of the most concern for management as the risk of EAB facilitation/dispersal combined with the potential ash loss in these areas is significant. These areas may be at the greatest risk because of the large abundance and high densities of ash that are located primarily on private property where no management interventions are currently planned.

Ash densities differed by status (public or private) and species (green or black) across the neighbourhoods of Winnipeg. Neighbourhoods with high densities of public trees were often different than neighbourhoods with high densities of private trees. The neighbourhoods with the highest densities and counts of public trees were typically located in more suburban developments such as River Park South, Richmond West, and Tyndall Park. This is because ash was used as the primary boulevard tree as a substitute for American elm (*Ulmus americana*) when these neighbourhoods were developed. The neighbourhoods with the highest densities and counts of private trees were typically located in neighbourhoods that bordered rivers such as

Perrault, Cloutier Drive, Royalwood, and Archwood. These neighbourhoods tend to have residential properties with backyards containing large amounts of ash that extend to the riverbank.

Neighbourhood ash densities also differed by species. Neighbourhoods with high densities of green ash were often found along riverbanks such as Perrault, St. Norbert, and Niakwa Park. High green ash counts also occurred in newer (developed post-1975) neighbourhoods such as River Park South and Dakota Crossing where green ash is the primary boulevard tree. The similarity between high private densities and high green ash densities suggests that private green ash trees heavily influence ash density hotspots. The top ten neighbourhoods in the all green ash count were quite different than the top ten for green ash density (Table 3.4). This is an interesting finding as it suggests some neighbourhoods with high green ash counts do not have as high density ratings. Neighbourhoods with high green ash counts such as Fort Richmond, River Park South, and Dakota Crossing have much lower density values (16.7 ash/ha, 13.3 ash/ha, and 14.1 ash/ha respectively) than the top ten dense neighbourhoods. This is likely because these neighbourhoods are influenced more by public green ash on boulevards and they are not located near riverbanks. The spacing of boulevard trees is relatively consistent based on City of Winnipeg planting guidelines which likely contributes to the lower ash densities in these neighbourhoods. Such spacing restrictions do not apply to trees that occur on private, natural, and riverbank areas.

It is also interesting to note that the top ten neighbourhoods for the private ash count (Table 3.3) and the top ten for the green ash count (Table 3.4) share eight of the same neighbourhoods and the top five are identical. These two inventories also share an identical top ten neighbourhoods for ash density. Neighbourhoods with high densities and counts of black ash were located quite randomly throughout the city, except that high densities of black ash are observed in newer (developed post-1975) neighbourhoods. Royalwood, Radisson, and Island Lakes are among the neighbourhoods that contain high black ash densities. Five neighbourhoods overlapped between the top ten black ash count and density lists suggesting that there is some degree of similarity between the sheer number of black ash trees and neighbourhood ash density values.

The various status and species combinations (private green, public green, private black, public black) were analyzed to determine if there were any noticeable differences when compared to the

stand-alone results (non-combinations). The private green ash had an identical top ten dense neighbourhoods as the all green ash with only a few neighbourhoods having a different ranking within the top ten. Private green and all green also shared eight (top ten) of the same neighbourhoods for ash tree count; and private green and all private had an identical top ten. The all private ash, all green ash, and private green ash had very similar count and density results.

The public green ash density results differ from the all green ash results in that the neighbourhoods along riverbanks are less dense. This can be especially seen along the Red River and the Seine River. This means that public green ash is not as influential on the all green ash density values as private green ash in neighbourhoods along riverbanks. Some neighbourhoods in the northern and eastern parts of Winnipeg had higher public green ash counts and densities when compared to the all green ash density. This is likely because green ash was widely planted as boulevard trees in these areas. The top ten neighbourhoods in public green ash count and density are very different than the top ten for all green ash with only three overlapping neighbourhoods for the count (River Park South, Dakota Crossing, and Pulberry) and zero overlapping neighbourhoods for density. This suggests that public green ash trees do not influence the all green ash density results as much as private green ash.

The private black ash density results differ from the all black ash results in that the neighbourhoods in the southern region of the city have higher densities. Most of these southern neighbourhoods are located near either the Red River or Seine River which may influence these results as many private ash trees (green and black) are found in residential backyards along the rivers. The top ten neighbourhoods in private black ash count and density are very different than the top ten for all black ash with only three overlapping neighbourhoods for the count (Island Lakes, St. Vital Perimeter, and River Park South) and one overlapping neighbourhood for density (Cloutier Drive). This suggests that private black ash trees do not influence the all black ash count results as much as public black ash. It is worth noting that the number of black ash trees in St. Vital Perimeter South is identical in both the all black ash and private black ash counts meaning that there are no public black ash trees in this neighbourhood.

The public black ash density results do not differ much from the all black ash density results in that the maps are quite similar. The eastern, northern, and western regions of the city are very similar between these two inventories with neighbourhoods tending to have a similar density

rating. These are subjective observations as statistic comparisons were not undertaken between density maps. The top ten neighbourhoods in public black ash count and density are similar to the top ten for all black ash with seven overlapping neighbourhoods for the count (Island Lakes, Royalwood, Westwood, Robertson, Radisson, Waverley Heights, and Kildare-redonda) and nine overlapping neighbourhoods for density (Radisson, Royalwood, Robertson, Island Lakes, Melrose, Fairfield Park, East Elmwood, Westwood, and Linden Ridge).

The St. Vital Perimeter South neighbourhood needs to be further explained as its results are quite misleading. This neighbourhood contains the highest ash counts for the all ash, all green ash, all black ash, all private green ash, and all private black ash inventories; and is ranked second for the all black ash inventory. However, it does not occur in any of the top ten density lists. The highest density it has for any inventory is for the all ash inventory (13.40 trees/ha) which ranks 35th out of the 230 neighbourhoods. The other inventories were as follows: all green ash (13.21 trees/ha) ranking 35th; all private ash (13.38 trees/ha) ranking 29th; green ash private (13.18 trees/ha) ranking 29th; all black ash (0.19 trees/ha) ranking 136th; and black ash private (0.19 trees/ha) ranking 58th. The large difference in ash count and ash density ranking is because of the large size (area) of this neighbourhood which significantly reduces ash density values. This neighbourhood is still important to manage due to the significant ash counts and proximity to the Seine and Red Rivers even if density values are low. Figures 3.13-3.15 can assist managers in determining where the ash hotspots are located in this neighbourhood.

3.4.2 Riverbanks

Rivers and creeks were analyzed to determine how trees along riverbanks influenced ash densities and the total percentage of the ash inventory that is located near these riverbanks. It was determined that the total area of all eight rivers/creeks with a 100m buffer in Winnipeg comprises 4.28% of Winnipeg's total area. It was then determined that 20.07% (100% - 79.93%) of the ash inventory is located within 4.28% of Winnipeg's total area. This is a very interesting result as it shows that 20% of Winnipeg's total ash canopy is located within 50m of a riverbank. This has significant management implications as rivers/creeks are likely to serve as potential corridors for EAB due to the amount and density of trees situated in a linear arrangement. The linearity and proximity of these trees would allow EAB to move through riverbank hosts without difficulty, especially as there is currently no management interventions for riverbank trees. The

buffers for the Seine River and the Red River (especially the southern half) contain high densities of ash, and these are primarily private trees. The high number of trees within the Seine River's buffer (n = 32,027) and the Red River's buffer (n = 22,477) comprise 15.99% of all ash trees in Winnipeg. These trees are also located in close proximity throughout the buffer zone and are among the largest ash hotspots in the city (Figures 3.13 and 3.14). What makes these areas so concerning is that they serve as potential corridors for EAB to move throughout the city due to the high ash counts and densities. Because most of these trees along the Seine and Red Rivers are private and thus are not managed by the city, these riverbanks may allow EAB to spread relatively unmanaged. The Seine and Red Rivers flow through many of the high dense neighbourhoods; therefore, a significant portion of the ash canopy will be immediately threatened should EAB use these riverbanks to spread throughout the city.

The density (trees/ha) was not calculated for the riverbank buffers as it would not have contributed any useful information. Determining ash densities within the 100m buffer area would not have been useful as the density would be averaged based on the entire length of the river/creek's buffer. Therefore, the density value would have applied to the entire river/creek even if different sections of the river may have few trees whereas other sections may be forested. Because I did not segment the rivers/creeks, assigning a density value for the buffers would not have been useful.

3.4.3 Spatial Autocorrelation

Using ash density data for each neighbourhood to derive indicators of spatial autocorrelation for each of the seven analyzed ash inventories will also help guide logistical planning for a city wide EAB management program in Winnipeg. The results from the spatial autocorrelation analyses can assist managers in determining the connectivity between ash as a whole or as a subset by species and status. Managers can also use these results to highlight the high influence points (neighbourhoods) in each ash inventory that may significantly contribute to potential EAB movement throughout the city.

The Moran plots can be used as a management tool for managers in Winnipeg as they indicate the spatial autocorrelation of neighbourhoods for specific ash inventories throughout the entire city. They are useful for determining high influence neighbourhoods in each respective quadrant which can allow managers to allocate more resources to EAB prevention and management in

neighbourhoods with high ash densities and with high density neighbours. The Moran plots are also useful for visualizing the number of neighbourhoods that fall into each quadrant in each ash inventory. This can assist managers in determining specific management measures for ash status (public or private), ash species (green or black), and the type of neighbourhood ash density (Q1-Q4). The correlograms can be used as a management tool for managers to determine the likelihood of any given neighbourhood having similar neighbours in terms of ash density. Should managers decide to implement some management method in a given neighbourhood, the correlograms may assist in determining how far to extend those management activities. Additionally, the correlograms show when spatial dependency ends (Moran's I brackets overlap 0) for each ash inventory. This may assist managers in determining the potential spread of EAB from a given neighbourhood based on the connectivity of hosts for any of the ash inventories.

The all ash, all green ash, and private green ash inventories showed very similar results in their respective Moran plots and correlograms. The Moran plots showed that neighbourhoods experienced high positive spatial autocorrelation (all ash = 64.7%; all green ash = 66.5%; private green ash = 83.0%; these values are obtained by adding the number of neighbourhoods in Q1 and Q3). This is especially true when looking at the private green ash inventory where 83% of Winnipeg's neighbourhoods are positively spatially autocorrelated. Additionally, the Moran plots of these three inventories had many overlapping high influence points including Turnball Drive, Perrault, Cloutier Drive, Omand's Creek Industrial, and West Perimeter South. The correlograms are almost identical between these three inventories which suggests that private green ash trees highly influence the spatial dependency between lags (neighbourhoods) in the all ash inventory. The fact that the all green ash and the private green ash inventories share such common characteristics with the all ash inventory suggests that the all ash inventory is significantly influenced by the all green and private green ash inventories. Given the high numbers of private green ash in Winnipeg, this is not a surprising result.

The all black ash and public black ash inventories shared similar results in their respective Moran plots and correlograms. The Moran plots showed that neighbourhoods experienced moderate positive spatial autocorrelation (all black ash = 57.9%; public black ash = 61.3%). These two inventories also shared several high influence points (neighbourhoods) including Victoria West, Kern Park, Westwood, East Elmwood, Griffin, and Transcona North. The number

of neighbourhoods found in each quadrant was quite similar between the two inventories (Q1 - 48, Q2 - 40, Q3 - 85, Q4 - 57 for all black ash; Q1 - 42, Q2 - 31, Q3 - 99, Q4 - 58 for public black ash). The correlograms are also similar as you can only get an indication of spatial autocorrelation one lag away for both inventories. Lags 2-7 (with the exception of the second lag from the all black ash correlogram) overlap zero; therefore, no indications of autocorrelation can be made. This similarity suggests that the density of public black ash has a more significant impact on the all black ash results than the private black ash inventory.

The private black ash inventory was quite different from the other black ash focused inventories in that the Moran plot showed significantly more positive spatial autocorrelation (70.5%). The number of neighbourhoods found in each quadrant was significantly different than the all black and public black inventories (Q1 - 54, Q2 - 29, Q3 - 108, Q4 - 39). The private black ash correlogram shows that up to five lags away there is positive spatial autocorrelation which is much different than the other black ash correlograms. The private black ash correlogram shows the most positive spatial autocorrelation (five lags) out of all seven inventories/correlograms.

The public green ash inventory was different from the other green ash focused inventories in that the Moran plot showed slightly less positive spatial autocorrelation (59.5%). However, what differs the most is that the public green inventory had a fairly uniform distribution of neighbourhoods. Each quadrant contained a closer to equal share of the total number of neighbourhoods. Figure 3.20 shows that the mean of the public green ash density (vertical dotted line) and the mean of lagged neighbours density (horizontal dotted line) is quite central in the plot which suggests that the points are fairly equal across the quadrants. When comparing to the private green ash Moran plot, the number of neighbourhoods found in each quadrant is significantly different (Q1 - 76, Q2 - 45, Q3 - 61, Q4 - 48 for the public green; Q1 - 69, Q2 - 14, Q3 - 122, Q4 - 25 for the private green).

Certain neighbourhoods are worthwhile highlighting as they relate to specific quadrants and ash inventories. Neighbourhoods located in Q2 can be thought of as ‘islands’ as they contain a high ash density but are surrounded by neighbourhoods with low density values. High influence points found in Q2 may be of special concern to city managers as these neighbourhoods are stand-alone high density areas. Neighbourhoods such as these may serve as transition points where EAB may ‘jump’ to other areas with high ash densities. These neighbourhoods are also

more important to manage than their neighbours because of their higher ash counts and densities. Knowing these island neighbourhoods allows managers to better allocate resources to defend such neighbourhoods against EAB. One example of an island is Omand's Creek Industrial which is a Q2 neighbourhood in the all ash, all green ash, and private green ash inventories. High influence island neighbourhoods often did not overlap between ash inventories; therefore, depending on the ash inventory being analyzed, refer to Appendix C for the entire list.

Neighbourhoods located in Q4 can be thought of as 'holes' as they contain a low ash density but are surrounded by neighbourhoods with high density values. High influence points found in Q4 may be of special concern to city managers as these neighbourhoods are often in the middle of neighbourhoods with high ash densities. Even if these neighbourhoods have low ash densities, they still may serve as a connection for EAB between high density neighbourhoods. Management activities such as pre-emptive ash tree removals and ash firewood removals may be more appropriate to do first in hole neighbourhoods to eliminate them as potential connections between high density neighbourhoods. High influence hole neighbourhoods often did not overlap between ash inventories; therefore, depending on the ash inventory being analyzed, refer to Appendix C for the entire list.

Neighbourhoods located in Q3 are positively spatially autocorrelated in that they contain a low ash density and are surrounded by neighbourhoods with low density values. High influence points found in Q3 will be neighbourhoods with some of the lowest ash densities and neighbourhoods adjacent to them will also have low densities. It is worthwhile to point out that there are agricultural areas within the legal boundary of Winnipeg and thus contain very little tree canopy. Some neighbourhoods that were commonly found in Q3 contain large amounts of agricultural area. The West Perimeter South neighbourhood is an example of this, hence the low ash densities and tree counts. These kinds of neighbourhoods may be of the least concern to managers as ash counts and densities are typically low as are the surrounding areas of such neighbourhoods.

Neighbourhoods located in Q1 are also positively spatially autocorrelated in that they contain a high ash density and are surrounded by neighbourhoods with high density values. High influence points found in Q1 will be neighbourhoods with some of the highest ash densities and counts for the respective ash inventory being examined. These neighbourhoods may be of the most concern

to managers as they contain high counts of ash that can be destroyed rapidly by EAB due to the high densities and proximity of trees. Many of these neighbourhoods are also found along riverbanks, namely the Seine, Red, and La Salle Rivers. These neighbourhoods should be considered as very high-risk areas where significant ash phloem could be lost and where EAB could rapidly spread to other areas of the city. There are several of these high-risk neighbourhoods that need to be mentioned. Turnbull Drive is a high influence point (Q1) in the all ash, all green ash, all black ash, private green ash, and the private black ash inventories; therefore, Turnbull Drive has high densities of private green and black ash trees. Turnbull Drive is also located along the Red and La Salle Rivers making it very susceptible to facilitating or being infested by EAB spread via these riverbanks. Neighbourhoods adjacent/near to Turnbull Drive including Perrault, St. Norbert, and Cloutier Drive are all high influence points in several of the ash inventories. This area of the city is one of the most susceptible to EAB based on ash density, ash counts, and proximity to riverbanks, and ash losses could be significant in this area. Royalwood is a high influence point (Q1) in the all ash, all green ash, all black ash, private green, and the public black ash inventories. Royalwood is also located along the Seine River which increases its susceptibility and the potential for EAB facilitation into other neighbourhoods. Neighbourhoods adjacent/near to Royalwood that are also along the Seine River include Niakwa Place, Niakwa Park, Archwood, and Island Lakes (especially for black ash) which are all high influence points in several of the ash inventories.

3.4.4 Literature Comparison

Several researchers have used a variety of regulatory and biological data in efforts to model EAB spread at local and regional scales. Regional models from the USA were usually based on the rate of new county or sub-county EAB detections over time (Muirhead et al., 2006; Prasad et al., 2010; Huset, 2013), while local models often incorporated EAB population dynamics, ash density and distribution, and the short-distance dispersal of adult beetles (BenDor et al., 2006; Kovacs et al., 2014; McCullough & Mercader, 2012; Mercader et al., 2011a, 2011b).

Mercader et al. (2011a) used a spatially explicit, coupled lattice model to examine the effects of different management options on localized spread of EAB. Their model incorporated the quantity of available ash phloem, emergence times of adult EAB, and adult beetle dispersal. This study highlighted that spatially examining EAB and host trees can improve the application of

management options. Mercader et al. (2011b) also developed a coupled map lattice model which was used to represent the spatially explicit growth and dispersal of an isolated EAB population following initial colonization. Variables accounted for included initial EAB population density and distribution, ash density and distribution, and EAB one-year versus two-year life cycles. This study highlighted that ash distribution, ash density, and tree health are large predictors of local EAB spread (Mercader et al., 2011b). McCullough & Mercader (2012) used a similar spatial modelling approach to that of (Mercader et al., 2011a; 2011b) to examine insecticide usages and treatment costs as a management option for EAB. These studies highlight how spatially analyzing EAB in local areas can improve the understanding of how different management options impact EAB. Like these studies, we used ash density and distribution as a main variable in determining how EAB may spread locally. Incorporating EAB population dynamics and EAB one vs two-year life cycles would greatly improve the estimates of our spatial analyses; however, such data is significantly limited in Winnipeg. Therefore, the results from Chapter 2 can act as these variables when considering the results of the spatial analyses.

BenDor et al. (2006) developed the first EAB spread model to incorporate EAB population dynamics, ash density and distribution, and short-distance dispersal of adult EAB. They constructed EAB spread scenarios using tree information and land use data for DuPage County, Illinois. It was assumed that EAB's dispersal decision is dependent upon the density of the adults present and the total area of host trees in each 60m x 60m cell (BenDor et al., 2006). Similarly, our study assumes that EAB's dispersal decision is dependent upon the density of ash hosts and the total number of trees throughout the neighbourhoods of Winnipeg. Kovacs et al. (2014) modelled the spatial dynamics of EAB in an urban forest in Twin Cities, Minnesota by focusing on the population of ash trees that are potential hosts for EAB. The model consisted of a grid of equal cells with ash trees being subdivided into public and private ownership classes (Kovacs et al., 2014). They considered variables such as the amount of susceptible and infested ash trees, ownership class, and assumptions about the dispersal of EAB females. The methodology used by Kovacs et al. (2014) is similar to our study in that we also examined how potential host populations and densities may influence how EAB spreads. We both also differentiated between public and private trees for management implications. The finer-scale sampling unit (60m x 60m) used by Bendor et al. (2006) is advantageous for modelling potential movements of adult beetles in areas where EAB is present. Our study had very limited EAB-known location data;

therefore, ash/ha was a more appropriate density unit to use as it provided density measurements for entire neighbourhoods which is useful for management purposes.

Muirhead et al. (2006) regionally modelled EAB by incorporating local diffusions of EAB populations and estimating long-distance dispersal in the region including Michigan, Ohio, Indiana, and Ontario. Local diffusion was modelled based on sub-county detections of EAB whereas long-distance dispersal was modelled based on human population size which was used as a surrogate of human activities that could transport EAB (Muirhead et al., 2006). They also included a model predicting firewood movement from infested areas. Prasad et al., (2010) spatially modelled regional EAB spread in Ohio, USA while incorporating dispersal parameters such as EAB and ash abundance, roads, campgrounds, distance from the original infestation, the wood products industry, and human population density. Using a SHIFT (Schwartz, 1992) model, they calculated the probability of EAB infestation in unoccupied cells (270mx270m) based on the abundance of EAB in the occupied cells, the availability of ash, and the distance between all occupied and unoccupied cells (Prasad et al., 2010). This modelling approach highlighted the importance of satellite populations and the potential importance of road networks for artificial movement of EAB (Prasad et al., 2010; Siegert et al., 2015). Huset (2013) modelled regional EAB spread in the state of New York to determine where ash trees face the greatest risk and which landscape features are most strongly associated with EAB presence. Climactic (temperature and precipitation) and anthropogenic (human population, wood products industry, and campgrounds) variables were modelled into logistic regression and Maxent models (Huset, 2013). Although these studies are regional in scope, they demonstrated the usefulness of spatially modelling EAB to predict the susceptibility of various areas.

The relationship between ash density and EAB infestation/EAB-induced tree mortality has been explored and used as a variable for spatial modelling by previous studies (BenDor et al., 2006; Kovacs et al., 2014; Mercader et al., 2011b). It has also been shown that ovipositing female EAB are attracted to areas with high ash tree densities (Mercader et al., 2009, 2011b; Siegert et al., 2010). However, not all studies have found such a relationship between ash density and EAB-induced ash mortality. Smith et al. (2015) found no relationship between EAB-induced ash mortality and ash density in southeast Michigan. Similarly, Knight et al. (2013) observed no relationship between ash density and percentage of ash mortality in Ohio. Low density ash stands

were just as susceptible to EAB infestation and ash mortality as high density stands (Knight et al., 2013; Smith et al., 2015). Smith et al. (2015) and Knight et al. (2013) sampled mixed forest stands across various forest habitats, not including urban forests. The results of these studies are not very applicable to the case of Winnipeg as their studies did not pertain to urban forests. The selection of ash stands and plots was not random; therefore, sample effort effects may have impacted their results. However, it is interesting that these studies found that ash stands of all densities were equally susceptible to EAB.

3.4.5 Limitations

There have been several other variables used in previous studies to model potential regional and local EAB movement patterns. Diameter at breast height (DBH) has been used as a variable to analyze ash crown condition and mortality associated with EAB infestation (Steiner et al., 2019). DBH has also been used to model ash basal area to improve spatial maps of ash abundance (Host et al., 2020). DBH was considered as a variable in the ash density and spatial autocorrelation analyses; however, the private ash datasets did not contain DBH values for the trees. Additionally, studies have indicated that the DBH of trees does not have a significant impact on how EAB selects hosts. McCullough (2020) found that ash trees ranging in size from 2.5cm to 90cm DBH have been killed by EAB, and Smith et al. (2015) found that ash mortality increased over time with little effect of tree size. Tree condition/health is a variable that has been used to assist in modelling EAB foraging behaviour (Mercader et al., 2011b) and ash decline in infested natural forests (Murfitt et al., 2016). This variable was also considered; however, the private ash dataset does not have a tree condition/health rating due to the difficulty of collecting information for such a large number of trees. The distance to known locations of EAB infestation is a variable that has been used to spatially model potential EAB spread such as in the works of (Prasad et al., 2010; Huset, 2013). This would have been a useful variable to include in this study; however, there is a significant lack of EAB presence data (known locations) in Winnipeg. There have only been fifteen identified infested trees in Winnipeg at the time of writing; therefore, EAB presence/absence analyses would not have produced meaningful results. Past studies (BenDor et al., 2006; Mercader et al., 2011b) have used estimated short and long-distance dispersal patterns of EAB to model potential spatial movement. However, challenges of quantifying short-distance and long-distance movement of adult EAB in the field remain exceptionally difficult (Siegert et al., 2015). Due to the lack of EAB-specific data in Winnipeg

and the difficulty with quantifying adult movement patterns, this was not considered in our analyses.

3.5 Conclusion

This study suggested that private green ash trees along riverbanks may be of most concern to city managers as these trees have significant potential to influence how EAB disperses throughout Winnipeg. The management (or lack of) for private green ash trees along riverbanks will prove to be a major variable in how successful EAB dispersal is throughout the city. Managing public ash alone may not be enough to control EAB spread due to the lower degree of connectivity of public ash. When comparing across the different ash inventories, the top ten neighbourhoods (in ash densities and counts) varied quite substantially, especially the private inventory vs the public inventory and the green inventory vs the black inventory. High influence neighbourhoods in the Moran plots also differed between ash inventories. The results of this study can better inform EAB management programs and decision-makers in Winnipeg. Managers can use these results to highlight neighbourhoods and areas of the city that may be more susceptible depending on the ash inventory being examined. Further management and research recommendations are explored in Chapter 4.

3.6 References

Anselin, L. (1995). Local Indicators of Spatial Association—LISA. *Geographical Analysis, 27(2),* 93-115. https://doi.org/10.1111/j.1538-4632.1995.tb00338.x

BenDor, T. K., Metcalf, S. S., Fontenot, L. E., Sangunett, B., & Hannon, B. (2006). Modeling the spread of the Emerald Ash Borer. *Ecological Modelling*, *197*(1), 221–236. https://doi.org/10.1016/j.ecolmodel.2006.03.003

Bivand, R., & Wong, D. (2018) Comparing implementations of global and local indicators of spatial association TEST, 27(3), 716-748. https://doi.org/10.1007/s11749-018-0599-x

Cappaert, D., Mccullough, D. G., Poland, T. M., & Siegert, N. W. (2005). Emerald Ash Borer in North America: A Research and Regulatory Challenge. *American Entomologist*, *51*(3), 152–165. https://doi.org/10.1093/ae/51.3.152

Herms, D., & McCullough, D. (2014). Emerald Ash Borer Invasion of North America: History, Biology, Ecology, Impacts, and Management. *Annual Review of Entomology*, *59*, 13–30. https://doi.org/10.1146/annurev-ento-011613-162051

Host, T. K., Russell, M. B., Windmuller-Campione, M. A., Slesak, R. A., & Knight, J. F. (2020). Ash Presence and Abundance Derived from Composite Landsat and Sentinel-2 Time Series and Lidar Surface Models in Minnesota, USA. *Remote Sensing*, *12*(8), 1341. https://doi.org/10.3390/rs12081341

Huset, R. (2013). *A GIS-based Analysis of the Environmental Predictors of Dispersal of the Emerald Ash Borer in New York.* 120.

Knight, K. S., Brown, J. P., & Long, R. P. (2013). Factors affecting the survival of ash (Fraxinus spp.) trees infested by emerald ash borer (Agrilus planipennis). *Biological Invasions*, *15*(2), 371–383. https://doi.org/10.1007/s10530-012-0292-z

Kovacs, K. F., Haight, R. G., Mercader, R. J., & McCullough, D. G. (2014). A bioeconomic analysis of an emerald ash borer invasion of an urban forest with multiple jurisdictions. *Resource and Energy Economics*, *36*(1), 270–289. https://doi.org/10.1016/j.reseneeco.2013.04.008

Liebhold, A. M., Berec, L., Brockerhoff, E., Epanchin-Niell, R., Hastings, A., Herms, D., Kean, J. M., McCullough, D. G., Suckling, D., Tobin, P., & Yamanaka, T. (2016). Eradication of Invading Insect Populations: From Concepts to Applications. *Annual Review of*

Entomology, *61*, 335–352. https://doi-org.uml.idm.oclc.org/10.1146/annurev-ento-010715-023809

Liebhold, A. M., & Kean, J. M. (2019). Eradication and containment of non-native forest insects: Successes and failures. *Journal of Pest Science*, *92*(1), 83–91. https://doi.org/10.1007/s10340-018-1056-z

Liebhold, A. M., & Tobin, P. (2008). Population Ecology of Insect Invasions and Their Management. *Annual Review of Entomology*, *53*, 387–408.

McCullough, D. G. (2020). Challenges, tactics and integrated management of emerald ash borer in North America. *Forestry*, *93*(2), 197–211. https://doi.org/10.1093/forestry/cpz049

McCullough, D. G., & Mercader, R. J. (2012). Evaluation of potential strategies to SLow Ash Mortality (SLAM) caused by emerald ash borer (Agrilus planipennis): SLAM in an urban forest. *International Journal of Pest Management*, *58*(1), 9–23. https://doi.org/10.1080/09670874.2011.637138

McCullough, D. G., Poland, T., & Cappaert, D. (2009b). Attraction of the emerald ash borer to ash trees stressed by girdling, herbicide treatment, or wounding. *Canadian Journal of Forest Research*, *39*(7), 1331–1345. https://doi-org.uml.idm.oclc.org/10.1139/X09-057

McCullough, D. G., Poland, T. M., Anulewicz, A. C., & Cappaert, D. (2009a). Emerald Ash Borer (Coleoptera: Buprestidae) Attraction to Stressed or Baited Ash Trees. *Environmental Entomology*, *38*(6), 1668–1679. https://doi.org/10.1603/022.038.0620

Mercader, R. J., Siegert, N. W., Liebhold, A. M., & McCullough, D. G. (2009). Dispersal of the emerald ash borer, Agrilus planipennis, in newly-colonized sites. *Agricultural and Forest Entomology*, *11*(4), 421–424. https://doi.org/10.1111/j.1461-9563.2009.00451.x

Mercader, R. J., Siegert, N. W., Liebhold, A. M., & McCullough, D. G. (2011a). Simulating the effectiveness of three potential management options to slow the spread of emerald ash borer (Agrilus planipennis) populations in localized outlier sites. *Canadian Journal of Forest Research*, *41*(2), 254–264. https://doi.org/10.1139/X10-201

Mercader, R. J., Siegert, N. W., Liebhold, A. M., & McCullough, D. G. (2011b). Influence of foraging behavior and host spatial distribution on the localized spread of the emerald ash borer, Agrilus planipennis. *Population Ecology*, *53*(2), 271–285. https://doi.org/10.1007/s10144-010-0233-6

Mercader, R. J., Siegert, N. W., & McCullough, D. G. (2012). Estimating the Influence of Population Density and Dispersal Behavior on the Ability to Detect and Monitor Agrilus planipennis (Coleoptera: Buprestidae) Populations. *Journal of Economic Entomology*, *105*(1), 272–281. https://doi.org/10.1603/EC11172

Mercader, R. J., McCullough, D. G., Storer, A. J., Bedford, J. M., Heyd, R., Siegert, N. W., Katovich, S., & Poland, T. M. (2016). Estimating local spread of recently established emerald ash borer, Agrilus planipennis, infestations and the potential to influence it with a systemic insecticide and girdled ash trees. *Forest Ecology and Management*, *366*, 87–97. https://doi.org/10.1016/j.foreco.2016.02.005

Muirhead, J. R., Leung, B., van Overdijk, C., Kelly, D. W., Nandakumar, K., Marchant, K. R., & MacIsaac, H. J. (2006). Modelling local and long-distance dispersal of invasive emerald ash borer Agrilus planipennis (Coleoptera) in North America. *Diversity and Distributions*, *12*(1), 71–79. https://doi.org/10.1111/j.1366-9516.2006.00218.x

Murfitt, J., He, Y., Yang, J., Mui, A., & De Mille, K. (2016). Ash Decline Assessment in Emerald Ash Borer Infested Natural Forests Using High Spatial Resolution Images. *Remote Sensing*, *8*(3), 256. https://doi.org/10.3390/rs8030256

Prasad, A. M., Iverson, L. R., Peters, M. P., Bossenbroek, J. M., Matthews, S. N., Davis Sydnor, T., & Schwartz, M. W. (2010). Modeling the invasive emerald ash borer risk of spread using a spatially explicit cellular model. *Landscape Ecology*, *25*(3), 353–369. https://doi.org/10.1007/s10980-009-9434-9

QGIS Development Team (2022). QGIS Geographic Information System. Open Source Geospatial Foundation Project. http://www.qgis.org

R Core Team (2022). R: A language and environment for statistical computing. R Foundation for Statistical Computing, Vienna, Austria. https://www.R-project.org/.

Sadof, C. S., Hughes, G. P., Witte, A. R., Peterson, D. J., & Ginzel, M. D. (2017). Tools for staging and managing emerald ash borer in the urban forest. *Arboriculture & Urban Forestry*, *43*(1), 15–26.

Schwartz, M. (1993). Modelling effects of habitat fragmentation on the ability of trees to respond to climatic warming. *Biodiversity & Conservation, 2,* 51-61. https://doi.org/10.1007/BF00055102

Shigesada, N., & Kawasaki, K. (1997). *Biological Invasions: Theory and Practice.* Oxford Univ. Press.

Siegert, N. W., Mccullough, D. G., Liebhold, A. M., & Telewski, F. W. (2014). Dendrochronological reconstruction of the epicentre and early spread of emerald ash borer in North America. *Diversity and Distributions*, *20*(7), 847–858. https://doi.org/10.1111/ddi.12212

Siegert, N. W., McCullough, D. G., Williams, D. W., Fraser, I., Poland, T. M., & Pierce, S. J. (2010). Dispersal of Agrilus planipennis (Coleoptera: Buprestidae) From Discrete Epicenters in Two Outlier Sites. *Environmental Entomology*, *39*(2), 253–265. https://doi.org/10.1603/EN09029

Siegert, N. W., Mercader, R. J., & McCullough, D. G. (2015). Spread and dispersal of emerald ash borer (Coleoptera: Buprestidae): estimating the spatial dynamics of a difficult-to-detect invasive forest pest. *The Canadian Entomologist*, *147*(3), 338–348. https://doi.org/10.4039/tce.2015.11

Smith, A., Herms, D. A., Long, R. P., & Gandhi, K. J. K. (2015). Community composition and structure had no effect on forest susceptibility to invasion by the emerald ash borer (Coleoptera: Buprestidae). *The Canadian Entomologist*, *147*(3), 318–328. https://doi.org/10.4039/tce.2015.8

Steiner, K. C., Graboski, L. E., Knight, K. S., Koch, J. L., & Mason, M. E. (2019). Genetic, spatial, and temporal aspects of decline and mortality in a Fraxinus provenance test following invasion by the emerald ash borer. *Biological Invasions*, *21*, 3439–3450. https://doi.org/10.1007/s10530-019-02059-w

Taylor, R. A. J., Bauer, L. S., Poland, T. M., & Windell, K. N. (2010). Flight performance of agrilus planipennis (Coleoptera: Buprestidae) on a flight mill and in free flight. *Journal of Insect Behavior*, *23*(2), 128–148. https://doi.org/10.1007/s10905-010-9202-3

Taylor, R. A. J., Poland, T. M., Bauer, L. S., Windell, K. N., & Lautz, J. (2007). *Emerald ash borer flight estimates revised. In: Mastro V, Lance D, Reardon R, Parra G (eds) Proceedings of 2006 Emerald Ash Borer Research and Technology Development Meeting, Cincinnati, OH. USDA-FS, FHTET-2007-04, Morgantown, pp 10–12*.

Wang, X., Yang, Z.-Q., Gould, J. R., Zhang, Y.-N., Liu, G.-J., & Liu, E. (2010). The Biology and Ecology of the Emerald Ash Borer, Agrilus planipennis , in China. *Journal of Insect Science*, *10*(128), 1–23. https://doi.org/10.1673/031.010.12801

Ward, S. F., Fei, S., & Liebhold, A. M. (2020). Temporal dynamics and drivers of landscape-level spread by emerald ash borer. *Journal of Applied Ecology*, *57*(6), 1020–1030. https://doi.org/10.1111/1365-2664.13613

Chapter 4: Summary, Conclusions, and Recommendations

4.1 Summary and Conclusions

There were two main objectives of this thesis: 1) to determine when adult EAB emergence and peak activity thresholds would have been reached in Winnipeg using weather station data from the past 50 years; and 2) to determine the potential susceptibility of neighbourhoods to EAB infestation based on ash density (trees/ha), total ash count, and the influence of riverbanks in Winnipeg. Prediction of first adult emergence and peak adult activity in Winnipeg will allow pest control managers to better plan and execute EAB control initiatives and develop long-term management strategies. The ash density and spatial autocorrelation models will allow managers to determine the degree of connectivity across neighbourhoods for various ash inventories and to determine high influence neighbourhoods that may be of special concern. This thesis was the first to explore estimated EAB emergence and peak activity periods in Winnipeg; and how different combinations of ash (status and species) are spatially distributed across Winnipeg.

In Chapter 2, historic annual temperature records from the past 50 years in Winnipeg were used to perform degree-day calculations that predict EAB adult emergence and peak activity. Each of the three degree-day models used threshold temperatures based on activity ranges provided by other EAB studies. This study suggested that climate change in the Winnipeg region would not have significantly impacted the date of first emergence for EAB over the study period; however, it has significantly impacted the date of peak activity (GDD 550 standard model). When comparing across the five decades, the earliest estimated emergence and peak activity dates for each model-threshold combination occurred in the 2010 decade. Managers should consider the results of all three models representing the range of days from (June 11 – June 15 for emergence; July 11 – July 13 for peak activity) when choosing a time to implement EAB monitoring and control measures.

In Chapter 3, public and private ash tree inventories were used to calculate ash densities, the total number of ash trees, and considered the influence of riverbanks across the neighbourhoods in Winnipeg. These ash inventories were further broken down by species to test for spatial autocorrelation and the degree of connectivity of trees across Winnipeg's neighbourhoods. This study suggested that private green ash trees along riverbanks may be of most concern to city managers as these trees have significant potential to influence how EAB disperses throughout

Winnipeg; particularly since the monitoring, management, and removal of private and riverbank trees is currently outside the City of Winnipeg's management mandate. Managers can use these results to highlight neighbourhoods and areas of the city that may be more susceptible depending on the ash inventory being examined.

4.2 Recommendations

There are several management tools that can help slow the spread and potential destruction of EAB. As previously mentioned in Chapter 2, some methods are better undertaken prior to the adult emergence date such as setting artificial pheromone traps, branch sampling, the establishment of trap trees by girdling them, and visual surveys of EAB symptoms in the canopy. In operational survey programs, traps do not necessarily need to capture the first EAB beetles, but they should be in place before peak flight activity (Poland et al., 2011). If trapping surveys are to be implemented in Winnipeg, managers need to have traps in place before peak flight activity - July 11 (191±5.4), July 11 (191±5.6), or July 13 (193±5.4) according to the double sine, single sine, and standard models respectively. Managers in Winnipeg should have traps setup by late June to early July (340-460 DD_{10}) to ensure that traps are in place for adult peak activity (Poland et al., 2011). Branch sampling is suitable for sampling open-grown ash in any landscape, but it is more important in urban areas with high-value ash trees (Ryall et al., 2011). Branch sampling can be performed at any time between September and May; however, because larvae continue to feed and grow in early fall, their galleries are easiest to see if branches are sampled after October (Ryall et al., 2011). Adult EAB beetles preferentially colonize unhealthy trees over healthy trees (Herms & McCullough, 2014; Klooster et al., 2014; McCullough, 2020); therefore, establishing trap trees by girdling them should be in place before peak activity to maximize trap catch. Conducting visual surveys to identify EAB-induced symptoms on ash trees is another tool that can be undertaken near emergence dates or in the late fall. Signs and symptoms of EAB infestation include crown thinning and dieback, epicormic shoots, woodpecker damage, bark splits, notched leaflets by adult feeding, D-shaped exit holes, and dead trees (City of Winnipeg, 2020a; Liu, 2018; Tluczek et al., 2011). Some of these symptoms such as woodpecker damage, bark splitting, and exit holes are easiest to detect during the leaf-off period from approximately October – May (K. La France, Pers. Comm., City of Winnipeg Urban Forestry Branch, August 5, 2020).

Alternatively, some methods are better undertaken just before or during the peak activity date such as visual surveys for adult beetles themselves, public outreach, and trap inspections. Conducting public outreach just prior to the peak activity date can raise public awareness of EAB symptoms and encourage vigilance and reporting which may assist managers in locating EAB problem areas. Additionally, increasing the frequency of trap (pheromone and girdled trees) inspections during peak activity may allow for more immediate detection and mitigation.

The use of insecticides is another effective way of slowing ash mortality and protecting high valued ash trees (McCullough, 2020). In urban landscapes, systemic insecticides have provided urban trees with a high level of protection (Herms & McCullough., 2014). Several insecticides have demonstrated effective ash tree protection against EAB including emamectin benzoate (Andrade et al., 2020; McCullough, 2020), azadirachtin (Herms et al., 2019; McKenzie et al., 2010), and imidacloprid (Herms et al., 2019; Poland et al., 2016). Emamectin benzoate has been reported to provide three years of protection (McCullough et al., 2019; Mercader et al., 2015) while azadirachtin and imidacloprid can provide 1-2 years of protection (Herms et al., 2019). Andrade et al. (2020) also found that a small proportion of ash trees treated with systemic insecticide provided detectable reductions in EAB population growth and distribution, suggesting a neighbouring effect for other trees. However, the use of insecticides does not come without potential disadvantages including affecting native pollinators, drilling wounds, labour, and cost (Andrade et al., 2020; McCullough, 2020). The recommended time to inject trees with insecticides depends on the product being used and location; however, spring treatments are consistently more effective than the same treatments applied in the fall (Herms et al., 2019). Tree injections are a pre-emptive management method that should implemented on high value ash trees before EAB is detected in an area. There are three active ingredients registered in Canada for controlling EAB by trunk injections which are acephate, imidacloprid, and azadirachtin (Government of Canada, 2015). The City of Winnipeg currently uses IMA-jet (imidacloprid) and TreeAzin (azadirachtin) for public tree injections (City of Winnipeg, 2022).

The spatial analyses showed that private green ash along riverbanks may have significant potential to influence how EAB disperses throughout Winnipeg. It is likely that the management of private green ash trees along riverbanks will prove to be a major variable in how successful EAB dispersal is throughout the city. Developing monitoring and management strategies will be

crucial to prevent EAB from using these hotspot corridors to disperse across the city. Management programs could be implemented similar to what the City of Winnipeg has in place for Dutch Elm Disease whereby city inspectors conduct neighbourhood level surveillance searching for diseased elm trees on public and private lands (City of Winnipeg, 2020b). Implementing this type of program for ash or even combining the surveillance of elm and ash together may be a management/monitoring option going forward. Riverbank surveillance along the Seine and Red Rivers that focuses on private ash is highly recommended. City inspectors could also identify unhealthy ash trees along riverbanks that could be used as trap (girdled) trees. Setting up trap trees along riverbanks may be useful for determining if EAB is present and approximate population densities.

Managing public ash is also important especially in the neighbourhoods that are adjacent to the Archwood neighbourhood as this is where EAB has been found in the city. Archwood itself has very low public ash densities (0.43 trees/ha for green ash which ranks 178th out of 230; and 0.0 trees/ha for black ash) due to pre-emptive removals done by the City of Winnipeg. However, the adjacent neighbourhoods of Niakwa Park, Glenwood, and Central St. Boniface contain much higher public ash densities (4.6 trees/ha, 3.0 trees/ha, and 1.7 trees/ha respectively) and 1,172 combined total public trees that should be closely monitored. The few remaining public ash trees in Archwood should also be closely monitored. Methods that are useful for monitoring and managing public trees include pre-emptive branch sampling, visual surveillance, and insecticides for high value trees. However, managing public ash is likely not enough to control EAB spread due to the lower degree of connectivity that public ash was found to have. It is also recommended for city managers to use the Moran plot results to better highlight neighbourhoods and areas of the city that may be more susceptible depending on the ash inventory being examined. Allocating further management resources to high influence neighbourhoods (Appendix C) may allow for improved EAB control in these influential neighbourhoods.

4.3 Research Recommendations

At the time of writing this thesis, there were very few (n= 15) known locations where individual trees were infested; therefore, the models and analyses undertaken as part of this thesis were predictions and estimations based on local parameters (ash inventories, temperature, and potential corridors) and studies from other jurisdictions. However, if EAB presents itself in

higher populations and densities in Winnipeg, further research should focus on several aspects. Determining developmental thresholds and life stage GDD accumulations that are specific to EAB in Winnipeg would improve the estimates for emergence and peak activity times. Further research should determine Winnipeg-specific life cycle lengths and the possible proportion of the EAB population that may take two years to develop to maturity. Understanding the life cycle (one or two years) and the proportion of the population that uses either cycle would significantly improve the timing of management activities.

Further research should investigate how EAB larvae experiences the underbark microclimate vs direct air temperatures across the various seasons in Winnipeg. The underbark microclimate often differs from direct air temperature (Vermunt et al., 2012) and understanding this in the context of EAB in Winnipeg may prove useful. Investigating how snow cover may provide insulation to overwintering larvae may assist in explaining winter mortality events as snow cover may act as a buffer for larvae (DeSantis et al., 2013). Examining the differences in sunlight exposure across ash trees to determine how trees differ in potential heat accumulation may be useful for determining which trees (i.e. boulevard, park, forest, etc.) allow for the most GDD accumulations in EAB larvae. Further research into how winter cold spells and temperatures affect EAB larvae in Winnipeg may be useful as demonstrated by Duell et al. (2022).

For future spatial analyses concerning EAB in Winnipeg, research should focus on using tree conditions/health as a potential modelling parameter. EAB is known to be more attracted to unhealthy trees (Herms & McCullough, 2014; Klooster et al., 2014); therefore, modelling this parameter may further pinpoint areas within the city that are most susceptible. Using tree condition/health as a variable for the entire ash inventory may not be feasible due to difficulty of obtaining health conditions for private trees. However, models that focus on public trees should incorporate this variable. The distance to known locations of EAB infestation is another variable that may be used in future spatial research. Studies have shown that EAB females lay the majority of their eggs within 100m of their emergence point (Mercader et al., 2009; Siegert et al., 2010) making this an incredibly useful modelling parameter. However, there are not enough EAB presence data (known locations) in Winnipeg yet to use this variable. Future research may investigate how anthropogenic transportation networks in Winnipeg may influence EAB spread throughout the city, similar to the work done by Prasad et al. (2010). Future research may also

investigate how tree species diversity impacts EAB dispersal and neighbourhood/area susceptibility. Areas with low tree species diversity are likely to be less resistant and resilient to EAB (Granger et al., 2020) and to non-native forest pests in general (Guo et al., 2019).

4.4 References

Andrade, R. B. de, Abell, K., Duan, J. J., Shrewsbury, P., & Gruner, D. S. (2020). Protective neighboring effect from ash trees treated with systemic insecticide against emerald ash borer. *Pest Management Science*, *77*(1), 474–481. https://doi.org/10.1002/ps.6041

City of Winnipeg. (2022). *Emerald Ash Borer Control Program 2022*. https://winnipeg.ca/publicworks/insectcontrol/insect/EABschedule.stm

City of Winnipeg. (2020a). *Emerald Ash Borer (EAB). Parks and Open Space.* https://winnipeg.ca/publicworks/parksopenspace/urbanforestry/EmeraldAsh.stm#18

City of Winnipeg. (2020b). *Dutch Elm Disease*. https://winnipeg.ca/publicworks/parksopenspace/urbanforestry/DED.stm

Duell, M. E., Gray, M. T., Roe, A. D., MacQuarrie, C. J. K., and Sinclair, B. J. (2022). Plasticity drives extreme cold tolerance of emerald ash borer (*Agrilus planipennis*) during a polar vortex. *Current Research in Insect Science.* 2:100031. https://doi.org/10.1016/j.cris.2022.100031

DeSantis, R., Moser, K., Gormanson, D., Bartlett, M., & Vermunt, B. (2013). Effects of climate on emerald ash borer mortality and the potential for ash survival in North America. *Agricultural and Forest Meteorology*, 120–128. https://doi.org/10.1016/j.agrformet.2013.04.015

Government of Canada. (2015). *Emerald ash borer.* https://www.exoticpests.gc.ca/control-details/insect/1

Granger, J. J., Zobel, J. M., & Buckley, D. S. (2020). *Differential Impacts of Emerald Ash Borer (Agrilus planipennis Fairmare) on Forest Communities Containing Native Ash (Fraxinus spp.) Species in Eastern North America*, *66*(1), 38–48. https://doi.org/10.1093/forsci/fxz063

Guo, Q., Fei, S., Potter, K., Liebhold, A., & Wen, J. (2019). Tree diversity regulates forest pest invasion. *PNAS, 116*(15), 7382-7386. https://doi.org/10.1073/pnas.1821039116

Herms, D., & McCullough, D. (2014). Emerald Ash Borer Invasion of North America: History, Biology, Ecology, Impacts, and Management. *Annual Review of Entomology*, *59*, 13–30. https://doi.org/10.1146/annurev-ento-011613-162051

Herms, D., Mccullough, D., Smitley, D., Clifford, C., & Cranshaw, W. (2019). Insecticide Options for Protecting Ash Trees from Emerald Ash Borer Insecticide, 3rd ed. *North Central Center Bulletin*, 1–16. http://www.emeraldashborer.info/documents/Multistate_EAB_Insecticide_Fact_Sheet.pdf

Klooster, W. S., Herms, D. A., Knight, K. S., Herms, C. P., McCullough, D. G., Smith, A., Gandhi, K. J. K., & Cardina, J. (2014). Ash (Fraxinus spp.) mortality, regeneration, and seed bank dynamics in mixed hardwood forests following invasion by emerald ash borer (Agrilus planipennis). *Biological Invasions*, *16*, 859–873. https://doi.org/10.1007/s10530-013-0543-7

Liu, H. (2018). Under Siege: Ash management in the wake of the emerald ash borer. *Journal of Integrated Pest Management*, *9*(1). https://doi.org/10.1093/jipm/pmx029

McCullough, D. G. (2020). Challenges, tactics and integrated management of emerald ash borer in North America. *Forestry*, *93*(2), 197–211. https://doi.org/10.1093/forestry/cpz049

McCullough, D. G., Poland, T. M., Tluczek, A. R., Anulewicz, A., Wieferich, J., & Siegert, N. W. (2019). Emerald Ash Borer (Coleoptera: Buprestidae) Densities Over a 6-yr Period on Untreated Trees and Trees Treated With Systemic Insecticides at 1-, 2-, and 3-yr Intervals in a Central Michigan Forest. *Journal of Economic Entomology*, *112*(1), 201–212. https://doi.org/10.1093/jee/toy282

McKenzie, N., Helson, B., Thompson, D., Otis, G., McFarlane, J., Buscarini, T., & Meating, J. (2010). Azadirachtin: An Effective Systemic Insecticide for Control of Agrilus planipennis (Coleoptera: Buprestidae). *Journal of Economic Entomology*, *103*(3), 708–717. https://doi.org/10.1603/EC09305

Mercader, R. J., McCullough, D. G., Storer, A. J., Bedford, J. M., Heyd, R., Poland, T. M., & Katovich, S. (2015). Evaluation of the potential use of a systemic insecticide and girdled trees in area wide management of the emerald ash borer. *Forest Ecology and Management*, *350*(2015), 70–80. https://doi.org/10.1016/j.foreco.2015.04.020

Mercader, R. J., Siegert, N. W., Liebhold, A. M., & McCullough, D. G. (2009). Dispersal of the emerald ash borer, Agrilus planipennis, in newly-colonized sites. *Agricultural and Forest Entomology*, *11*(4), 421–424. https://doi.org/10.1111/j.1461-9563.2009.00451.x

Poland, T. M., Ciaramitaro, T. M., & McCullough, D. G. (2016). Laboratory Evaluation of the Toxicity of Systemic Insecticides to Emerald Ash Borer Larvae. *Journal of Economic Entomology*, *109*(2), 705–716. https://doi.org/10.1093/jee/tov381

Poland, T. M., McCullough, D. G., & Anulewicz, A. C. (2011). Evaluation of Double-Decker Traps for Emerald Ash Borer (Coleoptera: Buprestidae). *Journal of Economic Entomology*, *104*(2), 517–531. https://doi.org/10.1603/EC10254

Prasad, A. M., Iverson, L. R., Peters, M. P., Bossenbroek, J. M., Matthews, S. N., Davis Sydnor, T., & Schwartz, M. W. (2010). Modeling the invasive emerald ash borer risk of spread using a spatially explicit cellular model. *Landscape Ecology*, *25*(3), 353–369. https://doi.org/10.1007/s10980-009-9434-9

Ryall, K., Fidgen, J., and Turgeon, J. (2011). Detection of Emerald Ash Borer in Urban Environments Using Branch Sampling. Natural Resources Canada – Canadian Forest Service, Sault Ste. Marie. https://epe.lac-bac.gc.ca/100/200/301/nrcan-rncan/frontline_forestry_research_applications-e/Fo123-1-111-eng.pdf

Siegert, N. W., McCullough, D. G., Williams, D. W., Fraser, I., Poland, T. M., & Pierce, S. J. (2010). Dispersal of Agrilus planipennis (Coleoptera: Buprestidae) From Discrete Epicenters in Two Outlier Sites. *Environmental Entomology*, *39*(2), 253–265. https://doi.org/10.1603/EN09029

Tluczek, A. R., Mccullough, D. G., & Poland, T. M. (2011). Influence of Host Stress on Emerald Ash Borer (Coleoptera: Buprestidae) Adult Density, Development, and Distribution in Fraxinus pennsylvanica Trees. *Environmental Entomology*, *40*(2), 357–366. https://doi.org/10.1603/EN10219

Vermunt, B., Cuddington, K., Sobek-Swant, S., Crosthwaite, J. C., Barry Lyons, D., & Sinclair, B. J. (2012). Temperatures experienced by wood-boring beetles in the under-bark microclimate. *Forest Ecology and Management*, *269*, 149–157. https://doi.org/10.1016/j.foreco.2011.12.019

Appendix A: Dataset Missing Values

1993
- March 9
- March 19
- March 24 – 25
- March 29
- April 8
- April 16
- April 26 – 27
- April 29
- May 1
- May 4
- May 13 – 16
- May 22
- May 24
- May 28
- June 1
- June 8
- June 13
- June 21 – 22
- August 5
- August 14
- August 17
- August 25
- September 1
- September 8
- September 13
- October 4 – 5

2007
- May 3 – 13 (data was obtained from Richard International Airport Weather Station)

2010
- September 14

2011
- March 16 – 21
- August 18 – 19

2012
- June 27
- July 12

2013
- March 20
- April 10
- May 3
- July 23

- September 9

2014
- June 6

2015
- June 2
- June 23

2016
- May 26
- June 6

2017
- April 18 – 19
- July 20

2018
- March 6
- September 10
- September 21

2019
- August 8
- September 8

Appendix B – Winnipeg Neighbourhood Index

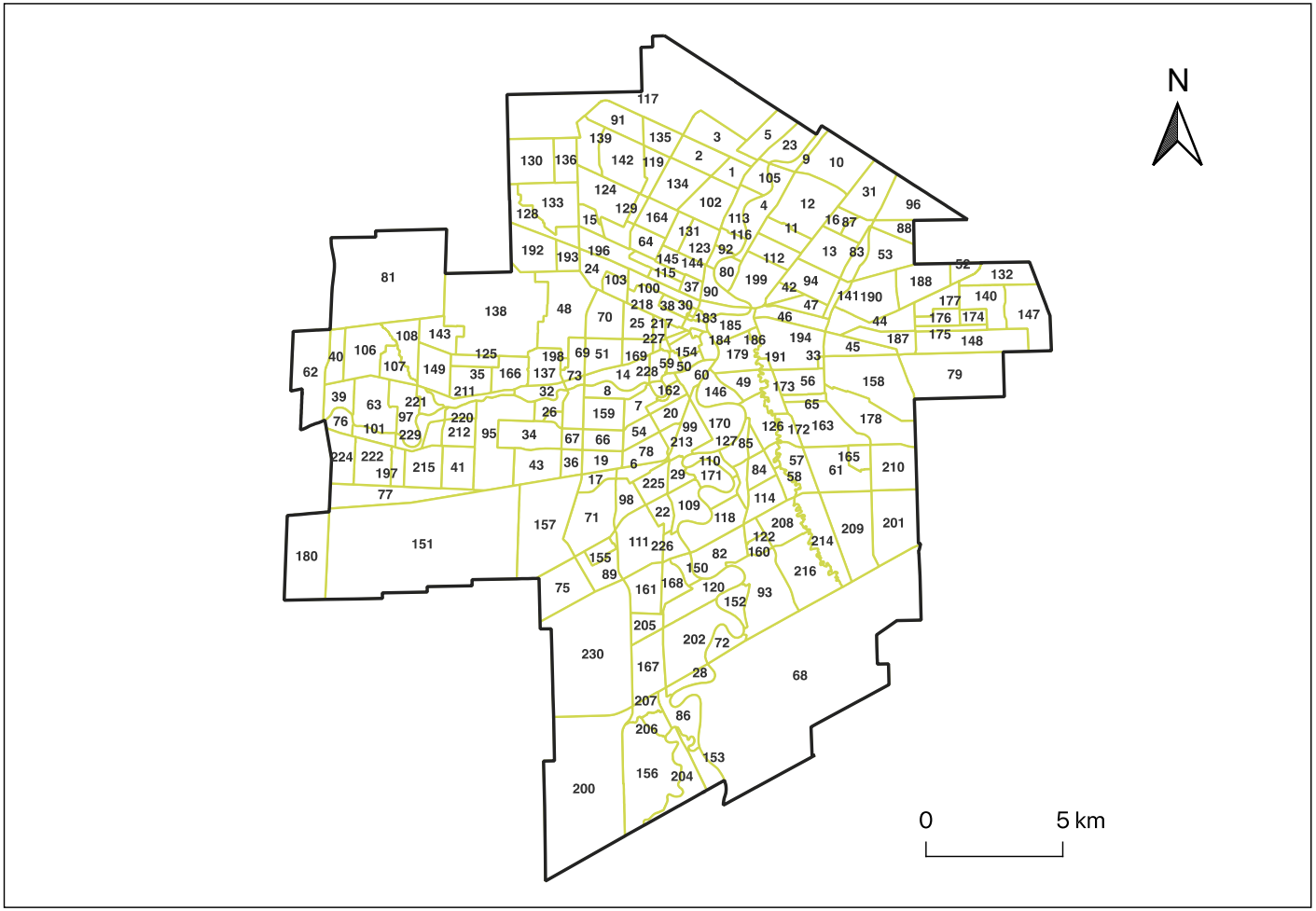

Figure B.1. Indexed City of Winnipeg Neighbourhood Map

Figure B.2. Indexed Map of Downtown Winnipeg

Table B.1. Indexed City of Winnipeg Neighbourhoods

1	Margaret Park	33	Holden	65	Maginot
2	Templeton-sinclair	34	Tuxedo	66	Central River Heights
3	West Kildonan Industrial	35	Silver Heights	67	J.B. Mitchell
4	Kildonan Drive	36	Mathers	68	St. Vital Perimeter South
5	Riverbend	37	Lord Selkirk Park	69	Polo Park
6	Parker	38	Centennial	70	Sargent Park
7	Crescentwood	39	Glendale	71	Linden Woods
8	Wellington Crescent	40	Buchanan	72	Maple Grove Park
9	Valhalla	41	Elmhurst	73	West Wolseley
10	River East	42	Talbot-grey	74	Edgeland
11	Rossmere-b	43	South Tuxedo	75	Whyte Ridge
12	Rossmere-a	44	Regent	76	River West Park
13	Valley Gardens	45	Dugald	77	Ridgewood South
14	Wolseley	46	Tyne-tees	78	Grant Park
15	Burrows-keewatin	47	East Elmwood	79	Transcona South
16	Mcleod Industrial	48	St. James Industrial	80	Glenelm
17	Brockville	49	Norwood East	81	Saskatchewan North
18	Roslyn	50	Broadway-assiniboine	82	Minnetonka
19	South River Heights	51	Minto	83	Eaglemere
20	Earl Grey	52	Griffin	84	St. George
21	Norberry	53	Grassie	85	Varennes
22	Maybank	54	Rockwood	86	St. Norbert
23	Rivergrove	55	Spence	87	Springfield South
24	Weston	56	Stock Yards	88	North Transcona Yards
25	Daniel Mcintyre	57	Niakwa Place	89	West Fort Garry Industrial
26	Old Tuxedo	58	Lavalee	90	North Point Douglas
27	Armstrong Point	59	Legislature	91	Amber Trails
28	Cloutier Drive	60	River-osborne	92	St. John's Park
29	Point Road	61	Southdale	93	River Park South
30	China Town	62	Assiniboia Downs	94	Munroe East
31	Margaret Park	63	Westwood	95	Assiniboine Park
32	Templeton-sinclair	64	Burrows-central	96	Kilcona Park

97	Kirkfield	129	Mynarski	161	Waverley Heights
98	Buffalo	130	North Inkster Industrial	162	Mcmillan
99	Lord Roberts	131	Inkster-faraday	163	Windsor Park
100	Logan-c.p.r.	132	Transcona North	164	Robertson
101	Southboine	133	Tyndall Park	165	The Mint
102	Jefferson	134	Garden City	166	Deer Lodge
103	Pacific Industrial	135	Leila North	167	Richmond West
104	Alpine Place	136	Inkster Gardens	168	Montcalm
105	Kildonan Park	137	King Edward	169	St. Matthews
106	Crestview	138	Airport	170	Riverview
107	Sturgeon Creek	139	Mandalay West	171	Wildwood
108	Heritage Park	140	Kildare-redonda	172	Niakwa Park
109	Crescent Park	141	Kildonan Crossing	173	Archwood
110	Kingston Crescent	142	The Maples	174	Kern Park
111	Chevrier	143	Murray Industrial Park	175	Melrose
112	Munroe West	144	William Whyte	176	Victoria West
113	Seven Oaks	145	Dufferin	177	Radisson
114	Worthington	146	Norwood West	178	Symington Yards
115	Dufferin Industrial	147	Canterbury Park	179	Central St. Boniface
116	Luxton	148	Transcona Yards	180	West Perimeter South
117	Rosser-old Kildonan	149	Booth	181	South Point Douglas
118	Pulberry	150	Agassiz	182	Civic Centre
119	Leila-mcphillips Triangle	151	Wilkes South	183	Exchange District
120	University	152	Normand Park	184	The Forks
121	Portage & Main	153	Turnbull Drive	185	North St. Boniface
122	St. Vital Centre	154	South Portage	186	Tissot
123	St. John's	155	Linden Ridge	187	Mission Gardens
124	Inkster Industrial Park	156	Trappistes	188	Meadows
125	Jameswood	157	Tuxedo Industrial	189	Victoria Crescent
126	Glenwood	158	St. Boniface Industrial Park	190	Peguis
127	Elm Park	159	North River Heights	191	Dufresne
128	Oak Point Highway	160	Vista	192	Omand's Creek Industrial

193	Brooklands	225	Beaumont
194	Mission Industrial	226	Pembina Strip
195	Shaughnessy Park	227	Colony
196	Weston Shops	228	West Broadway
197	Roblin Park	229	Ridgedale
198	Kensington	230	Waverley West
199	Chalmers		
200	La Barriere		
201	South St. Boniface		
202	Fort Richmond		
203	Sir John Franklin		
204	Perrault		
205	Fairfield Park		
206	Parc La Salle		
207	Richmond Lakes		
208	Meadowood		
209	Island Lakes		
210	Southland Park		
211	Birchwood		
212	Varsity View		
213	Ebby-wentworth		
214	Royalwood		
215	Eric Coy		
216	Dakota Crossing		
217	Central Park		
218	West Alexander		
219	Portage-ellice		
220	Vialoux		
221	Woodhaven		
222	Betsworth		
223	Marlton		
224	Westdale		

Appendix C: High Influence Points for Ash Inventories

Table C.1. High influence neighbourhoods in all seven ash inventories.

Ash Inventory	High density with high density neighbours	High density with low density neighbours	Low density with low density neighbours	Low density with high density neighbours
All Ash	Turnbull Drive, Perrault, Niakwa Park, Cloutier Drive, Victoria Crescent, Ridgedale, Royalwood, Wildwood	Beaumont, Canterbury Park, Tyndall Park, Linden Woods, Omand's Creek Industrial, Mission Gardens	West Perimeter South, Airport, Symington Yards, North Inkster Industrial, Saskatchewan North, Weston Shops, La Barriere	N/A
All Green Ash	Turnbull Drive, Perrault, Cloutier Drive, Royalwood, Victoria Crescent, Wildwood, Niakwa Park, Ridgedale, Norwood East	Beaumont, Canterbury Park, Tyndall Park, Linden Woods, Omand's Creek Industrial, Mission Gardens	West Perimeter South, Airport, Symington Yards, St. Boniface Industrial Park, North Inkster Industrial, Saskatchewan North, La Barriere	N/A
All Black Ash	Victoria West, Kern Park, University, Island Lakes, Fairfield Park, Melrose, Mathers, Turnbull Drive, Waverley Heights, Royalwood, Cloutier Drive, Radisson, Robertson	Grant Park, East Elmwood, Linden Ridge, Westwood	N/A	St. Vital Perimeter South, Griffin, Transcona North, Transcona Yards, Maple Grove Park
Private Green Ash	Turnbull Drive, Perrault, Victoria Crescent, Niakwa Park, Marlton, St. Norbert, Cloutier Drive, Wildwood, Royalwood, Archwood, Ridgedale, Niakwa Place, Lavalee,	Omand's Creek Industrial, Burrows-keewatin	West Perimeter South	Norwood West, Vista, Westwood, Worthington, St. George, Island Lakes

	Alpine Place, Roblin Park, Normand Park, Varsity View, Norwood East			
Public Green Ash	Exchange District, Daniel Mcintyre, Mandalay West	Kildonan Park	West Perimeter South, Holden	North Transcona Yards, Inkster Industrial Park
Private Black Ash	Maple Grove Park, St. Vital Perimeter South, Richmond West, University, Fort Richmond, Agassiz, Turnbull Drive, St. Norbert, Normand Park, Niakwa Place, Wilwood, Montcalm, Archwood	South Tuxedo, The Forks, Kildonan Crossing, Polo Park, Grant Park	N/A	Fairfield Park
Public Black Ash	Victoria West, Kern Park, Kildare-redonda, J. B. Mitchell, Meadows, Mathers, Melrose, Island Lakes, Radisson, Robertson, Mission Gardens, Waverley Heights, Fairfield Park, Royalwood	Burrows-keewatin, Mandalay West, Riverbend, East Elmwood, Linden Ridge, Westwood	N/A	Transcona North, Griffin, Transcona Yards, Inkster Industrial Park, Leila-McPhillips Triangle